

Copyright
by
Harish Ganapathy
2011

The Dissertation Committee for Harish Ganapathy
certifies that this is the approved version of the following dissertation:

**The Design Of Feedback Channels For Wireless
Networks: An Optimization-theoretic View**

Committee:

Constantine Caramanis, Supervisor

Jeffrey Andrews

Sanjay Shakkottai

Sriram Viswanath

John Hasenbein

**The Design Of Feedback Channels For Wireless
Networks: An Optimization-theoretic View**

by

Harish Ganapathy, B.S., M.S.

DISSERTATION

Presented to the Faculty of the Graduate School of

The University of Texas at Austin

in Partial Fulfillment

of the Requirements

for the Degree of

DOCTOR OF PHILOSOPHY

THE UNIVERSITY OF TEXAS AT AUSTIN

August 2011

Dedicated to my family.

Acknowledgments

I wish to thank my adviser Dr. Constantine Caramanis for an enriching five years of doctoral work at UT Austin and for standing by me through the crests and troughs that often punctuated this process. I often wondered where he found that infinite patience to guide me through the course. It would be safe to say that most of this work was done at JP's Java, which in addition to denting many-a-graduate-student's pocket, was the scene of numerous conversations, some leading to useful research but mostly amounting to hot air. The usual suspects here were Little John, BoFi, BigB, Kaushik, Vaze, and Reddy, a committed member of my siesta club, guys, thanks for the memories! On a more serious note, I must acknowledge the invaluable experience gained through my internship terms, which helped shape my approach to research; Pavan, Danlu, Jeremy, Kaushik, Mukundan, Malolan and Shiv, many thanks to you. Of course, I would not be in wireless had I not been privy to the teaching excellence and subsequent mentorship of Dr. Dimitris Pados at SUNY Buffalo through the course of my Bachelor's and Master's degrees. Finally, this would not have been possible without the support of my wife, Meghana, my parents, my grand parents and my sister ...

The Design Of Feedback Channels For Wireless Networks: An Optimization-theoretic View

Publication No. _____

Harish Ganapathy, Ph.D.
The University of Texas at Austin, 2011

Supervisor: Constantine Caramanis

The fundamentally fluctuating nature of the strength of a wireless link poses a significant challenge when seeking to achieve reliable communication at high data rates. Common sense, supported by information theory, tells us that one can move closer towards achieving higher data rates if the transmitter is provided with *a priori* knowledge of the channel. Such channel knowledge is typically provided to the transmitter by a feedback channel that is present between the receiver and the transmitter. The quality of information provided to the transmitter is proportional to the bandwidth of this feedback channel. Thus, the design of feedback channels is a key aspect in enabling high data rates. In the past, these feedback channels have been designed *locally*, on a link-by-link basis. While such an approach can be globally optimal in some cases, in many other cases, this is not true. In this thesis, we identify various settings in wireless networks, some already a part of existing standards, others under discussion in future standards, where the design of feedback channels

is a problem that requires global, *network-wide* optimization. In general, we propose the treatment of feedback bandwidth as a network-wide resource, as the next step en route to achieving Gigabit wireless.

Not surprisingly, such a global optimization initiative naturally leads us to the important issue of computational efficiency. Computational efficiency is critical from the point-of-view of a network provider. A variety of optimization techniques are employed in this thesis to solve the large combinatorial problems that arise in the context of feedback allocation. These include dynamic programming, sub-modular function maximization, convex relaxations and compressed sensing. A naïve algorithm to solve these large combinatorial problems would typically involve searching over an exponential number of possibilities to find the optimal feedback allocation. As a general theme, we identify and exploit special application-specific structure to solve these problems optimally with reduced complexity. Continuing this endeavour, we search for more intricate structure that enables us to propose approximate solutions with significantly-reduced complexity. The accompanying analysis of these algorithms studies the inherent trade-offs between accuracy, efficiency and the required structure of the problem.

Table of Contents

Acknowledgments	v
Abstract	vi
List of Tables	xi
List of Figures	xii
Chapter 1. Introduction	1
Chapter 2. Background	9
2.1 Sub-modular function maximization	9
2.1.1 Definitions and properties	10
2.1.2 Sensor selection	15
2.2 Compressed sensing	17
2.2.1 Mathematical preliminaries	20
2.2.2 Useful concentration inequalities	26
2.2.3 Recent RIP Results	29
Chapter 3. Feedback allocation with slow data scheduling	36
3.1 Introduction	36
3.2 System model	46
3.3 Long-term network objectives	48
3.3.1 Queue stability	49
3.3.2 Utility maximization	52
3.4 Optimal allocation through dynamic programming	54
3.5 Reduced-complexity resource allocation	57
3.5.1 Resource allocation through sub-modularity	60
3.5.2 Resource allocation for MIMO systems	62

3.5.2.1	Single-stream MIMO with limited feedback . . .	63
3.5.2.2	Time-scales and structure of rate vector $\boldsymbol{\mu}(\mathbf{m}, \mathbf{b})$	65
3.5.2.3	Relaxation and approximation guarantees . . .	71
3.6	Performance of relaxation-based algorithm	75
3.7	Concluding remarks	76
Chapter 4.	Feedback allocation, fast data scheduling and interference	79
4.1	Introduction	79
4.1.1	Prior work on feedback design	80
4.1.2	Our contributions	83
4.1.3	Chapter organization	84
4.2	System model	84
4.3	Part I: Feedback allocation under fast data scheduling	87
4.4	Part II: Feedback allocation with interference	95
4.5	Concluding remarks	102
Chapter 5.	Exploiting Sparse Dynamics for Controlling Whitespace Networks	103
5.1	Introduction	103
5.2	System model	108
5.3	Joint scheduling and feedback allocation with interference . . .	112
5.4	Exploiting Sparse Dynamics in Learning	115
5.4.1	Compressed Sensing	116
5.4.2	The feedback protocol	118
5.5	NSP of path-loss matrices	120
5.5.1	Preliminaries	120
5.5.2	Useful concentration inequalities	123
5.5.3	NSP of linearly-processed path-loss matrices \mathbf{A}	125
5.6	Joint Learning, Feedback Allocation and Scheduling	127
5.7	Simulations	129
5.8	Conclusion	132
Appendices		133

Appendix A. Appendix for Chapter 3	134
A.1 Proof of Theorem 10	134
A.2 Proof of Theorem 1	137
A.3 Proof of Theorems 12-14	139
A.3.1 Proof of Theorem 12	139
A.3.2 Proof of Theorem 13	140
A.3.3 Proof of Theorem 14	141
Appendix B. Appendix for Chapter 4	142
B.1 Proofs of Lemmas	142
B.1.1 Proof of Lemma 13	142
B.1.2 Proof of Lemma 23	143
B.1.3 Proof of Lemma 14	143
B.1.4 Proof of Lemma 15	144
B.1.5 Proof of Lemma 16	147
B.2 Proof of Theorem 23	149
B.3 Proof of Theorem 17	151
B.4 Proof of Theorem 5	152
Appendix C. Appendix for Chapter 5	154
C.1 Proof of Lemma 20	154
C.2 Proof of Lemma 21	158
Bibliography	161
Vita	178

List of Tables

3.1	Properties of proposed online feedback allocation algorithms . . .	77
-----	--	----

List of Figures

3.1	FDD Cellular uplink where the base-station has a feedback link to each user.	43
3.2	Single-stream beamforming and combining MIMO system. . .	64
3.3	Composite effects of small-scale fading and large-scale fading in a wireless channel with $D = 4$	66
3.4	Distribution of $\log_2 \left(1 + \max \left\{ \frac{1}{1-c_1(N_t, N_r) 2^{c_2(N_t, N_r)}}, \frac{1}{1-c_1(N_t, N_r)} \right\} \right)$ over 1000 codebook realizations.	75
3.5	The function $e(b)$ in Fig. 3.5 for a 2×2 MIMO system over a Rayleigh fading channel with a randomly chosen codebook and $B = 10$	76
4.1	Uplink interference neighbourhood	97
5.1	Network with interfering transmitters (not shown) uniformly distributed on the blue circle of radius r_p . There are $N_s = 8$ whitespace receivers in the network equally-divided across two circles ($q = 2$) of radii $r_{s,1}$ and $r_{s,2}$ respectively. This gives rise to partitions $\mathcal{C}_1 = \{1, 2, 3, 4\}$ and $\mathcal{C}_2 = \{5, 6, 7, 8\}$. The whitespace receivers are equally-spaced on each circle as shown.	110
5.2	Illustrative example of grid model used in simulations with $N = 25$ and $N_s = 4$	130
5.3	The average maximum queue lengths under the two different cases	132

Chapter 1

Introduction

The advent of wireless communication technology over the last two decades has significantly improved connectivity and access to information in general. Wireless devices have found a place in almost all walks of life, performing increasingly challenging tasks. There is an ever-growing demand from the end user for a device that is versatile, portable and yet efficient, and one that can support high-data rate services. Consequently, it is imperative on the part of the network designer to provide these high-data rate services in a computationally-efficient manner.

Fundamentally, the wireless medium is a shared medium of communication. Subsequently, any network of wireless nodes has the following two properties that differentiate it from a wireline network.

- Broadcast: When a single node transmits a signal, all nodes in the network receive an attenuated version of the signal.
- Superposition: When two nodes simultaneously transmit a signal, the received signal is a superposition of the two attenuated transmit signals.

These fundamental properties ensure that in order for any two nodes to com-

municate, they will have to endure fluctuations in the strength of the wireless link often called the *channel*. It is in general reasonable to believe that if the transmitter had *a priori* knowledge of the channel, it should be able to exploit this knowledge to achieve better communication rates. More formally, it is a well-known, fundamental, information-theoretic result that the use of up-to-date channel state information at the transmitter increases the communication rate. This brings into play the role of a feedback channel. Feedback refers to the process of communicating the current state of the channel, measured at the receiver, back to the transmitter. It is important in turn to ensure that the bandwidth of the feedback channel is large enough to ensure a sufficient quality of channel state information at the transmitter, since overly-corrupt and/or outdated information might not be useful. At a high level, this thesis deals with allocating feedback bandwidths on the network-wide scale so as to facilitate high data-rate communication. As networks seek to meet user demands through advanced technologies such as multiple-antenna communication, which call for increased levels and more sophisticated uses of feedback, the computational complexity of any feedback allocation scheme becomes a central issue; if an algorithm to determine optimal or near-optimal allocations cannot be implemented in larger systems due to prohibitive computational complexity, its usefulness is severely limited. Thus, in designing these feedback channels, this thesis focuses keenly on the topic of computational efficiency, which is an integral component of any viable system design.

Transmitter adaptation promises to be an indispensable part of almost

all future wireless systems. The advent of multiple-antenna technology has further fuelled the necessity for transmitter adaptation or *precoding* as it is commonly referred to. It is reasonable to assume that any network provider would be interested in consuming the least amount of cumulative feedback bandwidth (across the network) in order to enable high data rate transmissions on the “feedforward” link. Over the last decade, this has prompted much research into the field of limited feedback, which concerns the design the best possible transmit precoding systems under a constraint on the bandwidth of the feedback channel. However, much of this literature on limited feedback for multiple-input-multiple-output (MIMO) systems focuses on optimizing a single transmitter-receiver-transmitter closed-loop wireless system. For example, consider a single-stream beamforming MIMO system. For such a system, it is known that the rate-optimal strategy is for the receiver to measure the channel (matrix-valued in general) and feed back the right singular vector corresponding to the maximum singular value of the channel. Maximum-rate quantization codebooks have been designed for such systems under a bandwidth constraint on the feedback channel.

In this thesis, we propose the treatment of feedback channels as a *network-wide* resource that must allocated judiciously. Our work builds on the aforementioned body of research by identifying network scenarios where the feedback bandwidths across users in the system become *coupled*. Such scenarios demand a careful allocation of this resource. Two design criteria immediately come to mind, criteria that are well-established in the literature

on resource allocation: One can maximize the network-wide transmission rate given a constraint on the number of feedback resources or alternatively, one can minimize the number of feedback resources consumed, while offering a target quality-of-service. While these criteria have been applied in the context of other resource allocation problems such as power control, they have not been considered in the context of feedback allocation to the best of our knowledge. Accordingly, we take the perspective of a network controller by formulating and solving (exactly if possible) many important feedback resource allocation problems. In general, such allocations will be made as a function of the state (e.g., queue sizes, channel conditions, etc.) of the network.

The first problem we consider is that of feedback allocation in a traditional cellular uplink setting. Here, we have a group of users in a cell that are served orthogonally (no interference between the users) by a base station. The base station has a fixed/limited feedback budget with which to form its feedback packet. This packet communicates rate instructions to each user, thereby enabling link adaptation. A user that is assigned a larger chunk of bits within the feedback packet is able to perform *finer* rate adaptation. Thus, the rate seen by each user is a function of the size of its feedback partition within the feedback packet in addition to other system parameters. In this scenario, we are interested in optimally partitioning the feedback packet at each network scheduling instant in order to maximize system throughput. Note that in this case, the coupling amongst users that necessitates global optimization across all feedback links is induced by the total fixed feedback budget. The algorithms

proposed here are suitable for applications that do not require the aggressive, high-frequency data schedulers, i.e., the data schedules remain fixed for long periods of time.

The second problem builds on the first in that we now consider systems with high frequency data scheduling. Furthermore, we allow for groups of users to communicate on the same spectrum thereby generating inter-user interference. We cover both traditional cellular networks as well as future network architectures that include femtocells, microcells and distributed-antenna-systems. We design feedback allocation algorithms that operate in tandem with fast data schedulers in both interference-free and interference-limited environments. As the density of access points is only set to grow, interference becomes a major impediment to achieving high data rates in wireless networks. Therefore, designing feedback mechanisms that enable the application of interference cancellation techniques such as MIMO precoding is crucial. Note that any perfect MIMO interference cancellation technique would require an infinite-capacity feedback channel. Hence, a feedback channel with bandwidth constraints would immediately cause residual interference to the neighbouring access points. For such a setting as well as for others, we are interested in determining the minimum network-wide feedback budget that guarantees a given worst-case loss in throughput. Network-wide optimization is required in this case due to the coupling that is induced by the presence of interference amongst users.

The third research thrust focuses on a future network architecture in

the form of whitespace networks. Here we have a set of unlicensed users (called whitespace users) operating on the same spectrum as a group of primary users or incumbents. The whitespace users operate with the intention of improving spectral efficiency while not causing undue performance loss to the primary network. The whitespace network consists of a whitespace base station serving the group of whitespace users. We study the process of network state acquisition through feedback for the purposes of scheduling in the downlink of this whitespace network. As with the previous problem, we are interested in devising feedback strategies that consume the least amount of bandwidth while guaranteeing optimal or near-optimal throughput performance.

As one might imagine, feedback allocation problems are typically combinatorial in nature owing to the basic fact that the feedback bandwidth is modelled to be an integer number of bits. As the number of users and access points present in a network can be large in general, it is of primary interest for the controller to ensure that resource allocation algorithms are computationally efficient. In other words, it is imperative that the algorithmic solutions scale gracefully in the size of the problem. Through the course of this dissertation, we encounter several *large* combinatorial problems where a naïve solution would typically involve searching over an exponential number of possibilities. In order to reduce this exponential complexity, we search for, identify and exploit specific structure that is inherent in the application. As a general theme, we first propose optimal solutions that succeed in a significant reduction in complexity over the first order brute-force approach. Subsequently, we

identify more intricate structure that allow us to propose polynomial-time or pseudo-polynomial-time algorithms that solve the feedback allocation problem approximately. Often, we provide analytical guarantees on the accuracy of these algorithms. In some cases, we provide numerical evidence of near-optimal performance of these algorithms.

Some of the combinatorial optimization techniques employed in this research work have been used in other areas such as machine learning but have not often been used in the domain of wireless networks to the best of our knowledge. These include dynamic programming, sub-modular function optimization, greedy algorithms and compressed sensing. We strongly believe that the techniques introduced in this dissertation can be used to solve other important problems in the area of wireless networks.

Organization: In Chapter 2, we provide background on some of the combinatorial optimization techniques that will be used during the course of this dissertation. In Chapter 3, we introduce the first feedback allocation problem that aims to maximize throughput under a total feedback budget for networks without interference. The case with interference and the dual criterion – minimize feedback budget under quality-of-service constraints – is studied in Chapter 4. Chapter 5 considers the dual criterion in the specific context of whitespace networks.

Notation: We denote the (i, j) -th element of matrix \mathbf{X} by x_{ij} while x_i denotes element i of vector \mathbf{x} . Given matrices $\mathbf{X}, \mathbf{Y} \in \mathbb{R}^{p \times q}$, $X \leq Y$ denotes $x_{ij} \leq y_{ij}, \forall i = 1, \dots, p, j = 1, \dots, q$. We denote the transpose and Hermitian-

transpose operators by $(.)^T$ and $(.)^\dagger$ respectively. The sets \mathbb{R}_+ , \mathbb{N}_0 and \mathbb{N} represent the non-negative real numbers, non-negative integers and positive integers respectively. $[x]^+ = \max\{x, 0\}$ and $\|\cdot\|$ is the two-norm operator. Finally, the Frobenius norm of matrix \mathbf{X} is denoted by $\|\mathbf{X}\|_F$; $[x]^+ = \max\{x, 0\}$ and $[x]_1^+ = \min\{x, 1\}$.

Chapter 2

Background

In this chapter, we provide the basic background, as well as some key references, to some of the optimization techniques we use in the core chapters of this thesis. Section 2.1 introduces some basic concepts regarding sub-modular function optimization. Sub-modular functions are used in combinatorial optimization, and the basic result of interest says that if our objective has the property of “diminishing returns” then while combinatorial, it can nonetheless be efficiently approximated. The second section in this chapter, Section 2.2, introduces the topic of compressed sensing. Sparsity and structure are increasingly important concepts, and the need for computationally efficient tools that can exploit this structure is growing. Compressed sensing is precisely such a framework where sparsity can be exploited.

2.1 Sub-modular function maximization

The background in this section is most relevant to Chapter 3. This section presents a primer on sub-modular optimization (summarized from [67–69]) that will be useful for our purposes. We start with preliminary definitions and properties. Concluding this section is a recent application of sub-modularity

in solving a sensor selection problem [7].

2.1.1 Definitions and properties

A sub-modular function is defined as follows:

Definition (Sub-modular Function): Let E be a finite set and 2^E represent all its subsets. Then, $F : 2^E \rightarrow \mathbb{R}_+$ is a *non-decreasing, normalized, sub-modular* function if:

- $F(\emptyset) = 0$ (normalized)
- $F(A) \leq F(B)$ if $A \subseteq B \subseteq E$ (non-decreasing)
- $F(A \cup \{e\}) - F(A) \geq F(B \cup \{e\}) - F(B)$, $\forall A \subseteq B \subseteq E$ and $e \in E \setminus B$ (sub-modular)

The following property of sub-modular functions is useful for reasons that are obvious.

Lemma 1. *If F_k , $k = 1, \dots, K$, are sub-modular on set E , then $\sum_{k=1}^K w_k F_k(A)$, $A \subseteq E$ is a sub-modular function for $w_k \geq 0, \forall k$.*

Proof: The proof follows from direct application of the definition of sub-modularity. Let $F_k(A)$, $k = 1, \dots, K$, $A \subseteq E$, be sub-modular functions on set E . Then, for all $A \subseteq B \subseteq E$ and $e \in E \setminus B$, we have the property

$$\begin{aligned} \sum_{k=1}^K w_k F_k(A \cup \{e\}) - \sum_{k=1}^K w_k F_k(A) &= \sum_{k=1}^K w_k (F_k(A \cup \{e\}) - F_k(A)) \\ &\geq \sum_{k=1}^K w_k (F_k(B \cup \{e\}) - F_k(B)). \end{aligned} \tag{2.1}$$

□

Having provided the definition of sub-modularity along with a useful property, we now introduce the kinds of constraint sets that are typically considered in the context of sub-modular optimization.

Definition (Independence System): A set system (E, \mathcal{I}) where E is a finite set and \mathcal{I} is a collection of subsets of E is called an *independence system* if it satisfies the following properties:

- $\emptyset \in \mathcal{I}$
- $A \subseteq B$ and $B \in \mathcal{I}$, then $A \in \mathcal{I}$

Definition (Matroid): An independence system is called a *matroid* if it satisfies the following additional property; if $A, B \in \mathcal{I}$ and $|A| < |B|$, then there exists $e \in B \setminus A$ such that $A \cup \{e\} \in \mathcal{I}$.

We are interested in a special class of matroids called *uniform matroids*, defined as follows.

Definition (Uniform Matroid): \mathcal{I} is a uniform matroid if $\mathcal{I} = \{F \subseteq E : |F| \leq k\}$ for $k \in \mathbb{N}$.

The optimization problem that has been considered in the context of sub-modular functions and independence systems is

$$\begin{aligned} F^* &= \underset{\text{s.t}}{\text{maximize}} && F(A) \\ &&& A \in \mathcal{I}, A \subseteq E. \end{aligned} \tag{2.2}$$

Since many NP-hard problems can be reduced to a sub-modular function maximization over an independence system, significant research has focused on developing efficient approximation algorithms. In particular, the performance of the greedy algorithm in solving special cases of (2.2) has been extensively studied. Nemhauser et al. [70] considered problem (2.2) over uniform matroids and showed that the greedy algorithm provides a $(1 - \frac{1}{e})$ approximation factor for this special case.

At each step, this algorithm augments the existing subset solution with an additional element from the set E such that the new subset solution belongs to the independence system. The additional element is selected to maximize the incremental utility. Given sets $S, T \subset E$, we define

$$\rho_T(S) = F(S \cup T) - F(S) \quad (2.3)$$

and write the greedy algorithm (borrowing some notation from [67]) when \mathcal{I} is a uniform matroid, parametrized by size k , as follows.

Algorithm (*Greedy algorithm for maximizing non-decreasing, normalized, sub-modular functions over uniform matroids*):

- *Step 1:* Set $i = 1$ and $S_{g,0} = \emptyset$.
- *Step 2:* Select element $e_i \in E$ such that

$$e_i = \underset{\text{s.t } e \in E \setminus S_{g,i-1}}{\text{maximize}} \quad \rho_e(S_{g,i-1}) \quad (2.4)$$

- *Step 3:* Set $S_{g,i} = S_{g,i-1} \cup \{e_i\}$.
- *Step 4:* Stop if $i = k$; else set $i = i + 1$ and go to Step 2.

In the above, $S_{g,i}$ represents the set constructed by the greedy algorithm after i iterations. The approximation factor result is formally stated in Theorem 1 below. We re-state the proof of Theorem 1 as it provides insight into the operation of the greedy algorithm.

Theorem 1. *Let $F : 2^E \rightarrow \mathbb{R}_+$ be a normalized, non-decreasing, sub-modular function on set E , \mathcal{I} be a uniform matroid, and F_{greedy} be the solution provided by the greedy algorithm. Then $\frac{F_{greedy}}{F^*} \geq (1 - \frac{1}{e})$.*

Proof: Firstly, we present an alternate characterization of sub-modular functions from Nemhauser et al. [70] that is useful for the proof. For any two disjoint subsets S and $T = \{t_1, \dots, t_N\}$, $S, T \subseteq E$, we can write

$$F(S \cup T) = \left[\sum_{i=2}^N F(S \cup \{t_1, \dots, t_i\}) - F(S \cup \{t_1, \dots, t_{i-1}\}) \right] + (F(S \cup \{t_1\}) - F(S)) + F(S) \quad (2.5)$$

through telescoping. By the sub-modularity of F , we have

$$\begin{aligned} F(S \cup T) &\leq \left[\sum_{i=1}^N F(S \cup t_i) - F(S) \right] + F(S) \\ &= F(S) + \sum_{i=1}^N \rho_{t_i}(S) \end{aligned} \quad (2.6)$$

and furthermore, for $S \subseteq T$, this simplifies to

$$F(T) \leq F(S) + \sum_{t \in T \setminus S} \rho_t(S). \quad (2.7)$$

Now, let S^* and S_g be the optimal solution and the solution generated by the greedy algorithm respectively; ρ_i represents the incremental value that is obtained during the i -th iteration of the greedy algorithm. Then, by setting

$S = S_{g,0} = \emptyset$ in (A.11) and noting that $|S^*| \leq k$ since it is a uniform matroid, we calculate

$$F^* \leq \sum_{e \in T} F(\{e\}) \leq k\rho_1 = k \max_{e \in E} F(\{e\}). \quad (2.8)$$

Recalling that $F(S_{g,0}) = 0$ due to normalization and applying (A.11) to set $S_{g,j}$ generated by the greedy algorithm after j iterations, we have

$$\begin{aligned} F^* &\leq F(S_{g,j}) + \sum_{t \in T \setminus S_{g,j}} \rho_t(S_{g,j}) \\ &= \sum_{i=1}^j (F(S_{g,i}) - F(S_{g,i-1})) + \sum_{t \in T \setminus S_{g,j}} \rho_t(S_{g,j}) \\ &\leq \sum_{i=1}^j \rho_i + k\rho_{j+1}. \end{aligned} \quad (2.9)$$

By dividing both sides by k , re-arranging and adding $\sum_{i=1}^j \rho_i$ to both sides, we get

$$\sum_{i=1}^{j+1} \rho_i \geq \frac{1}{k} F^* + \frac{k-1}{k} \sum_{i=1}^j \rho_i. \quad (2.10)$$

The following result is proved through induction in order to solve the recursion.

$$\sum_{i=1}^j \rho_i \geq \left(\frac{k^j - (k-1)^j}{k^j} \right) F^*. \quad (2.11)$$

For $j = 1$, we get $\rho_1 \geq \frac{F^*}{k}$, which is true since, for $S^* = \{s_1^*, s_2^*, \dots, s_K^*\}$, we have

$$\begin{aligned} F^* &= F(S^*) \\ &= \sum_{i=2}^k \left[F(\{s_1^*, s_2^*, \dots, s_i^*\}) - F(\{s_1^*, s_2^*, \dots, s_{i-1}^*\}) \right] + F(\{s_1^*\}) \\ &\leq (k-1)F(\{s_1^*\}) + F(\{s_1^*\}) \\ &= kF(\{s_1^*\}). \end{aligned} \quad (2.12)$$

Assuming the statement holds true for $(j-1)$, and substituting it in (A.14),

we get

$$\begin{aligned}
\sum_{i=1}^j \rho_i &\geq \frac{1}{k} F^* + \frac{k-1}{k} \left(\frac{k^{j-1} - (k-1)^{j-1}}{k^{j-1}} \right) F^* \\
&= \frac{1}{k} F^* + (k-1) \left(\frac{k^{j-1} - (k-1)^{j-1}}{k^j} \right) F^* \\
&= \frac{k^{j-1} + (k-1)(k^{j-1} - (k-1)^{j-1})}{k^j} F^* \\
&= \left(\frac{k^j - (k-1)^j}{k^j} \right) F^*,
\end{aligned} \tag{2.13}$$

which proves the claim. Now, by setting $j = k$, we calculate

$$F_g = \sum_{i=1}^k \rho_i \geq \left(\frac{k^k - (k-1)^k}{k^k} \right) F^*, \tag{2.14}$$

or in other words,

$$\frac{F_g}{F^*} \geq \left(\frac{k^k - (k-1)^k}{k^k} \right) = 1 - \left(1 - \frac{1}{k} \right)^k. \tag{2.15}$$

The result follows since $\lim_{k \rightarrow \infty} \left(1 - \frac{1}{k} \right)^k = \frac{1}{e}$ and the fact that $\left(1 - \frac{1}{k} \right)^k$ is increasing in k . \square

Please refer to Goundan et al. [67], Calinescu et al. [68] and Vondrak [69] for a summary of related results on sub-modular function optimization over other families of constraint sets.

2.1.2 Sensor selection

In this section, we present a recent application of sub-modularity from Shamiah et al. [7] in developing efficient algorithms to approximately solve a sensor selection problem. The sensor selection problem can be described as follows. There are N sensors that form a network. All sensors in the system

observe a common phenomenon $\mathbf{x} \in \mathbb{R}^M$. The sensing or received signal model is

$$y_i = \mathbf{h}_i^T \mathbf{x} + n_i,$$

where n_i is additive white Gaussian noise such that $\mathbb{E}[n_i^2] = \sigma^2$, $\forall i$ and $\mathbb{E}[n_i n_j] = 0$, $i \neq j$. The signal is modelled as a zero-mean Gaussian random vector with $\mathbb{E}[\mathbf{x}\mathbf{x}^T] = \Sigma_x$. The channel follows the standard block fading model and is assumed known to the fusion center. The fusion center is interested in acquiring observations from only a subset of the sensors \mathcal{S} . More specifically, due to a constraint on the acquisition bandwidth, it is necessary for the queried set of sensors to satisfy $|\mathcal{S}| = k$.

Let $\mathbf{y}_{\mathcal{S}}$ denote the acquired observations. Then, the maximum *a posteriori* estimate of \mathbf{x} given $\mathbf{y}_{\mathcal{S}}$ is

$$\hat{\mathbf{x}} = \left(\sigma^{-2} \sum_{i \in \mathcal{S}} \mathbf{h}_i \mathbf{h}_i^T + \Sigma_x^{-1} \right)^{-1} \sum_{i \in \mathcal{S}} y_i \mathbf{h}_i.$$

The above estimate can also be shown to be optimal according to the minimum-mean-squared-error criterion. The estimation error $(\hat{\mathbf{x}} - \mathbf{x})$ under the above estimation criterion has a covariance matrix $\Sigma_{\text{map}}(\mathcal{S}) = (\sigma^{-2} \sum_{i \in \mathcal{S}} \mathbf{h}_i \mathbf{h}_i^T + \Sigma_x^{-1})^{-1}$. Often-used measures of quality in the sensor selection literature are mean radius of the error covariance matrix or the volume of its confidence ellipsoid. We refer the reader to [7, 144] for details about these metrics. Suffice it to say that these metrics are non-increasing functions of $\log \det(\Sigma_{\text{map}}(\mathcal{S}))$. Thus, it is of interest to solve the following problem

$$\max_{|\mathcal{S}|=k} \log \det \left(\sigma^{-2} \sum_{i \in \mathcal{S}} \mathbf{h}_i \mathbf{h}_i^T + \Sigma_x^{-1} \right),$$

which essentially finds the subset of sensors that minimize the error or provide maximum confidence. The authors [7] show that $\log \det (\sigma^{-2} \sum_{i \in \mathcal{S}} \mathbf{h}_i \mathbf{h}_i^T + \Sigma_x^{-1})$ is a monotone sub-modular function of \mathcal{S} . Thus, the constraint set can be rewritten $|\mathcal{S}| \leq k$ making it a uniform matroid. The greedy algorithm described in the previous section can hence be applied to solve this problem with an accuracy guarantee of $(1 - \frac{1}{e})$ according to Theorem 1.

2.2 Compressed sensing

The background in this section is most relevant to Chapter 5. Sparsity is naturally present or can be artificially induced in many real-world signals or data. It is this observation that prompted the development of the JPEG image compression scheme where the data (image in this case) is transformed into the frequency domain. In particular, the discrete cosine transform is used to create a sparse frequency map of the image owing to the fact that images predominantly contain low frequencies. For such settings, we are immediately charged with the task of storing this sparse data or signal using as little space as necessary. Thus, we are confronted twin goals which are clearly conflicting, that of low storage requirements along with the need to perfectly recovery the original data. As engineers, one immediately recognizes a tradeoff and asks the question “How small can we make the storage overhead while guaranteeing perfect recovery of our sparse signal?” In the sequel, we use the terms signal and data interchangeably.

Of course, an immediate and partial answer to this question would be

“It depends on the storage mechanism.”. The technique of *compressed sensing*, which has received tremendous interest in recent years, proposes a linear mechanism (that is independent of the signal) in that the acquired measurements are linear combinations of the sparse signal. Of course, the motivation for such a choice is clearly understood as simplicity of implementation. Mathematically, this can be written as

$$\mathbf{y} = \mathbf{M}\mathbf{x}, \quad (2.16)$$

where

$$\begin{aligned} \mathbf{x} \in \mathbb{R}^N & : \text{ signal or data, which has } S \text{ non-zero entries} \\ \mathbf{M} \in \mathbb{R}^{k \times N} & : \text{ sensing matrix} \\ \mathbf{y} \in \mathbb{R}^k & : \text{ acquired measurements.} \end{aligned} \quad (2.17)$$

Our twin goals can be re-phrased mathematically by saying that we are interested in recovering \mathbf{x} perfectly using any algorithm of our choice while using as few measurements k as possible. In some applications, we might be able to choose an appropriate sensing matrix \mathbf{M} while in some others such as the wireless application we will describe in Chapter 5, the sensing matrix will be provided by the underlying system. In either case, \mathbf{M} is assumed known as is \mathbf{y} . Given \mathbf{M} and \mathbf{y} , we would like to recover \mathbf{x} perfectly using any algorithm of our choice.

If $S = N$ or in other words, if there is no sparsity at all, then it is clear that one would need $k = \mathcal{O}(N)$ measurements in order to recover \mathbf{x} . A recover algorithm for this case would just be to perform matrix inversion. However, when $S \ll N$, can we do better?

In general, it has been shown that \mathbf{x} can be recovered perfectly using – what is arguably the most natural recovery algorithm one can think of – ℓ_0 -norm minimization. As this problem is combinatorial and NP-hard moreover, the natural convexification has been considered, where the $\|\cdot\|_0$ norm is replaced by its closest convex approximation, the $\|\cdot\|_1$ norm. It has been shown that \mathbf{x} can be recovered perfectly using ℓ_1 -norm minimization if the sensing matrix \mathbf{M} satisfies certain properties. Specifically, we can recover \mathbf{x} perfectly by solving the following ℓ_1 -norm minimization problem

$$\begin{aligned} & \text{minimize} && \|\mathbf{x}\|_1 \\ & \text{subject to} && \mathbf{M}\mathbf{x} = \mathbf{y} \end{aligned} \quad (2.18)$$

iff \mathbf{M} satisfies the *Null Space Property* (NSP), which will be defined later. These results, predominantly scattered across the statistics literature, are thus attractive from an algorithmic perspective as well.

Unfortunately, the NSP and other sufficient conditions such as the Restricted Isometry Property (RIP) that point to it are difficult to establish for any arbitrary deterministic matrix. This is where compressed sensing steps in. Recently, it was shown that it is possible to verify these conditions analytically for random matrices. The seminal papers by Donoho [10] and Cades et al. [11] show that Gaussian and Bernoulli matrices with independent, identically distributed (i.i.d.) entries satisfy the RIP with high probability when $k = \mathcal{O}(S \log N)$ thereby allowing for perfect recovery of \mathbf{x} through ℓ_1 -norm minimization (often called *Basis Pursuit* in the compressed sensing literature). Thus, by adopting a probabilistic selection rule, we buy ourselves analytical

guarantees on the goodness of these matrices. This initial result has given rise to a flurry of research activity over the last decade leading to many alternate recovery algorithms such as the greedy correlation approach [175], and the least absolute shrinkage and selection operator (LASSO) [177] given by

$$\text{minimize } \frac{1}{2} \|\mathbf{M}\mathbf{x} - \mathbf{y}\|^2 + \lambda \|\mathbf{x}\|_1. \quad (2.19)$$

The RIP has subsequently been proven for other random matrix ensembles such as sub-gaussian and sub-exponential ensembles [14, 18, 19, 21, 188]. To tie the above discussion back to the twin goals mentioned earlier, this means that perfect recovery with logarithmic storage is now possible for a large number of matrix distributions.

2.2.1 Mathematical preliminaries

We now step into the mathematical details. We define the null space property from Gribonval et al. [183]. Given a matrix \mathbf{M} , let $\mathcal{N}(\mathbf{M})$ denote its null space.

Definition (Null space Property): A matrix \mathbf{M} satisfies the null space property of order S if for all subsets $\mathcal{S} \subseteq \{1, 2, \dots, N\}$ with $|\mathcal{S}| \leq S$, the following holds

$$\|\mathbf{v}_{\mathcal{S}}\|_1 \leq \|\mathbf{v}_{\mathcal{S}^c}\|_1, \quad \forall \mathbf{v} \in \mathcal{N}(\mathbf{M}) \setminus \mathbf{0}.$$

where $\mathcal{S}^c = \{1, 2, \dots, N\} \setminus \mathcal{S}$. Based on this property, the following recovery result [183] has appeared both implicitly and explicitly in works such as [181, 184]. Let the support set of $\mathbf{x}(t)$ be denoted by \mathcal{S} . A vector $\mathbf{x}(t)$ is S -sparse if $|\mathcal{S}| \leq S$.

Theorem 2. Let $\mathbf{M} \in \mathbb{R}^{k \times N}$. Every S -sparse vector $\mathbf{x} \in \mathbb{R}^N$ is the solution to the ℓ_1 -norm minimization problem in (2.18) with $\mathbf{y} = \mathbf{M}\mathbf{s}$ iff \mathbf{M} satisfies the NSP of order S .

Proof [180]: Let every S -sparse vector be the solution to (2.18). In particular, let the generative S -sparse vector be \mathbf{v}_S where $S \subseteq \{1, 2, \dots, N\}$, $|S| = S$ and $\mathbf{v} \in \mathcal{N}(\mathbf{M})$. Then, the vector $-\mathbf{v}_{S^c}$ is also consistent with the set of observations because $\mathbf{M}\mathbf{v}_S = -\mathbf{M}\mathbf{v}_{S^c}$, which follows from the fact that $\mathbf{v} \in \mathcal{N}(\mathbf{M})$. Thus, $\|\mathbf{v}_S\|_1 < \|-\mathbf{v}_{S^c}\|_1 = \|\mathbf{v}_{S^c}\|_1$.

Assume the NSP of order S holds. Then let \mathbf{x} and \mathbf{z} be the *true* and *estimated* sparse vectors respectively that is consistent with the observations, i.e., $\mathbf{M}\mathbf{x} = \mathbf{M}\mathbf{z}$. Let the true support be $S = \text{support}(\mathbf{x})$. Then $\mathbf{x} - \mathbf{z} \in \mathcal{N}(\mathbf{M}) \setminus \mathbf{0}$. From the NSP, we can write

$$\begin{aligned}
\|\mathbf{x}\|_1 &= \|\mathbf{x} - \mathbf{z}_S + \mathbf{z}_S\|_1 \\
&\leq \|\mathbf{x} - \mathbf{z}_S\|_1 + \|\mathbf{z}_S\|_1 \text{ by the triangle inequality} \\
&= \|\mathbf{x}_S - \mathbf{z}_S\|_1 + \|\mathbf{z}_S\|_1 \text{ since } \mathbf{x} \text{ is } S\text{-sparse} \\
&= \|\mathbf{v}_S\|_1 + \|\mathbf{z}_S\|_1 \text{ by the definition of } \mathbf{v} \\
&\leq \|\mathbf{v}_{S^c}\|_1 + \|\mathbf{z}_S\|_1 \text{ by NSP} \\
&= \|-\mathbf{z}_{S^c}\|_1 + \|\mathbf{z}_S\|_1 \text{ since } \mathbf{x} \text{ is } S\text{-sparse} \\
&= \|\mathbf{z}\|_1.
\end{aligned} \tag{2.20}$$

□

The NSP is typically quite difficult to prove directly leading to the development of sufficient conditions that are easier to establish. One such sufficient condition is the *restricted isometry property* [186] that has become quite popular in recent years and is defined below.

Definition (Restricted Isometry Property): A matrix \mathbf{M} satisfies the Restricted Isometry Property (RIP) of order p if there exists $\epsilon_p(\mathbf{M}) \in (0, 1)$ such that

$$(1 - \epsilon_p(\mathbf{M}))\|\mathbf{v}_{\mathcal{T}}\|_2^2 \leq \|\mathbf{M}\mathbf{v}_{\mathcal{T}}\|_2^2 \leq (1 + \epsilon_p(\mathbf{M}))\|\mathbf{v}_{\mathcal{T}}\|_2^2, \quad \|\mathbf{v}\|^2 = 1 \quad (2.21)$$

holds for all sets \mathcal{T} with $|\mathcal{T}| \leq p$.

Here, $\epsilon_p(\mathbf{M})$ is called the *restricted isometric constant* of \mathbf{M} . The RIP essentially requires that all $k \times |\mathcal{T}|$ sub-matrices of \mathbf{M} be well-conditioned. Under such a conditioning, perfect recovery of \mathbf{x} is possible as described in the following theorem.

Theorem 3. [8] Let $\mathbf{M} \in \mathbb{R}^{k \times N}$. If \mathbf{M} satisfies the RIP with $\epsilon_{2S}(\mathbf{M}) \leq \frac{2(3-\sqrt{2})}{7} \approx 0.4531$, then every S -sparse vector $\mathbf{s} \in \mathbb{R}^N$ is the solution to the ℓ_1 -norm minimization problem in (2.18).

□

As the proof of the above theorem is quite involved, we will prove a weaker result from Rauhut [180] that uses mathematical machinery similar to that used in the proof of Theorem 21 above.

Theorem 4. [180] Let $\mathbf{M} \in \mathbb{R}^{k \times N}$. If \mathbf{M} satisfies the RIP with $\epsilon_{2S}(\mathbf{M}) \leq \frac{1}{3}$, then the NSP of order S is satisfied.

Proof: Let $\mathbf{v} \in \mathcal{N}(\mathbf{M})$. Let \mathcal{S}_o contain the S largest element of \mathbf{v} . Let \mathcal{S}_k , $k = 1, 2, \dots$ contain the S largest *absolute* elements of $\{1, \dots, N\} \setminus \bigcup_{i=0}^{k-1} \mathcal{S}_i$. Since

$\mathbf{v} \in \mathcal{N}(\mathbf{M})$, it follows that $\mathbf{A}\mathbf{v}_{\mathcal{S}_0} = -\mathbf{A}(\mathbf{v}_{\mathcal{S}_1} + \mathbf{v}_{\mathcal{S}_2} + \dots)$ and hence, from the RIP, we get

$$\begin{aligned}
\|\mathbf{v}_{\mathcal{S}_0}\|_2^2 &\leq \frac{1}{1-\varepsilon_S(\mathbf{M})} \|\mathbf{A}\mathbf{v}_{\mathcal{S}_0}\|_2^2 \\
&\leq \frac{1}{1-\varepsilon_{2S}(\mathbf{M})} \|\mathbf{A}\mathbf{v}_{\mathcal{S}_0}\|_2^2 \\
&= \frac{1}{1-\varepsilon_{2S}(\mathbf{M})} \mathbf{v}_{\mathcal{S}_0}^T \mathbf{M}^T \mathbf{M} (\mathbf{v}_{\mathcal{S}_1} + \mathbf{v}_{\mathcal{S}_2} + \dots) \\
&= \frac{1}{1-\varepsilon_{2S}(\mathbf{M})} \sum_i \mathbf{v}_{\mathcal{S}_0}^T \mathbf{M}^T \mathbf{M} \mathbf{v}_{\mathcal{S}_i} \\
&\leq \frac{1}{1-\varepsilon_{2S}(\mathbf{M})} \sum_i |\mathbf{v}_{\mathcal{S}_0}^T \mathbf{M}^T \mathbf{M} \mathbf{v}_{\mathcal{S}_i}|
\end{aligned} \tag{2.22}$$

where the second inequality follows from the fact that $\varepsilon_n(\mathbf{M})$ is non-decreasing in n .

We now argue that $|\mathbf{v}_{\mathcal{S}_0}^T \mathbf{M}^T \mathbf{M} \mathbf{v}_{\mathcal{S}_i}| \leq \varepsilon_{2S}(\mathbf{M}) \|\mathbf{v}_{\mathcal{S}_0}\|_2 \|\mathbf{v}_{\mathcal{S}_i}\|_2$. This is because

$$\begin{aligned}
\mathbf{v}_{\mathcal{S}_0}^T \mathbf{M}^T \mathbf{M} \mathbf{v}_{\mathcal{S}_i} &= [\tilde{\mathbf{v}}_{\mathcal{S}_0} \ \mathbf{0}_{\mathcal{S}_i}] \mathbf{M}_{\mathcal{S}_0 \cup \mathcal{S}_i}^T \mathbf{M}_{\mathcal{S}_0 \cup \mathcal{S}_i} [\tilde{\mathbf{v}}_{\mathcal{S}_i} \ \mathbf{0}_{\mathcal{S}_0}]^T \\
&= [\tilde{\mathbf{v}}_{\mathcal{S}_0} \ \mathbf{0}_{\mathcal{S}_i}] [\mathbf{M}_{\mathcal{S}_0 \cup \mathcal{S}_i}^T \mathbf{M}_{\mathcal{S}_0 \cup \mathcal{S}_i} - \mathbf{I}] [\tilde{\mathbf{v}}_{\mathcal{S}_i} \ \mathbf{0}_{\mathcal{S}_0}]^T.
\end{aligned} \tag{2.23}$$

The claim follows from standard inequalities concerning the matrix operator norm. Substituting this bound into (2.22), we get

$$\|\mathbf{v}_{\mathcal{S}_0}\|_2 \leq \frac{\varepsilon_{2S}(\mathbf{M})}{1-\varepsilon_{2S}(\mathbf{M})} \sum_{i \geq 1} \|\mathbf{v}_{\mathcal{S}_i}\|_2. \tag{2.24}$$

Now since *all* entries of $\mathbf{v}_{\mathcal{S}_{i-1}}$ are greater than $\mathbf{v}_{\mathcal{S}_i}$, it follows that

$$|v_j| \leq \frac{1}{S} \sum_{l \in \mathcal{S}_{i-1}} |v_l| \tag{2.25}$$

and hence $\|\mathbf{v}_{\mathcal{S}_i}\|_2 = \left(\sum_{j \in \mathcal{S}_i} |v_j| \right)^{\frac{1}{2}} \leq \frac{1}{\sqrt{S}} \|\mathbf{v}_{\mathcal{S}_{i-1}}\|_1$. From the Cauchy-Schwartz inequality

$$\begin{aligned}
\|\mathbf{v}_{\mathcal{S}_0}\|_1 \leq \sqrt{S} \|\mathbf{v}_{\mathcal{S}_0}\|_2 &\leq \frac{\varepsilon_{2S}(\mathbf{M})}{1-\varepsilon_{2S}(\mathbf{M})} \sum_{i \geq 1} \|\mathbf{v}_{\mathcal{S}_{i-1}}\|_1 \\
&= \frac{\varepsilon_{2S}(\mathbf{M})}{1-\varepsilon_{2S}(\mathbf{M})} [\|\mathbf{v}_{\mathcal{S}_0}\|_1 + \|\mathbf{v}_{\mathcal{S}_0^c}\|_1].
\end{aligned}$$

Since $\varepsilon_{2S}(\mathbf{M}) \leq \frac{1}{3}$, we get $\|\mathbf{v}_{s_0}\|_1 \leq \frac{1}{2}\|\mathbf{v}_{s_0^c}\|_1 \leq \|\mathbf{v}_{s_0^c}\|_1$ giving us the result. \square

Thus, the RIP with a sufficiently small constant immediately implies the NSP in the context of ℓ_1 -recovery. We are immediately confronted with the question “why is the RIP not a necessary condition as well in the context of ℓ_1 -recovery?”. This is because the RIP is extremely sensitive to left-multiplications. Consider multiplying the good sensing matrix by an invertible matrix that has a large condition number. This should not affect the recovery properties of the product matrix because the null spaces are invariant to invertible transformations. However, the condition number of the product matrix is quite large affecting adversely the RIP. This exposes a lack of robustness inherent in the RIP.

In fact, for the case when $\varepsilon_{2S}(\mathbf{M})$ is close to $\frac{1}{\sqrt{2}}$, Gribonval and Davies [9] have systematically constructed examples where all sparse vectors *cannot* be recovered. Surprisingly, for $\varepsilon_{2S}(\mathbf{M}) = 1$, they have constructed examples where all sparse vectors *can* indeed be recovered further illustrating the inherent weakness of the RIP in identifying the entire space of good sensing matrices.

As mentioned earlier, it was shown in the earlier part of the decade, that Gaussian and Bernoulli ensembles [10, 11] satisfy the RIP (with a sufficiently small RIP constant to enable ℓ_1 -recovery). Since then a number of other ensembles have been proven to lend themselves favourably to ℓ_1 -recovery. These

include i.i.d. ensembles with each matrix entry [21]¹ is given by

$$m_{ij} = \begin{cases} \sqrt{\frac{3}{N}}, & \text{w.p. } \frac{1}{3} \\ 0, & \text{w.p. } \frac{1}{3} \\ -\sqrt{\frac{3}{N}}, & \text{w.p. } \frac{1}{3} \end{cases},$$

Fourier ensembles [14] and i.i.d. sub-gaussian ensembles [13].

Recent research, which renders some of the above results special cases, includes matrices with:

- independent rows where each row is a correlated, Gaussian random vector (NSP) [15].
- independent rows where each row is a correlated, sub-gaussian random vector (NSP) [16].
- independent columns where each column is an uncorrelated, sub-gaussian random vector (RIP) [19, 188].
- independent rows/columns where each row is an uncorrelated, sub-exponential (heavy-tailed) random vector (RIP) [188].

We will reproduce two of these results along with proof sketches. In particular, we will present a recent result by Vershynin [188] that concerns matrices with independent rows where each row is an uncorrelated, sub-gaussian random vector. We will follow this up with a recent result by Vershynin [188] and

¹Achlioptas [21] proves that these ensembles make for good Johnson-Lindenstrauss (JL) embeddings. Baranuik et al. [12] subsequently provides the connection between JL-embeddings and the RIP.

Adamczyk et al. [19] that concerns matrices with independent columns where each column is an uncorrelated, sub-gaussian random vector. We present proof sketches instead of verbatim proof reproductions as the former would arguably be more useful for researchers that are looking for high-level summary of the pieces that constitute a typical RIP proof.

Before we summarize these recent RIP results, we present a primer on sub-gaussian and sub-exponential random variables along with some useful results from non-asymptotic matrix theory.

2.2.2 Useful concentration inequalities

We refer the reader to the tutorial paper by Vershynin [188] for a great introduction to non-asymptotic matrix theory. Lemmas 17-19 below are well-known past results that are summarized in this paper [188]. The proofs are not reproduced.

Lemma 2. *Let z be random variable. The following properties are equivalent with parameters $K_i > 0$ differing from each other by at most an absolute constant factor.*

- (i) *Tails:* $\Pr(|z| > t) \leq \exp(1 - \frac{t^2}{K_2})$ for all $t > 0$,
- (ii) *Moments:* $(\mathbb{E}[|z|^p])^{\frac{1}{p}} \leq K_2 \sqrt{p}$ for all $p \geq 1$,
- (iii) *Super-exponential moment:* $\mathbb{E}\left[\exp\left(\frac{z^2}{K_3}\right)\right] \leq e$.

Moreover, if $\mathbb{E}[z] = 0$ then properties (i)-(iii) are also equivalent to the following one:

- (iv) *Moment generating function:* $\mathbb{E}[\exp(tz)] \leq \exp(t^2 K_4)$ for all $t \in \mathbb{R}$.

□

A random variable that satisfies the above property is called a *sub-gaussian* random variable. Such random variables are often characterized by the ψ_2 -norm², which is defined as

$$\|z\|_{\psi_2} = \sup_{p \geq 1} \frac{(\mathbb{E}[|z|^p])^{\frac{1}{p}}}{\sqrt{p}}. \quad (2.26)$$

It follows that if the ψ_2 -norm of z is finite, then z is a sub-gaussian random variable with $\|z\|_{\psi_2} = K_2$. This is the case for bounded random variables with symmetric distributions.

Lemma 3. *Let z be a symmetrically distributed, bounded random variable with $|z| \leq M$, $M > 0$. Then, \mathbf{z} is a sub-gaussian random variable with $\|z\|_{\psi_2} \leq cM^2$, $c > 0$.*

□

Next, we present a large-deviations result for sums of independent, centered, sub-gaussian random variables.

Lemma 4. *Let $\{z_i\}_{i=1}^M$ be a collection of independent, zero-mean, sub-gaussian random variables with $\psi_{\max, z} = \max_i \|z_i\|_{\psi_2}$. Then, for every $\mathbf{a} \in \mathbb{R}^M$ and every $t > 0$, we have*

$$\Pr\left(\left|\sum_{i=1}^M a_i z_i\right| > t\right) \leq \exp\left(-\frac{ct^2}{\psi_{\max, z}^2 \|\mathbf{a}\|_2^2}\right).$$

²Alternate definitions of this norm have been adopted (such as in [19]) that are all equivalent to within a constant factor.

□

In higher dimensions, a random vector \mathbf{z} of dimension M is called sub-gaussian if $\mathbf{z}^T \mathbf{x}$ is sub-gaussian for every $\mathbf{x} \in \mathbb{R}^M$.

Lemma 5. *Let $\{z_i\}_{i=1}^M$ be a collection of independent, zero-mean, sub-gaussian random variables. Then, \mathbf{z} is a sub-gaussian random vector with $\|\mathbf{z}\|_{\psi_2} = C \max_i \|z_i\|_{\psi_2}$.*

□

One can make a similar characterization of sub-exponential random variables through the following lemma.

Lemma 6. *Let z be random variable. The following properties are equivalent with parameters $K_i > 0$ differing from each other by at most an absolute constant factor.*

- (i) *Tails:* $\Pr(|z| > t) \leq \exp(1 - \frac{t}{K_2})$ for all $t > 0$,
- (ii) *Moments:* $(\mathbb{E}[|z|^p])^{\frac{1}{p}} \leq K_2 p$ for all $p \geq 1$,
- (iii) *Super-exponential moment:* $\mathbb{E}\left[\exp\left(\frac{z}{K_3}\right)\right] \leq e$.

□

A random variable that satisfies the above property is called a *sub-exponential* random variable. The ψ_1 -norm of z is defined as

$$\|z\|_{\psi_1} = \sup_{p \geq 1} \frac{(\mathbb{E}[|z|^p])^{\frac{1}{p}}}{p}. \quad (2.27)$$

This immediately brings us to the next two lemmas, which explore the connection between sub-gaussian and sub-exponential random variables.

Lemma 7. z is a sub-gaussian random variable if and only if z^2 is a sub-exponential random variable. Furthermore, we have that $\|z\|_{\psi_2}^2 \leq \|z^2\|_{\psi_1} \leq 2\|z\|_{\psi_2}^2$.

□

The following lemma contains a large-deviations result for a sum of sub-exponential random variables.

Lemma 8. Let $\{z_i\}_{i=1}^M$ be a collection of independent, zero-mean, sub-exponential random variables and let $\psi_{\max,z} = \max_i \|z_i\|_{\psi_1}$. Then,

$$\Pr\left(\left|\sum_{i=1}^M z_i\right| > t\right) \leq \exp\left(-c \min\left\{\frac{t^2}{\psi_{\max,z}^2}, \frac{t}{\psi_{\max,z}}\right\}\right).$$

□

We are now ready to discuss the recent RIP results for matrices with independent, sub-gaussian columns and rows. Before we move on to this task, we require one more definition. A random vector \mathbf{m} of dimension M is called *isotropic* if $\mathbb{E}[|\mathbf{m}^T \mathbf{x}|^2] = \|\mathbf{x}\|^2$ for all $\mathbf{x} \in \mathbb{R}^M$.

2.2.3 Recent RIP Results

Typically, RIP proofs use the concept of ε -nets, which is defined as follows in the context of the unit sphere in Euclidean space:

Definition (Nets): Let U^{N-1} denote the unit sphere in \mathbb{R}^N . Then, a subset $\mathcal{N}_\varepsilon(N)$ is called an ε -net of U^{N-1} if for every $\mathbf{x} \in U^{N-1}$, we can find a point

$\mathbf{y} \in \mathcal{N}_\varepsilon$ such that $\|\mathbf{x} - \mathbf{y}\|_2 \leq \varepsilon$.

This brings us to the natural question “what is the minimum size of $\mathcal{N}_\varepsilon(N)$?”. This is called the *covering number* of U^{N-1} , denoted $CN(N, \varepsilon)$. This is answered in the following lemma [188]. The proof follows from standard Euclidean volume arguments and is not reproduced.

Lemma 9. *For every $\varepsilon > 0$, we have that*

$$CN(U^{N-1}, \varepsilon) \leq \left(1 + \frac{2}{\varepsilon}\right)^N.$$

□

We first present the result concerning matrices with independent, sub-gaussian rows. This result will be used to prove the subsequent result concerning matrices with independent, sub-gaussian columns. We essentially combine Theorem 39 and Theorem 64 from Vershynin [188].

Theorem 5. *(Sub-gaussian rows) Let $\tilde{\mathbf{M}} = \frac{1}{\sqrt{k}}\mathbf{M}$ be a $k \times N$ matrix containing independent, isotropic, sub-gaussian rows with worst-case sub-gaussian norm $\psi_{\max, m}$. Then, $\tilde{\mathbf{M}}$ satisfies for every $1 \leq S \leq \min\{k, N\}$, and every number $\varepsilon \in (0, 1)$:*

$$\text{if } k \geq C_{\psi_{\max, m}} \varepsilon^{-2} S \log\left(\frac{N}{S}\right) \text{ then } \varepsilon_S(\tilde{\mathbf{M}}) \leq \varepsilon$$

with probability at least $1 - 2\exp(-c_{\psi_{\max, m}} \varepsilon^2 k)$. Here, $c_{\psi_{\max, m}}$ and $C_{\psi_{\max, m}}$ depend only the worst-case sub-gaussian norm $\psi_{\max, m}$.

Proof sketch: The proof has three steps essentially:

Step 1: First, it proves the concentration $(1 - \varepsilon)\|\mathbf{x}_{\mathcal{T}}\|_2^2 \leq \|\mathbf{M}_{\mathcal{T}}\mathbf{x}_{\mathcal{T}}\|_2^2 \leq (1 + \varepsilon)\|\mathbf{x}_{\mathcal{T}}\|_2^2$ for a *particular choice* of subset \mathcal{T}^* and *any arbitrary vector* $\mathbf{x}_{\mathcal{T}^*} \in \mathbb{R}^{|\mathcal{T}^*|}$, $\|\mathbf{x}_{\mathcal{T}^*}\|_2^2 = 1$. This is established using the fact that $\|\mathbf{M}_{\mathcal{T}^*}\mathbf{x}_{\mathcal{T}^*}\|_2^2 = \frac{1}{k} \sum_{i=1}^k |\mathbf{m}_i^T \mathbf{x}_{\mathcal{T}^*}|^2$, where $\{\mathbf{m}_i\}$ are the rows of $\mathbf{M}_{\mathcal{T}^*}$, is a sum of independent, sub-exponential random variables. This follows from Lemma 7 and the fact that $\mathbf{m}_i^T \mathbf{x}_{\mathcal{T}^*}$ is a sub-gaussian random variable for each vector $\mathbf{x}_{\mathcal{T}^*} \in \mathbb{R}^{|\mathcal{T}^*|}$, $\|\mathbf{x}_{\mathcal{T}^*}\|_2^2 = 1$. Since we have a sum of independent, sub-exponential random variables, we can apply Lemma 8 to obtain a concentration.

Step 2: Now for the same fixed subset \mathcal{T}^* , we would like to show a concentration *for all* $\mathbf{x}_{\mathcal{T}^*} \in \mathbb{R}^{|\mathcal{T}^*|}$, $\|\mathbf{x}_{\mathcal{T}^*}\|_2^2 = 1$. The immediate use of the union bound is precluded since the space is uncountable. Thus, we turn to the concept of ε -nets. The idea here is if the concentration holds for every point in the ε -net of the sphere, then the concentration holds for the entire sphere since the net represents – within a distance of ε – all points of the sphere. More specifically, we can determine a worst-case magnification factor $\beta > 0$ such that $\sup_{\|\mathbf{z}\|=1} \left| \frac{1}{k} \|\mathbf{M}_{\mathcal{T}^*}\mathbf{z}\|_2^2 - 1 \right| \leq \beta \max_{\mathbf{z} \in \mathcal{N}_\varepsilon(|\mathcal{T}^*|)} \left| \frac{1}{k} \|\mathbf{M}_{\mathcal{T}^*}\mathbf{z}\|_2^2 - 1 \right|$. By Lemma 9, the condition number of the ε -net of a sphere and hence $|\mathcal{N}_\varepsilon(|\mathcal{T}^*|)|$ is finite allowing us to apply the union bound over the points contained in the net to

compute an exponential bound on

$$\begin{aligned} & \Pr \left(\beta \max_{\mathbf{z} \in \mathcal{N}_\varepsilon(|\mathcal{T}^*|)} \left| \frac{1}{k} \|\mathbf{M}_{\mathcal{T}^*} \mathbf{z}\|_2^2 - 1 \right| \geq \delta \right) \\ & \leq |\mathcal{N}_\varepsilon(|\mathcal{T}^*|)| \Pr \left(\kappa \left| \frac{1}{k} \|\mathbf{M}_{\mathcal{T}^*} \mathbf{z}\|_2^2 - 1 \right| \geq \delta \right) \end{aligned} \quad (2.28)$$

where $\kappa > 0$ is a constant.

Step 3: As the final step, we remove the *conditioning* on a specific set \mathcal{T}^* by applying the union bound on (2.28) over all sets $|\mathcal{T}| \leq S$. Note that there are $\binom{N}{S} \leq \left(\frac{eN}{S}\right)^S$ of them. \square

In order to present the result concerning matrices with independent sub-gaussian columns, we require the following decoupling technique for double arrays [22, 188]. The lemma essentially estimates the sum of a double array in terms of the sum across disjoint subsets of the array.

Lemma 10. *Consider a matrix \mathbf{M} with zeroes on the diagonal, i.e. $m_{ii} = 0$. Then,*

$$4 \min_{\mathcal{T} \in \{1, \dots, N\}} \sum_{i \in \mathcal{T}, j \in \mathcal{T}^c} a_{ij} \leq \sum_{i, j} a_{ij} \leq 4 \max_{i \in \mathcal{T} \in \{1, \dots, N\}} \sum_{i \in \mathcal{T}, j \in \mathcal{T}^c} a_{ij}.$$

\square

Theorem 6. (*Sub-gaussian columns*) *Let \mathbf{M} be a $k \times N$ matrix whose columns \mathbf{m}_i are independent, isotropic, zero-mean, sub-gaussian random vectors in \mathbb{R}^k with $\psi_{\max, m} = \max_i \|\mathbf{m}_i\|_{\psi_2}$. The columns satisfy the norm-concentration property $\|\mathbf{m}_i\|_2^2 = k$ almost surely. Let $\tilde{\mathbf{M}} = \frac{1}{\sqrt{k}} \mathbf{M}$ be the normalized version. Then, $\tilde{\mathbf{M}}$ satisfies for every $1 \leq S \leq \min\{k, N\}$, and every number $\varepsilon \in (0, 1)$:*

$$\text{if } k \geq C_{\psi_{\max, m}} \varepsilon^{-2} S \log \left(\frac{N}{S} \right) \text{ then } \varepsilon_S(\tilde{\mathbf{M}}) \leq \varepsilon$$

with probability at least $1 - 2\exp(-c_{\psi_{\max,m}}\varepsilon^2k)$. Here, $c_{\psi_{\max,m}}$ and $C_{\psi_{\max,m}}$ depend only the worst-case sub-gaussian norm $\psi_{\max,m}$.

Proof sketch: The proof has three main steps:

Step 1: As with the previous proof, it is sufficient to prove a concentration for a fixed vector in the ε -net, $\mathbf{x} \in \mathcal{N}_\varepsilon(|\mathcal{T}^*|)$, and for a fixed subset \mathcal{T}^* .

Step 2: For such a fixed $\mathbf{x} \in \mathcal{N}_\varepsilon(|\mathcal{T}^*|)$, we can write

$$\frac{1}{k} \|\mathbf{M}\mathbf{x}\|_2^2 = \frac{1}{k} \sum_{i=1}^N \|\mathbf{m}_i\|_2^2 x_i^2 + \frac{1}{k} \sum_{i=1}^N \sum_{j=1, i \neq j}^N \mathbf{m}_i^T \mathbf{m}_j x_i x_j.$$

Note that in contrast to the earlier proof sketch, we have replaced $\mathbf{x}_{\mathcal{T}^*}$ with \mathbf{x} for simplicity of exposition. It should be understood that \mathbf{x} is of dimension $|\mathcal{T}^*|$. By assumption, $\|\mathbf{m}_i\|_2^2 = k$ a.s. and $\|\mathbf{x}\|_2^2 = 1$. Substituting these assumptions in the above expression, we get

$$\left| \frac{1}{k} \|\mathbf{M}\mathbf{x}\|_2^2 - 1 \right| = \frac{1}{k} \left| \sum_{i=1}^N \sum_{j=1, i \neq j}^N \mathbf{m}_i^T \mathbf{m}_j x_i x_j \right| = \mathbf{x}^T \mathbf{G}_0 \mathbf{x}.$$

where \mathbf{G}_0 the off-diagonal part of the Gram matrix $\mathbf{M}^T \mathbf{M}$ with zeros on the diagonal. The elements of $\mathbf{x}^T \mathbf{G}_0 \mathbf{x}$ are not independent. As a first step towards *manufacturing* independence (and hence analytical tractability), we apply Lemma 10 to bound $\mathbf{x}^T \mathbf{G}_0 \mathbf{x}$ in terms of a sum over elements (i, j) where i and j come from disjoint sets. This gives us the following bound

$$\left| \frac{1}{k} \|\mathbf{M}\mathbf{x}\|_2^2 - 1 \right| = \mathbf{x}^T \mathbf{G}_0 \mathbf{x} \leq \frac{4}{k} \max_{v \subseteq \{1, \dots, N\}} |R_v(\mathbf{x})|.$$

where $R_{\mathcal{V}}(\mathbf{x}) = \sum_{i \in \mathcal{V}} \sum_{j \in \mathcal{V}^c} \mathbf{m}_i^T \mathbf{m}_j x_i x_j$ is the sum of correlations over disjoint sets. Note that our goal is prove an exponential bound on

$$\Pr \left(\frac{4}{k} \max_{\mathcal{V} \subseteq \{1, \dots, N\}} |R_{\mathcal{V}}(\mathbf{x})| \geq \varepsilon \right).$$

Since the number of subsets $\mathcal{V} \subseteq \{1, \dots, N\}$ is finite, we can apply the union bound and hence focus our attention on

$$\Pr \left(\frac{4}{k} |R_{\mathcal{V}}(\mathbf{x})| \geq \varepsilon \right)$$

instead.

Step 3: In the second and final step towards obtaining a sum of independent terms, we condition on a realization of vectors $\{\mathbf{m}_i\}_{i \in \mathcal{V}^c}$ and re-write the sum of correlations as

$$R_{\mathcal{V}}(\mathbf{x}) = \sum_{i \in \mathcal{V}} x_i \mathbf{m}_i^T \mathbf{z} \text{ where } \mathbf{z} = \sum_{j \in \mathcal{V}^c} x_j \mathbf{m}_j.$$

Upon conditioning, \mathbf{z} is fixed and hence $R_{\mathcal{V}}(\mathbf{x})$ now contains a sum of independent correlations. Furthermore, $\{\mathbf{m}_i^T \mathbf{z}\}_{i=1}^N$ is a set of independent, centered, sub-gaussian random variables and thus, we can form an exponential bound on

$$\Pr \left(\frac{4}{k} |R_{\mathcal{V}}(\mathbf{x})| \geq \varepsilon \mid \{\mathbf{m}_i\}_{i \in \mathcal{V}^c} \right)$$

by applying Lemma 4. Removing the conditioning on $\{\mathbf{m}_i\}_{i \in \mathcal{V}^c}$ is the final step, which is straightforward and will not hurt the exponential bound. \square

On comparing the above two RIP results for matrices with independent rows and columns respectively, one observes that the latter result requires a

concentration of the norm of each column. This additional assumption is required since the singular values of a matrix \mathbf{M} can be bounded as [188]

$$\min_i \|\mathbf{m}_i\| \leq \sigma_{\min}(\mathbf{M}) \leq \sigma_{\max}(\mathbf{M}) \leq \max_i \|\mathbf{m}_i\|.$$

This concludes the background section on optimization techniques. We now move on to the applications of such techniques to solve some important design problems in the field of wireless networks.

Chapter 3

Feedback allocation with slow data scheduling

In this chapter, we consider a cellular uplink problem where the base station has a fixed feedback budget, which it has to allocate across the users it is serving in an orthogonal manner. The feedback bandwidth allocated to a user determines the effective transmission rate seen by the user. The current state-of-the-art allocates an equal amount of feedback bandwidth to each user. We propose computationally-efficient dynamic feedback allocation algorithms that adapt to system parameters such as arrival rate and channel quality to improve the throughput of the system.

3.1 Introduction

In many currently-implemented wireless standards, channel state information (CSI) is fed back by the receiver to the transmitter to allow for the latter to adapt its transmit strategy. This includes power and rate adaptation, which is known to increase capacity over the case when there is no CSI at the transmitter (CSIT) and precoder adaptation for a fixed transmission rate in the case of multiple-input-multiple-output (MIMO) systems, which can be used to increase link reliability. Current state-of-the-art opportunistic

scheduling algorithms such as multi-user diversity and proportional fairness assume the availability of CSIT through feedback, thus allowing for the transmitters to adapt their respective transmission strategies as a function of their link quality and other network state information. An important example is multi-user diversity downlink scheduling. Here, the user with the best channel is scheduled in each time slot and the base station transmits (ideally) at the Shannon capacity of its link to that user. It is well-known (Sharif and Hassibi [26]) that for this scheduling policy, the sum-rate scales as $\Omega(\log \log K)^1$, where K is the number of users. However, as noted by Huang et al. [27] this increase comes with a linear increase in feedback rate. This observation has motivated the development of limited feedback techniques. Past literature on limited feedback, reviewed next, can be broadly classified into techniques for point-to-point links and for multi-user systems, with some overlap between the two.

The impact of limited feedback on the performance of MIMO point-to-point wireless links has been studied extensively. For a comprehensive survey of the current state-of-the-art in limited feedback techniques for point-to-point links, refer to the tutorial paper by Love et al. [79]. Two popular techniques are Grassmannian Quantization and Random Vector Quantization (RVA). The former [76] explores the merits of quantization on the Grassmann manifold. According to the latter technique [30,31], a codebook is constructed

¹ $f(n) = \mathcal{O}(g(n))$ if $\exists \bar{n}$ and $c_1 > 0$ such that $f(n) \leq c_1 g(n)$, $\forall n \geq \bar{n}$; $f(n) = \Omega(g(n))$ if $f(n) = \mathcal{O}(g(n))$ and $\exists \bar{n}$ and $c_2 > 0$ such that $f(n) \geq c_2 g(n)$, $\forall n \geq \bar{n}$.

by throwing points uniformly at random on the surface of a complex unit sphere. Bounds have been derived on some suitably-chosen measure of distortion [30, 31, 34–37, 76–78].

A parallel body of work [80–82] focuses on developing limited feedback protocols for multi-user systems. Here, past research efforts can be sub-divided into two categories. Work in the first category focuses on traditional single-antenna downlink orthogonal frequency-division multiple-access systems. Chen et al. [80] and Sanayei et al. [82] propose a limited feedback scheme where each user, with associated priority, is restricted to a feedback budget of one bit per tone, i.e., each user transmits a bit that indicates whether its channel is above a certain threshold. Given a set of users with good channels, the base station schedules the user with the highest priority on each tone. The authors compute thresholds that achieve the optimal tradeoff between feedback rate and data rate for this class of data and feedback scheduling policies. While the above work assumes that the feedback window has number of slots equal to the product of the number of users and tones, Agarwal et al. [81] relax this assumption by considering feedback windows of arbitrary size. They propose an opportunistic feedback scheme where a user contends for a feedback slot if their channel strength is greater than a pre-set threshold. Work in the second category focuses on limited feedback for MIMO multiple-access systems. Jindal [83] investigates the impact of finite rate feedback on a downlink space-division multiple-access network where a multiple-antenna base-station serves a number of single-antenna users. This work assumes that

the number of users is equal to the number of antennas at the base-station and that the latter uses a zero-forcing precoding transmission policy to simultaneously serve all users. Jindal shows that when each mobile uses an RVQ codebook, the feedback budget needs to scale linearly in the signal-to-noise-ratio in order to achieve the full multiplexing gain (equal to the number of users) offered by the channel. Huang et al. [84] study the ergodic sum-rate performance for a space-division multiple-access system that uses the *per-user unitary rate control* joint scheduling and feedback protocol (defined therein). The authors calculate the sum-rate scaling of this protocol in the number of users and antennas. Unlike time-division-duplexing networks where channel reciprocity cannot be exploited, explicit feedback for the uplink is required for current and future standards (such as Long Term Evolution) that employ frequency-division-duplexing (FDD), thus motivating limited feedback research specifically dealing with the uplink. Dai et al. [85] consider a MIMO uplink where the base-station obtains the channel perfectly for each user and feeds back (broadcasts) an index that maps to a collection of transmit covariance matrices, each for one mobile in the network. The mobile then uses this covariance matrix to design its Gaussian vector codeword. The quantizer design problem that they formulate is as follows: given a constraint on the number of quantization states (or feedback rate equivalently), they seek to find the optimal quantization policy that maximizes the ergodic sum-rate. As this problem is too difficult to solve in its most general form, Dai et al. [85] restrict their attention to a sub-optimal strategy as applicable to a scenario

where all users employ single-stream beamforming/combining, thus requiring knowledge of the right singular vector of the channel. The quantization codebook is a composite Grassmannian matrix and given a set of right singular vectors across the users, the base-station chooses an index or quantization point such that the sum-squared chordal distance is minimized. Jorswieck et al. [86] consider a MIMO successive interference cancellation uplink scheme where each mobile uses transmit precoding along with orthogonal-frequency-division-multiplexing. Here, the authors propose a limited feedback protocol that involves reducing the number of precoding matrices, which ideally would be equal to the number of sub-carriers.

While the aforementioned literature considers feedback strategies that are primarily *static* in nature, *dynamic* or *adaptive* feedback bandwidth control (that adapt to the current *state* of the system) has been recognized by Love et al. [79] as a promising future direction in limited feedback research. Zakhour and Gesbert take a first stride in this direction in a series of papers [45, 46] where they propose an adaptive feedback allocation strategy for a downlink system where the base station serves a subset of users (equal to the number of transmit antennas) using multi-user zero-forcing transmissions. The subset of users is chosen based on limited feedback that it receives during the initial control segment of the time slot. The users are allowed to adapt the quality of their feedback during this control segment, i.e., a user would provide higher-quality feedback if it anticipates being scheduled during this time slot. They essentially seek to design a channel-adaptive feedback scheme that maximizes

the expected throughput under an average feedback constraint. As the optimization is difficult to solve, they propose effective sub-optimal solutions to the problem without guarantees on accuracy.

In this chapter, we develop dynamic feedback allocation policies for the uplink of a cellular system. Fig. 3.1 depicts the uplink of an FDD cellular network where the base station serves multiple mobiles or users and has a limited feedback budget represented as a maximum number of feedback bits to communicate a transmit strategy to all users. Feedback allocation is necessary because limited feedback induces errors that predominantly stem from quantization and delay². Thus, for the uplink scenario under consideration, if the network objective is rate fairness across users for instance, then a user with a poor channel would demand more accurate CSIT. On the contrary, if the objective is sum-rate maximization, a stronger user might be provided with greater CSIT accuracy. More importantly, as a consequence of the total feedback constraint and independent of the choice of objective, the post-feedback uncertainties in CSIT (and hence throughputs) become coupled across the users even in the case when they transmit data on orthogonal channels.

A general transmission policy is a map from the entire content of the feedback packet to a collection of transmission strategies across users. Ide-

²Quantization error is encountered during the process of estimating the channel at the receiver and mapping it to a set of bits or states in order to be sent back to the transmitter. Delay error is due to the fact that the signal passing through the feedback channel is received at the transmitter after some delay depending on the user's location and the fact that the true channel might have changed over this period.

ally, this map should be selected dynamically as a function of the system state. However, very little work has gone into this approach, which requires high-dimensional optimization rendering it intractable as recognized by Dai et al. [85]. Thus, we focus on policies that partition the feedback broadcast packet into smaller chunks, each intended for one user. The partition is adapted based on the state of the system. We pursue this intuitively appealing partitioning approach in the interest of analytical tractability and implementability. Henceforth, all claims of optimality are with respect to this space of partitioning policies. A parallel, independent effort by Ouyang and Ying [163] considers OFDMA downlink with a similar partitioning model. In particular, each user reports CSI for at most F_i bands such that $\sum_{i=1}^N F_i \leq F$. This work assumes that all wireless links can be modelled as ON-OFF channels. In each time slot, the proposed Longest-Queue-First Feedback Allocation (LQF-FA) policy computes the optimal feedback partition $\{F_i^*\}$ as one that maximizes the queue-weighted expected throughput. A greedy algorithm is developed that solves the queue-weighted throughput maximization under a mean-field approximation on the channel without guarantees on accuracy.

Our work differs fundamentally from Ouyang and Ying [163] in that we have full observability of the channel and queue state in the uplink and are concerned with how to control the quality of CSIT that we distribute back to the users. This has not been considered before to the best of our knowledge. On the other hand, Ouyang and Ying [163] are interested in acquisition of partial CSI from the users, which is more applicable to the downlink. Further-

more, we deal extensively with the question of computational complexity by proposing a variety of algorithms with analytical guarantees on accuracy. The

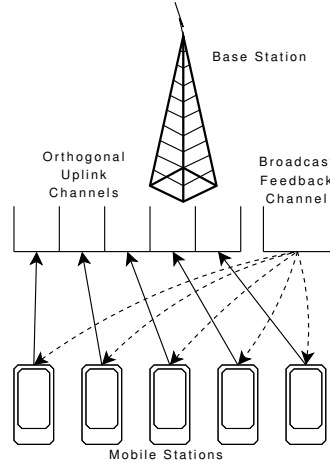


Figure 3.1: FDD Cellular uplink where the base-station has a feedback link to each user.

main contributions of this chapter are the following:

1. We propose a theoretical framework for limited feedback in cellular uplink that models this coupling in throughput performance across users. The scheme proposed by Jorswieck et al. [86] is a special case of our framework, as will be described later in Section 5.1.
2. Optimal – randomized and history-dependent online – multi-user feedback scheduling policies are designed for two long-term network objectives.
 - (a) Queue stability: This classical network objective [48, 52] is applicable to queueing systems where each user does not have infinitely

back-logged data to transmit, henceforth referred to as *unsaturated* systems.

- (b) Utility maximization: This second objective applies to systems that have infinitely back-logged data, called *saturated* systems [53].

Optimal throughput regions are determined in the process.

3. The optimal randomized policy can be obtained by solving a convex optimization problem with linear constraints and with an exponentially large number of variables. An optimal history-dependent online policy, which involves solving a weighted sum-rate maximization problem at each scheduling time slot, is presented as an alternative. The latter policy has the added advantage of not requiring *a priori* knowledge of the arrival rates in unsaturated systems.

While the above contributions introduce the proposed theoretical framework and the types of scheduling policies of interest for multi-user limited feedback in the uplink, implementability of these policies is an equally-critical design requirement. In light of this, the remaining contributions deal exclusively with the topic of computation complexity, which is the primary focus of this chapter. Here, we present a host of practical algorithms to solve the online optimization that explore the tradeoff between computational efficiency, accuracy, and required structure of the weighted sum-rate function. Following the seminal work on link schedul-

ing by Tassiulus and Ephremedis [48] where they show that throughput optimality can be achieved by solving a maximum-weight independent set problem at each scheduling time slot, there has long been immense interest in finding polynomial-time solutions to this problem for special cases. This has resulted in a variety of algorithmic approaches over the last decade (see eg. [49, 50] and references therein) for specific network structures. Prior to this work and the parallel contributions by Ouyang and Ying [163], the maximum-weight independent set problem has not been considered in the context of feedback allocations, to the best of our knowledge.

4. Notwithstanding the exponential size of the space of all possible feedback allocations, we develop a dynamic programming algorithm that solves the weighted sum-rate maximization with pseudo-polynomial complexity in the number of users and in the total feedback bit budget. This approach is exact and requires no assumptions on the structure of the weighted sum-rate function.
5. We show that in many practical wireless systems, the weighted sum-rate is non-decreasing and sub-modular. Using this observation, we then leverage sub-modular optimization results from combinatorial optimization (e.g. [67–69]) and propose a reduced-complexity feedback allocation algorithm with a multiplicative approximation guarantee of $(1 - \frac{1}{e})$.
6. Single-stream multiple-input-multiple-output beamforming and combin-

ing is being considered as a potential transmission mode in the Long Term Evolution standard [54]. For such systems, we show that when the popular RVQ codebooks are used, we are able to reduce the complexity even further. We provide additive approximation guarantees for this algorithm.

The rest of this chapter is organized as follows. In Section 3.2, we introduce the system model for multi-user feedback scheduling. In Section 3.3, we discuss the two long-term objectives that drive our choice of scheduling policies. We present a convex optimization approach to compute the throughput-optimal randomized feedback allocation policy, introduce an alternate throughput-optimal online feedback policy and provide a result useful later when we obtain approximate but computationally more efficient online feedback allocation schemes. In Section 3.4, we solve the optimal online feedback optimization problem for both objectives while in Section 3.5, we investigate methods of reducing the complexity of the optimal online optimization problem by exploiting more structure of the objective function. Section 3.6 contains a numerical study of the performance of some of the proposed algorithms. Concluding remarks are made in Section 3.7.

3.2 System model

Consider the uplink of a slotted-time cellular system with K users scattered across a cell. Each user-base-station channel is modeled as a finite-state

discrete-time process where the composite channel across users (in appropriate units) at time t , $\mathbf{m}[t]$, takes values in set \mathcal{M} , $|\mathcal{M}| = M$. For example, if we model all the channels as Gilbert-Eliot (or ON-OFF channels), then $\mathcal{M} = \{0, 1\}^K$. We assume that the base-station has perfect knowledge of the channel state $\mathbf{m}[t]$ in every time slot. Each user transmits on a separate frequency band thereby removing the need for data scheduling, since the focus of this work is primarily on feedback scheduling. To this effect, we assume that the base station has an error-free control channel that is broadcast in nature, which it uses for feedback purposes. Each feedback packet has a total size B bits and is intended to carry quantized channel state information back to all users. The base station has to allocate $b_k, k = 1, \dots, K$, bits of each feedback packet to user k such that $\sum_{k=1}^K b_k \leq B$. Let $\mathcal{B} = \{\mathbf{b} \in \mathbb{N}_0^K : \sum_{k=1}^K b_k \leq B, B \in \mathbb{N}\}$ represent the set of allowable bit allocation vectors. In each time slot, the base station decides on a bit allocation that it will use to form the feedback packet. An insufficiently large budget B will lead to loss of information in the quantization process. In addition to quantization effects, we assume the presence of delay in the feedback link, the combination of which motivates the following general transmission model. In channel state $\mathbf{m} \in \mathcal{M}$, user k chooses its transmission rate $\mu_k(m_k, b_k) \in \mathbb{R}_+$ based on the bit allocation b_k , the quantized CSIT that it receives and its inherent tendency towards tolerating outage or packet drops. Since we assume that maximum tolerable outage probability remains fixed over the entire period that the user is in the system, we do not explicitly include it in the functional

definition of rate $\mu_k(m_k, b_k)$. We assume that the channel process $\{\mathbf{m}[t]\}$ is an ergodic Markov chain and that the feedback link has zero-delay, for simplicity. The limited feedback policy proposed by Jorswieck et al. [86] falls within our framework since their protocol allocates an equal number of bits to each user, i.e. $b_k = \frac{B}{K}$, and given b_k bits, a user transmits at a rate that is determined by the collection of precoding matrices it is assigned by the base-station according to some utility. The above model can also account for delayed feedback with independent and identically distributed (i.i.d.) channels. Here, the user would choose a transmission rate according the distribution of the current channel state conditioned on the delayed channel information received through the feedback link.

3.3 Long-term network objectives

In Sections 3.3.1 and 3.3.2, we define the two objectives that we briefly introduced earlier – queue stability and utility maximization – and justify the use of SSS policies, which are randomized policies by definition, to characterize the system rate region for each objective. In the context of feedback, such a characterization has not been made in the past to the best of our knowledge. This characterization immediately allows for the computation of an optimal randomized scheduling policy (under either objective) by solving a convex optimization problem with linear constraints, but one that has an exponential number of variables. Once we establish this initial result, we proceed by proposing an alternate computationally less-demanding online allocation pol-

icy that takes into account the history of allocation decisions. We show that in order to achieve either long-term objective, the online allocation problem to be solved is a weighted sum-rate maximization. This allows us to propose an optimal history-dependent feedback allocation algorithm in Section 3.4, which solves this weighted sum-rate maximization problem at every scheduling instant.

3.3.1 Queue stability

Assume that each user k , $k = 1, 2, \dots, K$, has a queue of untransmitted packets with queue-length $q_k[t]$ and associated arrival rate λ_k . The state of the system at time t is given by $\mathbf{S}[t] = \{\mathbf{m}[t], \mathbf{q}[t]\}$ ³ where $\mathbf{q}[t]$ is the vector of queue lengths. A mapping H from the state $\mathbf{S}[t]$ to a probability distribution $H(\mathbf{S}[t])$ on the set of bit allocations \mathcal{B} is called a feedback scheduling or allocation policy. This means that when the system is in state $\mathbf{S}[t]$, bit allocation \mathbf{b} is picked according to the probability distribution $H(\mathbf{S}[t])$.

Let $a_k[t]$ denote the packet arrival process for user k . For simplicity, let us assume that $a_k[t]$ is an ergodic Markov chain and that the arrival processes are mutually independent across users. Under these standard assumptions, the queue-state process is Markov and evolves according to

$$\mathbf{q}[t] = \mathbf{q}[t-1] + \mathbf{a}[t] - \mathbf{d}[t],$$

³A general policy, in principle, is allowed to depend on the entire history of the state (e.g. channel, queues, etc.) of the system but it is well-known [51] that it is sufficient to consider stationary scheduling policies that depend only on the current state at time t .

where $d_k[t] = \min\{q_k[t], \mu_k(m_k[t], b_k^*[t])\}$; $\mathbf{b}^*[t]$ is the allocation decision at time t . *Queue stability* is traditionally defined as the positive recurrence of the queue-state process $\mathbf{q}[t]$ under a given scheduling policy.

Let \mathcal{V} be the system rate region, i.e., the set of all long-term stabilizable service rates under all possible feedback allocation policies. While a general policy as introduced above can depend on both queue and channel state, we characterize this set through the use of Static Service Split (SSS) scheduling rules, which are a simplification of it, following the approach pursued by Andrews et al. [52]. We will comment shortly on why it is sufficient to consider SSS feedback allocation policies in order to characterize the system rate region. An SSS rule can be described as follows. In channel state \mathbf{m} , the scheduler chooses bit allocation \mathbf{b} with probability $\phi_{\mathbf{mb}}$; a SSS policy is completely characterized by a stochastic matrix Φ . The long-term rate region for this space of policies is written as

$$\mathcal{V} = \left\{ \boldsymbol{\nu}(\Phi) : \sum_{\mathbf{b} \in \mathcal{B}} \phi_{\mathbf{mb}} = 1, \phi_{\mathbf{mb}} \in [0, 1], \forall \mathbf{m}, \mathbf{b} \right\}, \quad (3.1)$$

where $\boldsymbol{\nu}(\Phi) = \sum_{\mathbf{m} \in \mathcal{M}} \pi_{\mathbf{m}} \sum_{\mathbf{b} \in \mathcal{B}} \phi_{\mathbf{mb}} \boldsymbol{\mu}(\mathbf{m}, \mathbf{b})$ and

$$\boldsymbol{\mu}(\mathbf{m}, \mathbf{b}) = [\mu_1(m_1, b_1) \mu_2(m_2, b_2) \dots \mu_K(m_K, b_K)]^T;$$

$\boldsymbol{\nu}(\Phi)$ is the long-term average rate under scheduling policy Φ since $\sum_{\mathbf{b} \in \mathcal{B}} \phi_{\mathbf{mb}} \boldsymbol{\mu}(\mathbf{m}, \mathbf{b})$ represents the expected rate while in channel state \mathbf{m} , which is subsequently averaged over all channel states.

The following theorem states that if some feedback allocation policy (possibly randomized) can stabilize a system, then there exists a SSS policy,

as given in (3.1), that can also stabilize the system. In particular, the theorem says that one can obtain a throughput-optimal feedback allocation strategy by solving a linear program.

Theorem 7. *If a scheduling rule H exists under which the system is stable, then there exists an SSS scheduling policy Φ such that the system is stable, i.e., $\lambda < \nu(\Phi)$.*

□

The proof of the theorem follows very similar lines as the proof in the paper by Andrews et al. [52]. Here, the authors prove the above claim under a definition of scheduling policies that maps the state $\mathbf{S}[t]$ to a probability distribution on the users indices $\{1, \dots, K\}$ as opposed to a probability distribution on the set of bit allocations \mathcal{B} . The core idea of the proof involves a marginalization across the queue states $\mathbf{q}[t]$ in order to compute an equivalent SSS probability that picks an allocation or user in a given channel state $\mathbf{m}[t]$.

This theorem, in particular, justifies our use of SSS policies in order to characterize the rate region or stability region⁴, equivalently, of an unsaturated system. The above theorem directly motivates the computation of a stabilizing SSS policy Φ^* given arrival rate vector λ , through the following linear program

$$\begin{aligned} \Phi^* &= \underset{\text{s.t.}}{\operatorname{argmin}} \quad c \\ &\quad \lambda \leq c\nu(\Phi) \\ &\quad \sum_{\mathbf{b} \in \mathcal{B}} \phi_{\mathbf{mb}} = 1, \quad \forall \mathbf{m} \in \mathcal{M} \\ &\quad \phi_{\mathbf{mb}} \in [0, 1], \quad \forall \mathbf{m}, \mathbf{b} \end{aligned} \quad (3.2)$$

⁴The stability region of an unsaturated system is defined as the set of arrival rates $\Lambda \subset \mathbb{R}_+^K$ that are stabilizable under any scheduling policy.

This linear program characterizes the throughput region and also provides the optimal feedback allocation policy. However, there are two key issues. The first issue is that the linear program requires the scheduler to have *a priori* knowledge of the arrival rates. To alleviate the requirement on *a priori* knowledge of arrival rates, Tassiulus and Ephremedis [48] proposed the well-known *max-weight* or *back-pressure* online scheduling algorithm. Observing the natural connection between the independent sets defined by Tassiulus and Ephremedis in [48] and the feedback bit allocations in our model, it follows that if $\boldsymbol{\lambda} < \boldsymbol{\nu}(\bar{\boldsymbol{\phi}})$ for some SSS scheduling matrix $\bar{\boldsymbol{\phi}}$, then the following per-instant scheduling rule

$$\mathbf{b}^*[t] = \operatorname{argmax}_{\mathbf{b} \in \mathcal{B}} \mathbf{q}[t]^T \boldsymbol{\mu}(\mathbf{m}[t], \mathbf{b}) \quad (3.3)$$

stabilizes the system.

The second issue is more fundamental and it concerns computational complexity. The linear program (3.2) has an exponential number of variables since the stochastic matrices $\boldsymbol{\Phi}$ have dimension $|\mathcal{M}| \times |\mathcal{B}| = M \times \binom{B+K-1}{K-1}$. Furthermore, the per-instant scheduling rule of Tassiulas and Ephremides in (3.3) also requires optimization over the set \mathcal{B} , which may have exponentially many facets. We take up the issue of complexity starting in Section IV.

3.3.2 Utility maximization

The following alternate long-term network objective, proposed in [53], is applicable to saturated systems where each user has an infinite amount of data to be served (transmitted). For such systems, the state is given by

$\mathbf{S}[t] = \mathbf{m}[t]$ and hence, any scheduling rule is automatically a SSS scheduling rule thereby giving us the same characterization of rate region⁵ \mathcal{V} as in (3.1). In such systems, we are concerned with optimizing the vector of long-term service rates $\boldsymbol{\nu}(\phi)$ such that we maximize some utility function $H(\boldsymbol{\nu})$ over the region \mathcal{V} introduced earlier, i.e., we are interested in

$$\text{maximize}_{\boldsymbol{\nu} \in \mathcal{V}} H(\boldsymbol{\nu}). \quad (3.4)$$

The following two classes of long-term utility functions are defined in [53]:

- (i) Type I Utility Function - $H(\mathbf{u})$ is a continuous strictly concave function on \mathbb{R}_+^K . In addition, $H(\mathbf{u})$ is continuously differentiable, i.e., the gradient ∇H is finite and continuous everywhere in \mathbb{R}_+^K .
- (ii) Type II Utility Function - $H(u) = \sum_{k=1}^K H(u_k)$ where each $H(u_k)$ is a strictly concave continuously differentiable function, defined for all $u_k > 0$ and such that $H(u_k) \rightarrow -\infty$ as $u_k \rightarrow 0$, e.g. $H(\mathbf{u}) = \sum_{k=1}^K \log(u_k)$.

For the aforementioned utility functions, we have a convex optimization problem with linear constraints in (3.4). As an alternative to solving this problem, which again has a large number of variables, Stolyar [53] shows that using the following gradient-weighted sum-rate maximization at each instant solves (3.4) for δ sufficiently small

$$\mathbf{b}^*[t] = \operatorname{argmax}_{\mathbf{b} \in \mathcal{B}} \nabla H(\boldsymbol{\mu}_{emp}^\delta[t])^T \boldsymbol{\mu}(\mathbf{m}[t], \mathbf{b}) \quad (3.5)$$

⁵the notion of rate region is slightly different here since we are not stabilizing anything – here it is the region of long term average rates that the system provides

where

$$\boldsymbol{\mu}_{emp}^\delta[t] = (1 - \delta)\boldsymbol{\mu}_{emp}^\delta[t] + \delta\boldsymbol{\mu}(\mathbf{m}[t], \mathbf{b}^*[t])$$

is the empirical rate vector measured till time t . Formally stated, the statement proven in [Theorem 2, [53]] says:

Theorem 8. *Let \mathcal{A} be a bounded subset of \mathbb{R}_+^K . Then, for any $\varepsilon > 0$, there exists $T > 0$ (depending on ε and \mathcal{A}) such that*

$$\lim_{\delta \rightarrow 0} \sup_{\boldsymbol{\mu}_{emp}^\delta[0] \in \mathcal{A}, t > \frac{T}{\delta}} P(\|\boldsymbol{\mu}_{emp}^\delta[t] - \boldsymbol{\nu}^*\| > \varepsilon) = 0.$$

□

As is the case for the stability objective, solving this problem requires optimizing over the set \mathcal{B} . The computational burden this presents may be non-trivial. We turn to this now.

3.4 Optimal allocation through dynamic programming

In Section 3.3, we have established that for queue stability in (3.12) and for Type I/II utility maximization in (3.5), we are interested in the following online weighted sum-rate maximization problem

$$\text{maximize}_{\mathbf{b} \in \mathcal{B}} \quad \mathbf{w}^T \boldsymbol{\mu}(\mathbf{m}[t], \mathbf{b}), \quad (3.6)$$

where $\mathbf{w} = [w_1, \dots, w_K]^T$ is a vector of non-negative weights. The form of the function $\boldsymbol{\mu}(\mathbf{m}[t], \mathbf{b})$ would, in general, depend on the underlying system. In fact, for complex modulation/coding schemes the function might only be available as a look-up table. While the optimization problem characterizes optimal

performance, solving it exactly may be computationally prohibitive. Thus, the focus of this chapter becomes algorithmic. We propose novel solutions to (3.6) through Theorems 9-14 that explore the natural tradeoffs between accuracy, complexity and the structure of the weighted sum-rate function. We start by showing that using Dynamic Programming, the exact solution can be obtained in pseudo-polynomial time.

Theorem 9. *The online resource allocation problem (3.6) can be solved exactly in time $\mathcal{O}(KB^2)$.*

Proof: Order the users arbitrarily. We choose to work with the existing order w.l.o.g. Define

$$A(i, j) \triangleq w_i \mu_i(m_i, j) \quad (3.7)$$

to be the weighted sum-rate for user i given we allocate j bits to this user and define

$$R(k, b) \triangleq \text{maximize}_{\sum_{i=1}^k b_i \leq b, b_i \in \mathbb{N}_0} \sum_{i=1}^k w_i \mu_i(m_i, b_i) \quad (3.8)$$

to be the maximum weighted sum-rate if we have b bits to allocate amongst the first k users with $R(0, b) = 0$. It follows that $R(1, b) = A(1, b), b = 0, \dots, B$. We can write a recursion

$$R(k, b) = \text{maximize}_{j=0, \dots, b} \{R(k-1, b-j) + A(k, j)\}. \quad (3.9)$$

The optimality of the recursion (3.9) can be established using standard induction arguments. This rule gives rise to a table with a total of $K(b+1)$ elements.

In order to compute element (k, b) in the table, using our recursion, we incur a complexity of $\mathcal{O}(b + 1)$. Hence, the total complexity can be calculated as

$$\begin{aligned}
\sum_{k=1}^K \sum_{b=0}^B (b + 1) &= K \sum_{b=0}^B (b + 1) \\
&= K \left(B + 1 + \frac{B(B+1)}{2} \right) \\
&= K \frac{(B+1)(B+2)}{2} \\
&= \mathcal{O}(KB^2).
\end{aligned} \tag{3.10}$$

□

Thus, we have proposed an exact solution using dynamic programming, which has pseudo-polynomial⁶ complexity $\mathcal{O}(KB^2)$ and which is applicable to any type of weighted sum-rate function.

It is clear that the complexity of this algorithm depends critically on how the bit budget B scales in the number of users K . If $B = \mathcal{O}(1)$ and is a small constant, then the algorithm provides an implementable linear-complexity solution in the number of users. However, in order to prevent a throughput ceiling, it is necessary for the bit budget to scale with the number of users [98]. In LTE, a *physical downlink control channel (PDCCH)* carries resource assignments to a user. Each PDCCH can vary in size ranging from 72 bits to 576 bits per user depending on the user's channel conditions and required robustness [55, 56]. The standard is expected to accommodate an average of 100 users (indoor, high-speed etc.) for services such as VoIP services [58] thus resulting in a complexity of roughly $KB^2 = 100 \times 100 \times 100 = 10^6$ operations for dynamic programming. Here, we are assuming a feedback packet

⁶An algorithm has pseudo-polynomial complexity if its running time is a polynomial in the size of the input in unary. The size of the input to (3.6) in unary is at most $KB A_{max} + B = \mathcal{O}(KB)$ where $A_{max} = \max_{(i,j)} A(i, j)$.

size of 100 bits, a number that will only grow with the advent of technologies such as MIMO-OFDMA coupled with high-data rate applications such as video and gaming. While complexity might not be too large for some applications, others might demand faster running times.

This motivates the development of algorithms with faster running times that might be less accurate. This forms the focus of the remainder of this chapter.

3.5 Reduced-complexity resource allocation

In this section, we develop more computationally efficient algorithms that approximately solve (3.6) for a special class of weighted sum-rate functions. We provide theoretical lower bounds on their performance. The long-term performance of these approximate algorithms in achieving queue stability is characterized by Theorem 10 below.

We say that an algorithm is a multiplicative β -approximation, $\beta \in (0, 1]$, to (3.3) if it provides a solution \mathbf{b}_{alg} such that

$$\mathbf{w}^T \boldsymbol{\mu}(\mathbf{m}[t], \mathbf{b}_{alg}) \geq \beta \max_{\mathbf{b} \in \mathcal{B}} \mathbf{w}^T \boldsymbol{\mu}(\mathbf{m}[t], \mathbf{b}).$$

We say that an algorithm is an additive β -approximation to (3.3) if it provides a solution \mathbf{b}_{alg} such that

$$\max_{\mathbf{b} \in \mathcal{B}} \mathbf{w}^T \boldsymbol{\mu}(\mathbf{m}[t], \mathbf{b}) - \mathbf{w}^T \boldsymbol{\mu}(\mathbf{m}[t], \mathbf{b}_{alg}) \leq \beta \mathbf{w}^T \mathbf{1}.$$

The following theorem is a generalization of the original result by Tassiulus

and Ephremedis. It essentially states that local approximation is consistent with the long-term objectives we consider.

Theorem 10. *(i) (Multiplicative) If $\lambda < \beta\nu(\bar{\phi})$, $\beta \in (0, 1]$ for some SSS scheduling matrix $\bar{\phi}$, then a β -approximation to the following per-instant scheduling rule*

$$\mathbf{b}^*[t] = \operatorname{argmax}_{\mathbf{b} \in \mathcal{B}} \mathbf{q}[t]^T \boldsymbol{\mu}(\mathbf{m}[t], \mathbf{b}) \quad (3.11)$$

stabilizes the system.

(ii) (Additive) If $\lambda + \beta < \nu(\bar{\phi})$ where $\beta = \beta\mathbf{1}$, $\beta > 0$ for some SSS scheduling matrix $\bar{\phi}$, then the approximate bit allocation policy $\bar{\mathbf{b}}[t]$ satisfying

$$\mathbf{q}[t]^T \boldsymbol{\mu}(\mathbf{m}[t], \bar{\mathbf{b}}[t]) \geq \mathbf{q}[t]^T [\boldsymbol{\mu}(\mathbf{m}[t], \mathbf{b}^*[t]) - \beta] \quad (3.12)$$

stabilizes the system. Here, $\mathbf{b}^[t] = \max_{\mathbf{b} \in \mathcal{B}} \mathbf{q}[t]^T \boldsymbol{\mu}(\mathbf{m}[t], \mathbf{b})$.*

Proof: See Appendix A.1. □

The theorem essentially states that for unsaturated systems: *(i)* If we calculate a multiplicative β -approximate solution, $\beta \in (0, 1]$ to (3.3) in every time slot, one can achieve a β -fraction of the stability region \mathcal{V} , and *(ii)* if we calculate a solution that is within $\beta\mathbf{q}[t]^T\mathbf{1}$, $\beta > 0$ of (3.3) in every time slot, one can achieve all rates within the region $(\mathcal{V} - \beta\mathbf{1})^+$, where $(x)^+ = \max\{0, x\}$. This is the set formed by subtracting $\beta\mathbf{1}$ from each vector in \mathcal{V} . Of course, it is understood that if β is large leading to vectors with negative elements, these elements are made zero since we cannot have negative rates. This result

paves the way for the design of computationally efficient algorithms for the long-term objectives, by constructing approximations to (3.6).

In Section 3.5.1, we consider weighted sum-rate functions that are non-decreasing and sub-modular in the bit allocation. In short, sub-modularity, as discussed in Section 2.1, refers to *diminishing returns* with respect to the allocation of resources. This is a property that is exhibited quite frequently by wireless systems in general since transmission rates typically behave logarithmically. Sub-modularity enables us to propose a *greedy* bit allocation algorithm that has complexity $\mathcal{O}((B + K)\log_2 K)$ with multiplicative approximation factor $(1 - \frac{1}{e})$. In the example above, this reduces the running time from 10^6 operations to roughly 10^3 operations. Our main contributions are contained in Lemma 11 and Theorem 11. We review the basic concepts and definitions of sub-modular function optimization in Section 2.1.

In Section 3.5.2, we focus on a class of weighted sum-rate functions that arise in uplink scenarios where all nodes (including the base-station) are equipped with multiple antennas and the adopted transceiver scheme is single-stream beamforming and combining with quantized beamformer feedback. Single-stream beamforming and combining MIMO systems have been extensively studied in the past [30, 31, 34, 37, 64, 65, 76]. This is an attractive method for achieving reliable data transmission through significant diversity and array gain making them part of standards such as W-CDMA [66] and LTE [55]. We show that for this choice of physical layer signalling protocol, the weighted sum-rate maximization problem in (3.6) is sub-modular for

certain types of beamformer quantizers. More importantly, this sub-class of non-decreasing, sub-modular functions allows for the development of an approximation algorithm with a further-reduced complexity of $\mathcal{O}(K \log_2 K)$ thus reducing the running time even further from 1000 operations to roughly 600 operations in the example above. We prove an additive approximation factor for this algorithm that is a function of the beamformer quantizer parameters.

3.5.1 Resource allocation through sub-modularity

In this section we show that under some mild assumptions, bit allocation has sub-modular structure. Roughly speaking, this means that a users' performance exhibits diminishing returns with respect to the number of feedback bits received. This allows us to leverage results from sub-modular function optimization. Preliminary definitions and results on sub-modular function maximization are presented in Chapter 2.

We now show that the optimal bit allocation problem in (3.6) is indeed a sub-modular function maximization over a uniform matroid. Let $\mathcal{G} = (U, V, E)$ be a bipartite graph where U contains K *user nodes* and V contains B *bit nodes*, both ordered arbitrarily, i.e. $|U| = K$ and $|V| = B$. Let E contain the set of all edges $E = \{e_{kb} : i = 1, \dots, K \text{ and } j = 1, \dots, B\}$. Given $A \subseteq E$, we define $|A|_i \triangleq |\{e_{kb} \in A : k = i\}|$ to represent the number of bits allocated to user i , i.e., $|A|_i = b_i$. The independence we are interested in is $\mathcal{I} = \{A \subseteq E : |A| \leq B\}$ where B is the total bit budget. By definition, \mathcal{I} is a uniform matroid and furthermore, \mathcal{I} is the set of *all* valid allocations since if $A \in \mathcal{I}$, then

$\sum_{k=1}^K b_k = \sum_{k=1}^K |A|_k \leq B$ and if $A \notin \mathcal{J}$, then $\sum_{k=1}^K b_k = \sum_{k=1}^K |A|_k = |A| > B$.

Now the weighted sum-rate maximization problem in (3.6) when the channel is in state $\mathbf{m}[t]$ in time slot t as

$$\begin{aligned}
& \text{maximize}_{\mathbf{b} \in \mathcal{B}} \quad \sum_{k=1}^K w_k \mu_k(m_k[t], b_k) \\
\equiv & \text{maximize} \quad \sum_{k=1}^K w_k \mu_k(m_k[t], b_k) - \mu_k(m_k[t], 0) \\
& \text{s.t.} \quad b_k = |A|_k, \quad \sum_k |A|_k \leq B, \quad A \subseteq E \\
= & \text{maximize}_{A \in \mathcal{J}} \quad \sum_{k=1}^K w_k \mu_k(m_k[t], |A|_k) - \mu_k(m_k[t], 0).
\end{aligned} \tag{3.13}$$

The following result becomes immediate.

Lemma 11. *If the function $\mu_k(m_k, b_k)$ is non-decreasing and sub-modular in the bit allocation $b_k = |A|_k$, $A \subseteq E$ for all users $k = 1, \dots, K$, and channel states $\mathbf{m} \in \mathcal{M}$, then $\sum_{k=1}^K w_k \mu_k(m_k[t], |A|_k) - \mu_k(m_k[t], 0)$ is a normalized, non-decreasing, sub-modular function on set E for all channel states $\mathbf{m} \in \mathcal{M}$.*

Proof: The result follows from Lemma 1. □

Hence, the result in Theorem 1 is applicable and the greedy algorithm can be used to solve the optimal bit allocation problem in (3.13) with approximation factor $(1 - \frac{1}{e})$. The greedy algorithm for the specific case of our bit allocation problem in time slot t can be written as follows where

$$u_k(b_k) \triangleq w_k (u_k(m_k[t], b_k + 1) - u_k(m_k[t], b_k)) \tag{3.14}$$

is the increase in rate or marginal utility if user k is given one extra bit.

Algorithm (*Greedy algorithm for feedback bit allocation*):

- *Step 1*: Set $b = 1$ and $b_k = 0, \forall k$, which is essentially a bit counter for each user.
- *Step 2*: Compute $u_k(b_k), \forall k$.
- *Step 3*: Sort this list of marginal utilities.
- *Step 4*: Assign a bit to user k^* who is on top of this list, update $b_{k^*} = b_{k^*} + 1$ and re-compute $u_{k^*}(b_{k^*})$
- *Step 5*: If $b < B$, set $b = b + 1$, and go to Step 3; else exit.

We end this section by investigating the complexity of the above algorithm in the following theorem.

Theorem 11. *The greedy algorithm has complexity $\mathcal{O}((B + K)\log_2 K)$ when applied to the optimal bit allocation problem in (3.6).*

Proof: Step 2 of this algorithm incurs complexity $\mathcal{O}(K\log_2 K)$ for the first iteration $b = 1$. Subsequently, every re-sort in Step 3 costs $\mathcal{O}(\log_2 K)$ with a maximum of B such re-sorts. Thus, the total complexity is $\mathcal{O}((B + K)\log_2 K)$. \square

3.5.2 Resource allocation for MIMO systems

By assuming that the rate $\mu_k(m_k, b)$ is a non-decreasing sub-modular function in the bit allocation b in every channel state m_k , we use the greedy algorithm in Section 3.5.1 to approximately solve the online feedback allocation problem in (3.6) with complexity $\mathcal{O}((B + K)\log_2 K)$. In this section,

we show that when single-stream beamforming and combining with quantized beamformer feedback is used as the physical layer transmission scheme, the weighted-sum-rate maximization problem in (3.6) is non-decreasing and sub-modular for a broad class of quantizers. Thus, we are able to develop an approximation algorithm with a further-reduced complexity of $\mathcal{O}(K\log_2 K)$ with an additive guarantee that depends on the parameters of the quantizer. The technique involves relaxing the integral constraint on the bits, solving the weighted sum-rate maximization using fractional bits under an assumed form on the expected post-quantization signal-to-noise ratio (SNR) or quantized SNR in short, followed by rounding to obtain the integer solution. Thus, aside the usual impact on precision that are typically omitted from running time calculations, the running time of our algorithm no longer depends on the feedback budget B .

We begin this section by investigating the effects of limited feedback on the aforementioned class of MIMO systems.

3.5.2.1 Single-stream MIMO with limited feedback

The classical $N_t \times N_r$ single-stream beamforming and combining MIMO link for a typical user (shown in Fig. 3.2) can be described using the following received signal model,

$$y = \sqrt{\alpha} \mathbf{z}^\dagger \mathbf{H} \mathbf{g} s + \mathbf{z}^\dagger \mathbf{n}, \quad (3.15)$$

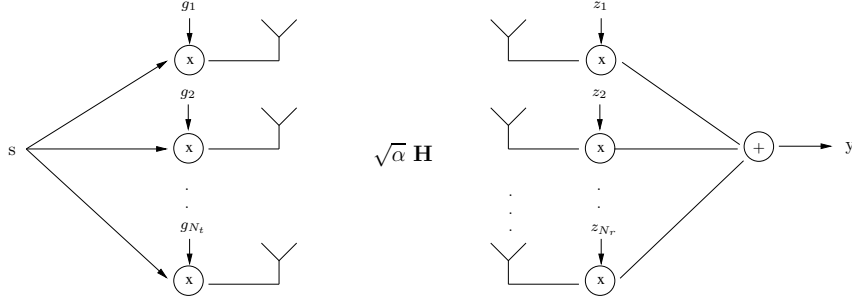


Figure 3.2: Single-stream beamforming and combining MIMO system.

where

$$\begin{array}{ll}
 \mathbf{s} & \sim \text{Complex Gaussian transmit codeword with } \mathbb{E}[|s|^2] = P \\
 \mathbf{n} \in \mathbb{C}^{N_r} & \sim \mathcal{CN}(0, N_o \mathbf{I}) \text{ is additive white Gaussian noise} \\
 \mathbf{g} \in \mathbb{C}^{N_t} & : \text{Transmit beamformer with } \|\mathbf{g}\|^2 = 1 \text{ to satisfy} \\
 & \text{the transmit power constraint} \\
 \mathbf{z} \in \mathbb{C}^{N_r} & : \text{Receive combiner} \\
 \mathbf{H} \in \mathbb{C}^{N_r \times N_t} & : \text{Complex-valued MIMO channel} \\
 \alpha \in \mathbb{R}_+ & : \text{Large-scale fading gain}
 \end{array}
 .$$

The model in (3.15) is a comprehensive description of the wireless channel in that it explicitly accounts for the composite effects of small-scale (SS) fading and large-scale (LS) fading. We use α to represent the path-loss or shadowing effects of the channel, henceforth referred to as *LS effects*, while the matrix \mathbf{H} denotes SS fading. Composite models have been used in past literature (see [61] and references therein). The SNR for this system can be written as

$$\text{SNR} = \frac{|\mathbf{z}^\dagger \mathbf{H} \mathbf{g}|^2}{\|\mathbf{z}\|^2} \frac{P\alpha}{N_o}. \quad (3.16)$$

For simplicity, we assume that all users have the same number of antennas N_t although all results presented in the remainder of this section can be extended to scenarios where this is not true. It is well-known that the SNR in (5.3) can

be maximized by setting $\mathbf{g}^* = \mathbf{v}$ and $\mathbf{z}^* = \mathbf{H}\mathbf{g}^*$ where \mathbf{v} is the right singular vector corresponding to the maximum singular value σ of the channel matrix \mathbf{H} . By introducing user indices, the maximum SNR for user k can be written as

$$\text{SNR}_{k,PF} = \frac{\alpha_k P_k \|\mathbf{H}\mathbf{v}_k\|^2}{N_o} = \frac{\alpha_k P_k \sigma_k^2}{N_o}. \quad (3.17)$$

The choice of notation reflects the fact that the user requires Perfect Feedback of the right singular vector \mathbf{v}_k from the base-station in order to achieve this maximum SNR. However, feedback in realistic systems is imperfect due to limited feedback budgets, the primary motivation for this work. Through the remainder of this section, we restrict our attention to quantization error: error that is introduced when the base-station quantizes the optimal precoder \mathbf{v}_k using b_k bits in preparation for feedback, the feedback link is assumed to be delay- and error-free. We assume that user k uses a quantized beamformer $\hat{\mathbf{v}}_k$ for which we can write the SNR with Imperfect Feedback as

$$\text{SNR}_{k,IF} = \frac{\alpha_k P_k \|\mathbf{H}_k \hat{\mathbf{v}}_k\|^2}{N_o}. \quad (3.18)$$

3.5.2.2 Time-scales and structure of rate vector $\boldsymbol{\mu}(\mathbf{m}, \mathbf{b})$

In this section, we describe the structure of rate vector $\boldsymbol{\mu}(\mathbf{m}, \mathbf{b})$ that arises out of employing the single-stream MIMO physical layer scheme described earlier.

We consider changing feedback allocations once every LS fading coherence time, which typically spans mutiple SS fading coherence times, say D of

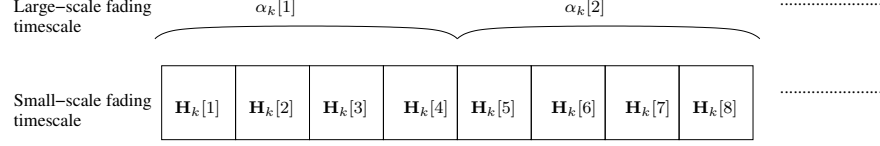


Figure 3.3: Composite effects of small-scale fading and large-scale fading in a wireless channel with $D = 4$.

them, as shown in Fig. 3.3. In other words, we provide feedback about the faster time-scale (small-scale fading) and the quality of feedback is varied at a slower time-scale (large-scale fading). Such a design choice has two benefits: First, it might require too much overhead to compute and communicate optimal allocations on the SS fading time-scale, which typically spans a few milliseconds. Second, this allows each user to estimate their LS coefficient α_k without the need for feedback from the base-station by exploiting reciprocity on the downlink. This is possible since path-loss and/or shadowing are dependent solely on the distance between the user and the base-station. The increasing availability of GPS-enabled devices also offers the user an alternate means to compute their path-loss.

Capturing the two separate time-scales, we define the channel state as

$$\mathbf{m}[t] = \{\alpha[t], [\mathbf{H}_k[(t-1)D+1], \dots, \mathbf{H}_k[tD]]\}, \quad k = 1, \dots, K\}$$

for the single-stream MIMO system we are considering. We assume that $\{\alpha[t]\}$, is a finite-state process that is either (i) i.i.d. across time or (ii) an ergodic Markov chain⁷, taking values from the set \mathcal{P} with a unique stationary distri-

⁷Markovian and i.i.d. models for user mobility in a cell (and hence path-loss) have been

bution $\{\pi_\alpha\}_{\alpha \in \mathcal{P}}$. On the faster time-scale, we assume that

$$\{[\mathbf{H}_k[(t-1)D+1], \dots, \mathbf{H}_k[tD]], k = 1, \dots, K\}$$

is again a finite-state process that is either i.i.d. across time or ergodic Markov taking values from the set \mathcal{H} . Traditionally, each element of the channel matrix \mathbf{H}_k is modeled as a complex Gaussian random variable. However, we can consider a finite-state process by discretizing this random variable and creating set \mathcal{H} by sampling the support of its probability density function sufficiently finely. As is the case in past literature (see [61] and references therein), large-scale fading is assumed to be independent of the small-scale fading. Finally, the small-scale fading channels are assumed to be identically distributed across users.

In each state $\mathbf{m} \in \mathcal{M} = \mathcal{P} \times \mathcal{H}$, given bit allocation b , we assume that user k transmits at a rate $\mu_k(\alpha_k, b_k)$ that is independent of the realization $\{[\mathbf{H}_k[(t-1)D+1], \dots, \mathbf{H}_k[tD]], k = 1, \dots, K\}$. Given a fixed α_k and bit allocation b_k through the course of a large coherence time, we define $\mu_k(\alpha_k, b_k)$ to be the *goodput* (a notion that is discussed by Lau et al. [62]) when transmitting at the maximum possible rate $\gamma_k^*(\alpha_k, b_k)$ while allowing for an outage probability of at most ϵ_k , i.e.,

$$\mu_k(\alpha_k, b_k) \triangleq \gamma_k^*(\alpha_k, b_k)(1 - \epsilon_k).$$

utilized by El Gamal et al. [59] and Toumpis et al. [60] respectively in studying how mobility impacts the performance of a wireless network.

In this framework, outages arise due to delay constraints that dictate that a packet must be decoded within a SS coherence time. This means that a particular SS fading realization within the larger coherence time might not be able to support the chosen transmission rate in accordance with Shannon's capacity formula.

To compute $\gamma_k^*(\alpha_k, b_k)$, we need to quantify the outage probability of the single-stream beamforming/combining MIMO system. From (3.18), the SNR with imperfect feedback is a random variable whose distribution depends on the joint distribution of σ_k^2 and \mathbf{v}_k along with the quantization policy. Thus, the outage probability for user k that transmits at rate $\gamma_k(\alpha_k, b_k)$ can be written as

$$\mathbb{P} \left(\frac{\alpha_k P_k \|\mathbf{H}_k \hat{\mathbf{v}}_k\|^2}{N_o} \leq 2^{\gamma_k(\alpha_k, b_k)} - 1 \right). \quad (3.19)$$

We can use the Markov inequality to bound (3.19):

$$\begin{aligned} \mathbb{P} \left(\frac{\alpha_k P_k \|\mathbf{H}_k \hat{\mathbf{v}}_k\|^2}{N_o} \leq 2^{\gamma_k(\alpha_k, b_k)} - 1 \right) &= \mathbb{P} \left(\frac{N_o}{\alpha_k P_k \|\mathbf{H}_k \hat{\mathbf{v}}_k\|^2} \geq \frac{1}{2^{\gamma_k(\alpha_k, b_k)} - 1} \right) \\ &\leq \frac{N_o}{\alpha_k P_k} \mathbb{E} \left[\frac{1}{\|\mathbf{H}_k \hat{\mathbf{v}}_k\|^2} \right] (2^{\gamma_k(\alpha_k, b_k)} - 1) \\ &\quad \text{by Markov's inequality.} \end{aligned} \quad (3.20)$$

From Jensen's inequality, we know that $\mathbb{E} \left[\frac{1}{\|\mathbf{H}_k \hat{\mathbf{v}}_k\|^2} \right] > \frac{1}{\mathbb{E}[\|\mathbf{H}_k \hat{\mathbf{v}}_k\|^2]}$. In order to proceed, we note that one can find a function $e(\cdot)$ such that

$$\mathbb{E} \left[\frac{1}{\|\mathbf{H}_k \hat{\mathbf{v}}_k\|^2} \right] = e(b_k) \frac{1}{\mathbb{E}[\|\mathbf{H}_k \hat{\mathbf{v}}_k\|^2]}. \quad (3.21)$$

While it is true that $e(\cdot)$ is dependent on the quantization codebook/policy and the channel distribution as well, we do not explicitly write down this dependence since we are interested only in optimizing bit allocations. This

function can be computed numerically at the beginning of the communication session and furthermore, we can find a bound $e_{max} = \max_k e(b_k)$ such that

$$\mathbb{E} \left[\frac{1}{||\mathbf{H}_k \hat{\mathbf{v}}_k||^2} \right] \leq e_{max} \frac{1}{\mathbb{E} [||\mathbf{H}_k \hat{\mathbf{v}}_k||^2]}, \quad \forall k. \quad (3.22)$$

For our analysis, we use the popular *Random Vector Quantization* (RVQ) technique [30, 31]. According to this approach, a codebook $\mathcal{C}_k(b)$ for user k , corresponding to a bit allocation of b bits, is constructed by throwing 2^b points uniformly at random on the surface of a complex unit sphere. These codebooks offer the combined advantages of analytical tractability along with implementability [34]. On the other hand, Grassmannian codebooks [35, 76], which are optimal maximum-SNR fixed codebooks for single-stream transmission over a Rayleigh fading channel are unfortunately not available for all combinations of feedback bits and transmit antennas [34]. Recent results [34, 36, 37] quantify the loss in SNR due to quantization when using RVQ codebooks. In these works, the authors show that the expected SNR with feedback quantization using b bits for a single-stream beamforming/combining MIMO system can be described accurately by a function of the form

$$\mathbb{E}_{\mathcal{C}(b), \mathbf{H}} [||\mathbf{H} \hat{\mathbf{v}}||^2] = \mathbb{E}[\sigma^2] (1 - c_1(N_t, N_r) 2^{-c_2(N_t, N_r)b}), \quad (3.23)$$

where $c_1(N_t, N_r) \in (0, 1]$, $c_2(N_t, N_r) > 0$. Some user indices have been dropped in the above expression since all users transmit through i.i.d. Rayleigh MIMO channels and employ the same codebook, i.e., $\mathcal{C}_k(b) = \mathcal{C}(b)$, $\forall k$. Now since (3.23) is true on an average over all realizations of the codebook $\mathcal{C}(b)$, it follows

that there exists at least one codebook $\mathcal{C}^*(b)$ with quantized SNR

$$\mathbb{E}_{\mathbf{H}} [||\mathbf{H}\hat{\mathbf{v}}||^2 | \mathcal{C}^*(b)] \geq \mathbb{E}[\sigma^2] (1 - c_1(N_t, N_r) 2^{-c_2(N_t, N_r)b}). \quad (3.24)$$

We can collect codebooks across all $b = 0, \dots, B$, to form a *super* codebook $\mathcal{C}^* = \bigcup_{b=0}^B \mathcal{C}^*(b)$. Through the remainder of our analysis, we assume that the system uses such a codebook \mathcal{C}^* and do not include an explicit dependence on \mathcal{C}^* in our notation henceforth.

Substituting (3.22) and (3.24) in (3.20), we get

$$\begin{aligned} & \mathbb{P} \left(\frac{\alpha_k P_k ||\mathbf{H}_k \hat{\mathbf{v}}_k||^2}{N_o} \leq 2^{\gamma_k(\alpha_k, b_k)} - 1 \right) \\ & \leq \frac{N_o}{\alpha_k P_k} \mathbb{E} \left[\frac{1}{||\mathbf{H}_k \hat{\mathbf{v}}_k||^2} \right] (2^{\gamma_k(\alpha_k, b_k)} - 1) \\ & = \frac{N_o}{\alpha_k P_k} \frac{e_{max}}{\mathbb{E}[\sigma^2] (1 - c_1(N_t, N_r) 2^{-c_2(N_t, N_r)b_k})} (2^{\gamma_k(\alpha_k, b_k)} - 1) \\ & = \frac{N_o}{\alpha_k P_k} \frac{e_{max}}{\mathbb{E}[\sigma^2] (1 - c_1(N_t, N_r) 2^{-c_2(N_t, N_r)b_k})} (2^{\gamma_k(\alpha_k, b_k)} - 1). \end{aligned}$$

Therefore, by using $\left\{ \frac{N_o}{\alpha_k P_k} \frac{e_{max}}{\mathbb{E}[\sigma^2] (1 - c_1(N_t, N_r) 2^{-c_2(N_t, N_r)b_k})} (2^{\gamma_k(\alpha_k, b_k)} - 1) \leq \varepsilon_k \right\}$ as our outage event, we are being conservative. We enforce the maximum outage probability constraint of ε_k and explicitly compute $\gamma_k^*(\alpha_k, b_k)$ as

$$\begin{aligned} \varepsilon_k & \geq \frac{N_o}{\alpha_k P_k} \frac{e_{max}}{\mathbb{E}[\sigma^2] (1 - c_1(N_t, N_r) 2^{-c_2(N_t, N_r)b_k})} (2^{\gamma_k(\alpha_k, b_k)} - 1) \\ \Rightarrow \gamma_k^*(\alpha_k, b_k) & = \log_2 \left(1 + \frac{\alpha_k P_k \varepsilon_k}{e_{max} N_o} \mathbb{E}[\sigma^2] (1 - c_1(N_t, N_r) 2^{-c_2(N_t, N_r)b_k}) \right), \end{aligned}$$

Thus, we have computed the goodput when transmitting at $\gamma_k^*(\alpha_k, b_k)$ while incurring outage probability of at most ε_k as

$$\mu_k(\alpha_k, b_k) \triangleq \log_2 (1 + a_k \Delta(b_k)) (1 - \varepsilon_k).$$

where $a_k = \frac{P_k \alpha_k \varepsilon_k}{e_{max} N_o}$ and $\Delta(b_k) = \mathbb{E}[\sigma^2] (1 - c_1(N_t, N_r) 2^{-c_2(N_t, N_r)b_k})$, $c_1(N_t, N_r) \in (0, 1]$, $c_2(N_t, N_r) > 0$ is the *quantizer SNR function*. Recall that $\gamma_k^*(\alpha_k, b_k)$ rep-

resents the maximum possible transmission rate that obeys the outage constraints.

From (3.1), the rate region for a system that employs the single-stream MIMO physical layer structure described thus far can be expressed in terms of

$$\begin{aligned}\nu(\Phi) &= \sum_{\mathbf{m} \in \mathcal{M}} \pi_{\mathbf{m}} \sum_{\mathbf{b} \in \mathcal{B}} \phi_{\mathbf{m}\mathbf{b}} \boldsymbol{\mu}(\mathbf{m}, \mathbf{b}) \\ &= \sum_{\boldsymbol{\alpha} \in \mathcal{P}} \pi_{\boldsymbol{\alpha}} \sum_{\mathbf{b} \in \mathcal{B}} \phi_{\boldsymbol{\alpha}\mathbf{b}} \boldsymbol{\mu}(\boldsymbol{\alpha}, \mathbf{b}) \\ &= \sum_{\boldsymbol{\alpha} \in \mathcal{P}} \pi_{\boldsymbol{\alpha}} \sum_{\mathbf{b} \in \mathcal{B}} \phi_{\boldsymbol{\alpha}\mathbf{b}} [\log_2(1 + a_1 \Delta(b_1)) (1 - \epsilon_1) \dots \\ &\quad \dots \log_2(1 + a_K N_o \Delta(b_K)) (1 - \epsilon_K)]^T\end{aligned}$$

and the optimization in (3.6) takes the specific form

$$\text{maximize}_{\mathbf{b} \in \mathcal{B}} \quad \sum_{k=1}^K w_k \log_2(1 + a_k \Delta(b_k)) (1 - \epsilon_k) . \quad (3.25)$$

We absorb the success probability $(1 - \epsilon_k)$ into weight w_k henceforth.

While the above analysis calls for the use of a specific super codebook \mathcal{C}^* , in Section 3.6, we consider a $N_t = N_r = 2$ MIMO system with a randomly-generated super codebooks. We estimate the constants $c_1(N_t, N_r)$ and $c_2(N_t, N_r)$ thereby forming a lower bound (3.24) on quantized SNR for many codebook realizations. We also compute the function $e(b)$ (and hence e_{max}) to demonstrate the feasibility of this approach.

3.5.2.3 Relaxation and approximation guarantees

In Theorems 12-14 below, we develop an approximation algorithm to solve (3.25) in closed-form while incurring a complexity of $\mathcal{O}(K \log_2 K)^8$. We

⁸We recognize that there is an additional storage cost of $\mathcal{O}(\log B)$.

provide an additive approximation guarantee of

$$\log_2 \left(1 + \max \left\{ \frac{1}{1 - c_1(N_t, N_r) 2^{c_2(N_t, N_r)}}, \frac{1}{1 - c_1(N_t, N_r)} \right\} \right).$$

In Section 3.6, we show through numerical experiments that

$$\log_2 \left(1 + \max \left\{ \frac{1}{1 - c_1(N_t, N_r) 2^{c_2(N_t, N_r)}}, \frac{1}{1 - c_1(N_t, N_r)} \right\} \right) \approx 2 \text{ bits per second.}$$

Theorem 12. *Consider the following continuous relaxation of (3.25):*

$$\mathbf{b}^*[t] = \operatorname{argmax}_{\sum_k b_k \leq B, b_k \in \mathbb{R}_+} \max_{\mathbf{b} \in \mathcal{B}} \sum_{k=1}^K w_k \log_2 \left(1 + \frac{P_k \alpha_k}{N_o} \Delta(b_k) \right) (1 - \epsilon_k).$$

The solution to this relaxation is

$$b_k^* = (N_t - 1) \left[\log_2 \left(\left(1 + \frac{1}{(N_t - 1)\eta^*} \right) \left(\frac{a_k(\mathbb{E}[\sigma^2] - N_r)}{a_k \mathbb{E}[\sigma^2] + 1} \right) \right) \right]^+ \quad (3.26)$$

where η^* is chosen such that $\sum_k b_k^* = B$.

Proof: See Appendix A.3. □

Now, we argue that the weighted sum-rate function in (3.25) is non-decreasing and sub-modular on set $E = \{e_{kb} : i = 1, \dots, K \text{ and } b = 1, \dots, B\}$.

Lemma 12. *The weighted sum-rate function in (3.25) where $b_k = |A|_k$, $A \subseteq E$, $E = \{e_{kb} : i = 1, \dots, K \text{ and } b = 1, \dots, B\}$ is non-decreasing and sub-modular on this set E .*

Proof: By setting $b_k = |A|_k$, $A \subseteq E$ and defining a function $F : b_k \rightarrow \mathbb{R}$ on the bit allocation for the k -th user, we observe that it is sufficient to show

that $F(b_k)$ is (i) non-decreasing in $b_k \in \mathbb{N}_0$ and that (ii) $F(b_k + n) - F(b_k) \geq F(\bar{b}_k + n) - F(\bar{b}_k)$, $b_k \leq \bar{b}_k$, $b_k, \bar{b}_k \in \mathbb{N}_0$, $n \in \mathbb{N}$ in order to prove the claim.

Consider the relaxed function $f : b_k \rightarrow \mathbb{R}$, $b_k \in \mathbb{R}_+$ (of course $f(b_k) = F(b_k)$ for $b_k \in \mathbb{N}_0$) and assume that this function is non-decreasing, concave, and twice differentiable. Then, the conditions (i) is trivially satisfied while condition (ii) is satisfied due to following argument. Since $f(b_k)$ is concave and twice differentiable, we know that $f'(b_k) \geq f'(\bar{b}_k)$ for $b_k \leq \bar{b}_k$. Thus, for any $y \in \mathbb{R}_+$, we can write

$$\frac{d}{db_k} [f(b_k + y) - f(b_k)] = f'(b_k + y) - f'(b_k) \leq 0,$$

which implies that condition (ii) is satisfied. Since the continuous relaxation of (3.25) is non-decreasing, concave, and twice differentiable, the result follows. \square

Theorem 13. *Computing the above solution in (3.26) incurs a complexity of $\mathcal{O}(K \log_2 K)$.*

Proof: See Appendix A.3. \square

Comparing the results in Theorems 11 and 13, we see that by assuming less about the exact form of the communication system, we are incurring an added complexity cost of $\mathcal{O}(B \log_2 K)$, while providing a system-independent multiplicative approximation guarantee of $(1 - \frac{1}{e})$.

Once we solve for b_k^* , we apply a floor operation in order to enforce the

integer constraints, i.e., we set

$$b_{k,INT}^* = \begin{cases} \lfloor b_k^* \rfloor, & b_k^* \geq 1 \\ 0, & b_k^* < 1 \end{cases}$$

This leads us to the task of quantifying loss due to integrality, which we address in Theorem 14 below.

Theorem 14. *The bit allocation obtained by relaxing integer constraints followed by flooring gives an additive approximation factor of*

$$\log_2 \left(1 + \max \left\{ \frac{1}{1 - c_1(N_t, N_r) 2^{c_2(N_t, N_r)}}, \frac{1}{1 - c_1(N_t, N_r)} \right\} \right) \left(\sum_{k=1}^K w_k \right).$$

Proof: See Appendix A.3. □

By applying Theorem 10 with $\mathbf{w} = \mathbf{q}$, we can conclude that the proposed relaxation-based algorithm will result in a throughput loss of at most $\log_2 \left(1 + \max \left\{ \frac{1}{1 - c_1(N_t, N_r) 2^{c_2(N_t, N_r)}}, \frac{1}{1 - c_1(N_t, N_r)} \right\} \right)$ bits per second for unsaturated systems. Furthermore, the result in Theorem 14 tells us that for single-stream beamforming/combining MIMO systems, the performance of relaxation-based algorithm approaches the optimal as $c_1(N_t, N_r)$ and $c_2(N_t, N_r)$ approach zero. This agrees with intuition because as $c_1(N_t, N_r)$ becomes small, the loss due to quantization decreases. Similarly, as $c_2(N_t, N_r)$ becomes small, we are dealing with codebooks that exhibit a slow rate of decay. This would mean that the flooring operation to obtain integral bits would not impact the SNR too much.

3.6 Performance of relaxation-based algorithm

In this section, we evaluate the accuracy of the convex-relaxation-based algorithm by plotting the distribution of the approximation factor

$$\log_2 \left(1 + \max \left\{ \frac{1}{1 - c_1(N_t, N_r)2^{c_2(N_t, N_r)}}, \frac{1}{1 - c_1(N_t, N_r)} \right\} \right)$$

over many RVQ codebook realizations. The goal of these experiments is to demonstrate that the quantized SNR functional form proposed in (3.24) is accurate for RVQ codebooks.

We generate an RVQ codebook, compute $c_1(N_t, N_r)$ and $c_2(N_t, N_r)$ for each codebook and the resulting approximation factor. We repeat this process for 1000 codebooks and plot the distribution of the approximation factor in Fig. 3.4. The distribution in Fig. 3.4 shows us that the convex relaxation

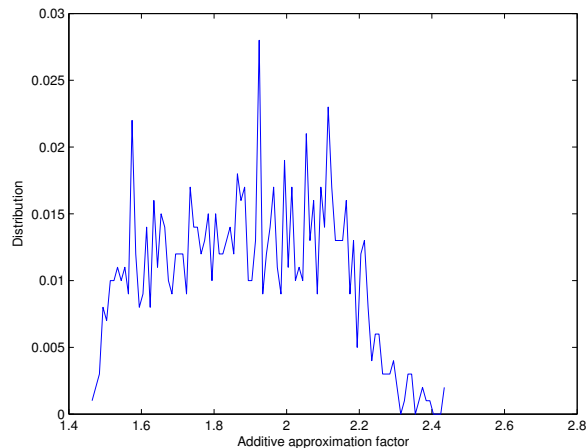


Figure 3.4: Distribution of $\log_2 \left(1 + \max \left\{ \frac{1}{1 - c_1(N_t, N_r)2^{c_2(N_t, N_r)}}, \frac{1}{1 - c_1(N_t, N_r)} \right\} \right)$ over 1000 codebook realizations.

technique offers us a guarantee of roughly 2 bits per second. Note that the

computation of $c_1(N_t, N_r)$ and $c_2(N_t, N_r)$ for each codebook is not optimized meaning that the above guarantee is conservative.

Finally, we compute $e(b)$ in Fig. 3.5 for one such RVQ codebook in order to demonstrate the implementability of this approach. From Fig. 3.5, it

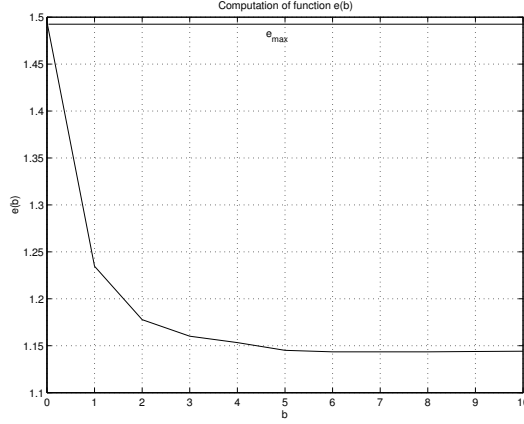


Figure 3.5: The function $e(b)$ in Fig. 3.5 for a 2×2 MIMO system over a Rayleigh fading channel with a randomly chosen codebook and $B = 10$.

is clear that $e_{max} \approx 1.5$ for this codebook.

3.7 Concluding remarks

We summarize the algorithmic contributions presented in Sections 3.4 and 3.5 in Table 3.1 where $M = \max \left\{ \frac{1}{1-c_1(N_t, N_r)2^{c_2(N_t, N_r)}} \frac{1}{1-c_1(N_t, N_r)} \right\}$. We observe from the table that these algorithms explore the tradeoffs between accuracy, computational efficiency and the structure of the weighted sum-rate function.

An interesting question and future direction pertaining to the section

on single-stream MIMO systems is whether such an analysis can be extended to cover other commonly-deployed MIMO architectures. Finally, the design of joint data scheduling and feedback allocation policies is another direction for future research.

In summary, we propose optimal feedback allocation policies for cellular uplink systems where the base station has a limited feedback budget. The optimality is in the sense of queue stability for unsaturated queueing regimes and long-term utility maximization for saturated queueing regimes. We show that a randomized optimal allocation policy can be computed by solving a convex optimization problem with linear constraints and with an exponentially large number of optimization variables. An optimal online allocation policy, one that involves solving a weighted sum-rate maximization problem at every scheduling instant, is presented as an alternative. This problem is solved using dynamic programming incurring pseudo-polynomial complexity in the number of users and the total bit budget. When the weighted sum-rate is a

Table 3.1: Properties of proposed online feedback allocation algorithms

Algorithm	Required structure on weighted sum-rate	Complexity	Multiplicative/Additive approximation factor
Dynamic Programming	None	$\mathcal{O}(KB^2)$	$1/0$
Greedy	Sub-modular weighted sum-rate	$\mathcal{O}((B + K)\log_2 K)$	$(1 - \frac{1}{\epsilon})/-$
Convex Relaxation	Sub-modular weighted sum-rate for specific MIMO systems	$\mathcal{O}(K\log_2 K)$	$-\log_2(1 + M)$

non-decreasing sub-modular function, we leverage the theory of sub-modular function maximization to propose a greedy algorithm with polynomial complexity that has a multiplicative approximation guarantee of $(1 - \frac{1}{e})$. For single-stream beamforming and combining MIMO physical layer communication schemes with quantized beamformer feedback, we recognize that the weighted sum-rate function is non-decreasing and sub-modular for RVQ codebooks. More importantly, it takes a special form that allows us to develop an approximation algorithm based on convex relaxations that can be solved in closed-form, incurring further-reduced complexity than the greedy algorithm. We connect the performance of the proposed approximate online algorithms to the long-term stability region of the system.

Chapter 4

Feedback allocation, fast data scheduling and interference

In the previous chapter, we considered systems where the data schedule was fixed and where users did not experience inter-user interference. We were only concerned with controlling the amount of self-interference, due to limited feedback, that each user experienced. In this chapter, we examine two extensions of the previous chapter. In the first part, we are interested in designing feedback allocation algorithms that operate in conjunction with fast frequency-domain scheduling (in contrast to Chapter 3) but in the absence of interference. In the second part, we study more general network structures where feedback allocation must take into account interference from other cells, however, under slow data scheduling as in Chapter 3. We show that convex relaxation, a technique that was used in Chapter 3, is applicable under both these wireless network settings.

4.1 Introduction

Over the last decade, there has been an ever-increasing demand for data-rate in wireless systems coupled with a growing scarcity in spectrum.

This calls for the network service providers to utilize available spectrum in as efficient a manner as possible to support these throughput demands. At the physical layer, it is well-known that the availability of channel state information at the transmitter (CSIT) and subsequent adaptation of the transmit strategy leads to an increase in link throughput. This availability of CSIT is made possible by the presence of feedback channels between every receiver and transmitter in the network. Feedback channels are a regular feature in most past, current and future wireless standards such as IS-95, GSM, Long-Term Evolution, WiMAX, etc. [73].

These feedback channels, which are a key enabler of future multiple-input-multiple-output enhancements in standards such as Long Term Evolution Advanced (LTE-A) [71, 72] and IEEE 802.16m [74], are unfortunately bandwidth-limited as well. This has prompted significant research into the impact of limited feedback bandwidth on the throughput of a system.

4.1.1 Prior work on feedback design

Past literature on feedback design for multi-user cellular systems can be broadly classified based on a physical versus network layer perspective. The former approach is typically applicable to *saturated* systems with infinitely-backlogged data. The weighted sum-rate per scheduling slot and the ergodic sum-rate are often-used metrics in this setting. For example, Chen et al. [80] and Agarwal et al. [81] design feedback protocols for orthogonal frequency-division multiple-access (OFDMA) per-instant weighted sum-rate scheduling.

Here, a set of channel thresholds are chosen that permit only a subset of users to report channel information, thereby achieving feedback reduction over a full CSI system where all users report channel states on all sub-bands. Dai et al. [85] and Jorswieck et al. [86] study the impact of limited feedback on MIMO uplink in terms of the ergodic sum-rate. Sanayei et al. [82] propose limited feedback schemes for a downlink single-antenna OFDMA system that achieves the same *scaling* in ergodic sum-rate as a full CSI system. Jindal [83] and Huang et al. [84] perform a similar analysis for a downlink space-division multiple-access system. Another online (per-instant) scheduling metric that has been considered extensively in the literature, as an alternative to the weighted sum-rate, is the weighted signal-to-noise-ratio (SNR) [87–94]. For example, the *normalized proportional fairness* scheduling rule, where the weights are set to be the inverse of the average SNR, has been studied in detail owing to its favourable fairness properties. Results have been reported both under ideal and quantized CSI settings [95–98].

In contrast to the above predominantly-physical-layer approaches, there has been research on the impact of limited feedback on queueing or unsaturated systems [101, 102, 161, 163], where the feedback constraint has been modelled in a variety of ways. For instance, Gopalan et al. [161] consider a setting where only a subset of users are allowed to feedback their CSI following which MaxWeight scheduling is performed [48] for data transmission, i.e., the user with the largest weighted rate is scheduled. The task of the decision-maker in this case is to determine which subset of users to sample prior to MaxWeight

scheduling. Huang et al. [101] consider a zero-forcing space-division-multiple-access downlink transmission scheme and analyse the loss in throughput due to limited feedback from the mobile to the base-station. The authors quantify the number of feedback bits per mobile necessary to achieve a given loss in throughput. Ouyang et al. [163] consider the downlink of an orthogonal-frequency-division-multiple-access network with a limited feedback model where the base station is able to acquire channel state information on a restricted number of frequency bands. In particular, each user is instructed to report CSI for at most F_i bands such that $\sum_i F_i$ does not exceed the total feedback budget. Following CSI acquisition, MaxWeight scheduling is performed. The authors prove throughput-optimality of the Longest-Queue-First Feedback Allocation policy under the ON-OFF channel model along with a mean approximation. The authors also quantify the shrinkage in the rate region under the same policy as a function of the limited feedback budget but without the mean approximation. In Chapter 3 of this thesis, we introduced a limited feedback model for uplink systems where the base-station is constrained in the number of bits that form the feedback packet that is broadcast to the users. Computationally-efficient algorithms were presented that compute the optimal (or near-optimal) feedback partitioning across users as a function of the channel and queue state as well as other network parameters. A key assumption made in the earlier chapter was that the data scheduling decisions were already made, i.e., each user was assigned to one frequency band prior to feedback optimization.

4.1.2 Our contributions

This chapter contains two extensions to the model in Chapter 3 as opposed to single-cell uplink that was treated earlier.

In the first part of the chapter, we consider a setting where data transmission occurs on the faster time-scale (for example, one millisecond in the case of LTE) and feedback allocation is done less often on the time scale of large-scale fading. This is in contrast to Chapter 3 where we assume fixed data schedules prior to feedback optimization. Single-cell downlink OFDMA systems are considered with weighted-SNR scheduling. We show that under uniform quantization, the resulting feedback allocation problem is convex thereby admitting efficient solutions using standard convex optimization-based techniques.

In the second part of the chapter, we consider the reverse setting where feedback allocation occurs on the faster time-scale and the data schedules change very slowly reverting back to the setup in Chapter 3. However, we now study interference-limited networks and the impact of feedback allocation on the same, a scenario that was not considered in the previous chapter. More specifically, we consider a multi-cell uplink system with one multiple-antenna user active per frequency per cell, pre-computed by the data scheduler. All mobiles in the system adopt the zero-forcing interference-cancellation strategy. Ideally, under infinite capacity feedback, we are able to eliminate completely the interference contributions to the neighbouring links. Under limited feedback however, perfect interference cancellation is not possible under zero-

forcing making the allocated feedback bandwidth the sole cause of interference, thereby requiring careful management. Here, we show that resulting feedback allocation problem is convex under the popular Random Vector Quantization (RVQ) codebooks.

4.1.3 Chapter organization

The rest of this chapter is organized as follows. In Section 4.2, we introduce the network model with emphasis in the role of feedback channel. In Section 4.3, we study feedback allocation for multi-antenna systems with interference. We move on to the second part of the chapter where we consider a single-cell OFDMA system in Section 4.4. We conclude the chapter with some remarks in Section 4.5.

4.2 System model

Consider a network comprised of K wireless transceiver pairs (i.e., a one-hop network). Time is slotted and in each time slot, a subset of these links are scheduled. Note that once scheduled, the transmissions might still interfere with each other as is the case in many common scenarios. Examples of such scenarios include an adhoc network with uncoordinated transmissions or a cellular network with full frequency re-use where each cell employs orthogonal signalling. On the other hand, the subset of scheduled links can also be interference-free as is the case in a hexagonally-deployed cellular network with a frequency re-use factor of six and intra-cell orthogonal multiple-access.

Channel State and achievable rate: The channel state of the network at time t is given by $\left\{ \left(g_{ij} \left\lfloor \frac{t}{T_{LS}} T_{LS} \right\rfloor, H_{ij}[t] \right) \right\}_{(i,j) \in \{1, \dots, K\}^2}$ where $g_{ij} \left\lfloor \frac{t}{T_{LS}} \right\rfloor$ models the large-scale (fading channel between transmitter i and receiver j and $T_{LS} \in \{1, 2, 3, \dots\}$ denotes the large-scale fading coherence time counted in terms of scheduling slots; $\mathbf{H}_{ij}[t] \in \mathbb{C}^{N_{r,j} \times N_{t,i}}$ denotes the small-scale fading matrix channel between transmitter i with $N_{t,i}$ antennas and receiver j with $N_{r,j}$ antennas. Note that in some specific cases such as single-cell multi-user uplink, the index j becomes redundant since the base station is the sole receiver here. For ease of notation, we will collect together the large-scale and small gains to form sets $G[t] = \{g_{ij}[t]\}_{i,j}$ and $H[t] = \{\mathbf{H}_{ij}[t]\}_{i,j}$ respectively. We denote the channel state of the system by $C[t] = (G[t], H[t])$. We assume that each scheduling slot is designed to span a small-scale fading coherence time. We assume that each large-scale fading coefficient g comes from a *finite* state space \mathcal{S}_l with probability distribution $\{p_g\}_{g \in \mathcal{S}_l}$ that is independent and identical across all (i, j) ¹. Each small-scale fading coefficient h comes from a *continuous* state space \mathcal{S}_s with probability density function $f_h(x)$, $x \in \mathcal{S}_s$, (e.g., Rayleigh distribution) that is independent and identical across all (i, j) . For convenience, we define the joint probability density functions $f_G(\mathbf{X}) = \prod_{(i,j)} p_{x_{ij}}$ and $f_H(\mathbf{X}) = \prod_{(i,j)} f_{\mathbf{H}}(x_{ij})$.

¹This assumption is not necessary for our results to hold and is in place for ease of notation.

Quantization and Feedback: We assume that the large-scale fading channel state $\mathbf{G}[t]$ is known perfectly to the decision makers in the system since this is a slowly-varying quantity that is typically position-dependent². With respect to the small-scale fading channel state, we assume that receiver j can measure $\mathbf{h}_j[t] = [h_{1j}[t] \ h_{2j}[t] \ \dots \ h_{Kj}[t]]^T$ perfectly. This can be accomplished through the transmission of pilots by all the appropriate transmitters. Now, once this is measured, we require a mechanism to (i) communicate this information to the decision makers in order to facilitate link scheduling and (ii) advise the transmitters of the rate at which they must transmit. In general, these two tasks are accomplished through the insertion of feedback channels into the network. If these feedback channels were of infinite capacity, there would be no loss of information in this process but in practice, this is of course not the case. Feedback channels are bandwidth-limited and hence, we need to understand how this can potentially affect the throughput of the network.

Let us consider the case of uplink. Here, the receivers (base stations) are the decision-makers and have access to perfect (but maybe local) channel information. Once a scheduling decision has been made, rate instructions must be transferred to the transmitter-side through the feedback channel. This immediately leads to a loss in throughput as quantized feedback precludes transmission at the true rate offered by the channel. In the downlink scenario, the situation is slightly different. Here the decision-makers reside at the

²This assumption is not unreasonable given the increasing trend towards GPS-enabled devices.

transmitter-side while the receivers have access to perfect (but maybe local) channel information. Quantized feedback from the receivers to the transmitters in this setting means that the scheduling decisions at the transmitter-side can never be based on perfect information. This in turn leads to a loss in throughput.

We now introduce some notation in order to formalize the above arguments. Let the bandwidth of the feedback channel serving transceiver pair j be denoted by b_j . Then, given channel state $\mathbf{h}_j[t]$ and a serving feedback channel with bandwidth b_j , the corresponding quantized channel state is given by $\mathbf{h}_j^{b_j}[t]$. Here, we make an implicit assumption that a separate codebook is used for each link following the approach of recent literature on multi-user limited feedback. Furthermore, we assume that these codebooks are pre-decided. We collect these feedback budgets and resulting quantized small-scale channel gains across all transceiver pairs to form a feedback allocation vector \mathbf{b} and quantized channel $H^{\mathbf{b}}[t]$. We can then define the corresponding quantized composite channel state $C^{\mathbf{b}}[t] = (G[t], H^{\mathbf{b}}[t])$. Note that there is no quantization under infinite feedback bandwidth, i.e., $C[t] = C^\infty[t] = (G[t], H^\infty[t])$, $\forall t$.

4.3 Part I: Feedback allocation under fast data scheduling

In this section, we consider the downlink of an OFDMA cellular network with sufficiently small frequency re-use to ensure that there is no inter-cell

interference. This means that it suffices to study the throughputs in a single cell. Furthermore, we study the throughputs on a single sub-band since the cell throughput scales linearly in the number of sub-bands. We consider feedback allocation under single-cell weighted-SNR scheduling and show that the resulting problem is convex and hence admits efficient, though sub-optimal, algorithmic solutions.

The K wireless links in the context of a single-cell OFMDA system where we are interested in per-band throughputs correspond to the channels between the base station and the K users it serves. The SNR for link i is given by

$$\text{SNR}_i[t] = \frac{P g_{ii} [\bar{t} T_{LS}] h_{ii}[t]}{N_o}.$$

The family of weighted-SNR scheduling policies [87–94] under infinite feedback chooses user

$$i^* = \operatorname{argmax}_i w_i [\bar{t} T_{LS}] \text{SNR}_i[t]. \quad (4.1)$$

at each instant. Then, the per-band average rate for link i in the ideal case (without quantization), through the course of T_{LS} scheduling slots where the path-loss coefficients $\{g_{ii}\}_i$ remain constant, can be bounded as

$$\begin{aligned} & \bar{\mu}_i^* [\mathbf{w}, \operatorname{diag}\{\mathbf{G}\}] \\ = & \Pr(\text{link } i \text{ is chosen}) \mathbb{E}_{\mathbf{h}} \left[\log_2 \left(1 + \frac{P g_{ii} h_{ii}}{N_o} \right) \mid \text{link } i \text{ is chosen} \right] \\ & \text{where } \mathbf{h} = \operatorname{diag}\{\mathbf{H}\} \\ = & \Pr \left(i = \arg \max_j w_j \frac{P g_{jj} h_{jj}}{N_o} \right) \mathbb{E}_{\mathbf{h}} \left[\log_2 \left(1 + \frac{P g_{ii} h_{ii}}{N_o} \right) \mid i = \arg \max_j \beta_j h_{jj} \right] \\ = & \Pr (i = \arg \max_j \beta_j h_{jj}) \mathbb{E}_{\mathbf{h}} \left[\log_2 \left(1 + \frac{P g_{ii} h_{ii}}{N_o} \right) \mid i = \arg \max_j \beta_j h_{jj} \right] \\ \leq & \Pr (i = \arg \max_j \beta_j h_{jj}) \mathbb{E}_{\mathbf{h}} \left[\log_2 \left(1 + \frac{P g_{ii} h}{N_o} \right) \right], \end{aligned} \quad (4.2)$$

where $\beta_j = \frac{Pg_{ji}w_i}{N_o}$. The last step follows since $\mathbb{E}_h \left[\log_2 \left(1 + \frac{Pg_{ii}h}{N_o} \right) \right]$ is the best-possible rate the user can achieve assuming no other user in the system is served. As would be expected, the rate obtained by the users in system critically depend on the ratios

$$\sigma_{ij} = \frac{\beta_i}{\beta_j}, \quad (4.3)$$

as we will precisely characterize later in this section.

Now, a more realistic system with quantization and feedback operates as follows. The mobile quantizes the small-scale fading channel gain h_{ii} and reports channel gain $[h_{ii}]_{b_i}$. We use a simple uniform quantization policy that is comprised of 2^{b_i} levels in the range $[0, M]$; M is chosen such that

$$M = \max\{\gamma_1\sigma_{\max}, \gamma_2\} \quad (4.4)$$

where γ_1, γ_2 are large positive constants and $\sigma_{\max} = \max_{ij}\{\sigma_{ij}\}$. The quantized state is given by

$$[h_{ii}]_{b_i} = \left\lfloor \frac{h_{ii}2^{b_i}}{M} \right\rfloor \frac{M}{2^{b_i}}. \quad (4.5)$$

Then, the rate for link i with quantization is

$$\begin{aligned} & \bar{\mu}_i[\mathbf{w}, \mathbf{G}[\bar{t}T_{LS}], \mathbf{b}] \\ = & \Pr(i = \arg \max_j \beta_j [h_{jj}]_{b_j}) \mathbb{E}_{\mathbf{h}} \left[\log_2 \left(1 + \frac{Pg_{ii}[h_{ii}]_{b_i}}{N_o} \right) \mid i = \arg \max_j \beta_j [h_{jj}]_{b_j} \right]. \end{aligned} \quad (4.6)$$

Having expressed the average rates through one large-scale coherence time of T_{LS} time slots in (4.2) and (4.6), we now describe our proposed two time-scale feedback allocation and data scheduling policy below:

Algorithm 1 Joint feedback allocation and data scheduling

- 1: **for** $t = \bar{t}T_{LS}, \dots, \bar{t}T_{LS} - 1$ **do**
- 2: (*Slow feedback allocation*): The feedback allocation vector \mathbf{b} is given as the solution to

$$\begin{aligned} \mathbf{b}^* = \arg \min \quad & c(\mathbf{b}) \\ \text{s.t.} \quad & \bar{\mu}_i[\mathbf{w}, \mathbf{G}[\bar{t}T_{LS}], \mathbf{b}] \geq \delta \bar{\mu}_i^*[\mathbf{w}, \mathbf{G}[\bar{t}T_{LS}]], \quad \forall i \\ & b_k \in \{0, 1, \dots, \infty\}. \end{aligned} \quad (4.7)$$

where $c(\mathbf{b}) = \sum_k \gamma_k b_k$ or $c(\mathbf{b}) = \min \max_k \gamma_k b_k$.

- 3: (*Fast data scheduling*): Given \mathbf{b}^* , the users are scheduled according to

$$i^* = \arg \max_i w_i[\bar{t}T_{LS}] \frac{Pg_{ii}[\bar{t}T_{LS}][h_{ii}[t]]_{b_i^*}}{N_o}. \quad (4.8)$$

- 4: **end for**
-

In what follows, we derive a lower bound on the ratio $\frac{\bar{\mu}_i[\mathbf{w}, \mathbf{G}[\bar{t}T_{LS}], \mathbf{b}]}{\bar{\mu}_i^*[\mathbf{w}, \mathbf{G}[\bar{t}T_{LS}]]}$. This lower bound possesses the property that as $\mathbf{b} \rightarrow \infty$ element-wise and as $M \rightarrow \infty$, the bound approaches one, which agrees with intuition and means that (4.7) is feasible for any δ . Most importantly, we show that the bound is convex in \mathbf{b} . The bound is derived using the following four lemmas. The first two lemmas derive a lower and upper bound on $\Pr(i = \arg \max_j \beta_j h_{jj})$ and $\Pr(i = \arg \max_j \beta_j [h_{jj}]_{b_j})$ respectively. The third lemma derives a lower bound on

$$\mathbb{E}_{\mathbf{h}} \left[\log_2 \left(1 + \frac{Pg_{ii}[h_{ii}]_{b_i}}{N_o} \right) \mid i = \arg \max_j \beta_j [h_{jj}]_{b_j} \right].$$

Lemma 13. *Given any set of non-negative, constants $\{\kappa_i\}_{i=1}^N$ with $\kappa_1 = 1$,*

the following relationship holds for $N \geq 2$

$$\int_{x_k \kappa_N} \int_{x_{k-1} \kappa_{k-1}} \dots \int_{x_2 \kappa_2} e^{-w} \prod_{i=2}^{k-1} e^{-x_i} dw dx_2 dx_3 \dots dx_{k-1} = \left[\prod_{i=1}^{k-1} \frac{1}{\delta_i} \right] e^{-\delta_{k-1} \kappa_k x_k}. \quad (4.9)$$

where $\delta_1 = 1$ and $\delta_i = \delta_{i-1} \kappa_i + 1$.

Proof. Refer to Appendix B.1. □

For the purposes of the next few lemmas, we introduce some notation. Let \mathcal{P}_k denote the set of all permutations of $\{1, 2, \dots, K\}$ with k as the first element of the sequence, i.e., for all $\mathbf{p} = (i_1, i_2, \dots, i_K) \in \mathcal{P}_k$, we have that $i_1 = k$.

Lemma 14. *The probability of user k begin scheduled in the case where there is no quantization can be computed as*

$$Pr \left(k = \arg \max_j \beta_j h_{jj} \right) = \sum_{\mathbf{p} \in \mathcal{P}_k} \prod_{j=1}^K \frac{1}{\delta_j^{\mathbf{p}}}$$

where $\delta_1^{\mathbf{p}} = 1$ and $\delta_j^{\mathbf{p}} = \delta_{j-1}^{\mathbf{p}} \sigma_{p(j)k} + 1$.

Proof. Refer to Appendix B.1. □

Extending the above analysis to cover the case with quantization poses significant analytical challenges as we will see. Nevertheless, we infuse analytical tractability and obtain insightful closed-form expressions by making the simple approximation $\exp \left(-\frac{M}{\sigma_{\max}} \right) \approx 0$. This is reasonable because, by definition in (4.4), M scales with σ_{\max} and $\exp \left(-\frac{M}{\sigma_{\max}} \right) \leq \exp(-\gamma_1)$ which can be

made as small as we wish for γ_1 sufficiently large. For convenience, we will use $x \doteq y$ to mean “ x is equal to y under the approximation $\exp\left(-\frac{M}{\sigma_{\max}}\right) = 0$ ” and $x \dot{\geq} y$ to mean “ x is greater than or equal to y under the approximation $\exp\left(-\frac{M}{\sigma_{\max}}\right) = 0$ ”.

Lemma 15. *The probability of user k begin scheduled in the case where there is quantization and when \mathbf{b} satisfies the added constraints*

$\left\{ \sum_{j=1}^{K-2} \sigma_{ji} 2^{-b_j} \leq 1 - \frac{1}{\gamma_3}, \forall i \right\}$ can be bounded as

$$\begin{aligned} Pr(k = \arg \max_j \beta_j [h_{jj}]_{b_j}) &\dot{\geq} \sum_{\mathbf{p} \in \mathcal{P}_k} e^{-M \sum_{i=1}^K \gamma_i^{\mathbf{p}} \delta_i^{\mathbf{p}}} \left[\prod_{j=1}^K \frac{1}{\delta_j^{\mathbf{p}}} \right] \\ &\geq \left(e^{-M \max_{\mathbf{p} \in \mathcal{P}_k} \sum_{i=1}^K \gamma_i^{\mathbf{p}} \delta_i^{\mathbf{p}}} \right) \sum_{\mathbf{p} \in \mathcal{P}_k} \prod_{j=1}^K \frac{1}{\delta_j^{\mathbf{p}}} \end{aligned}$$

where $\delta_1^{\mathbf{p}} = 1$ and $\delta_j^{\mathbf{p}} = \delta_{j-1}^{\mathbf{p}} \sigma_{p(j)k} + 1$.

Proof. Refer to Appendix B.1. □

Lemma 16. (a) *Let $i^* = \arg \max_j \beta_j$ be the user with highest priority. Then, for this user, the rate with quantization can be bounded as*

$$\begin{aligned} &\mathbb{E}_{\mathbf{h}} \left[\log_2 \left(1 + \frac{Pg_{ii}[h_{ii}]_{b_i}}{N_o} \right) \mid i = \arg \max_j \beta_j [h_{jj}]_{b_j} \right] \\ &\geq (1 - 2^{-b_{i,\min}}) \mathbb{E}_{h_{kk}} \left[\log_2 \left(1 + \frac{Pg_{ii}h_{kk}}{N_o} \right) \mid h_{kk} \in \left[\frac{M}{2^{b_j}}, M \right] \right], \end{aligned}$$

where $b_{i,\min} = \min_{j \neq i} b_j$.

(b) *For the remaining users, the rate with quantization can be bounded as*

$$\begin{aligned} &\mathbb{E}_{\mathbf{h}} \left[\log_2 \left(1 + \frac{Pg_{ii}[h_{ii}]_{b_i}}{N_o} \right) \mid i = \arg \max_j \beta_j [h_{jj}]_{b_j} \right] \\ &\geq (1 - 2^{-b_{i,\min}}) \mathbb{E}_{h_{kk}} \left[\log_2 \left(1 + \frac{Pg_{ii}\sigma_i^* h_{kk}}{N_o} \right) \mid h_{kk} \in \left[\frac{M}{2^{b_j}}, M \right] \right]. \end{aligned}$$

Proof. Refer to Appendix B.1. □

By applying the results in Lemmas 14, 15 and 16, we now present the main result of this section.

Theorem 15. *Given priority vector \mathbf{w} , large-scale gains $\mathbf{G}[\bar{t}T_{LS}]$ and bit allocation \mathbf{b} that satisfies the constraints $\{\sum_{j=1}^{K-2} \sigma_{ji} 2^{-b_j} \leq 1 - \frac{1}{\gamma_3}, \forall i\}$, the loss in rate due to quantization is given by*

$$\frac{\bar{\mu}_i[\mathbf{w}, \mathbf{G}[\bar{t}T_{LS}], \mathbf{b}]}{\bar{\mu}_i^*[\mathbf{w}, \mathbf{G}[\bar{t}T_{LS}]]} \geq \left(e^{-M \max_{\mathbf{p} \in \mathcal{P}_i} \sum_{i=1}^K \gamma_i^{\mathbf{p}} \delta_i^{\mathbf{p}}} \right) (1 - 2^{-b_{i,\min}}).$$

Proof. Refer to Appendix B.2. □

By applying the result in Theorem 15 and including the extra constraints mentioned therein, we can re-write problem (4.7) as

$$\begin{aligned} \min \quad & \sum_i c(\mathbf{b}) \\ \text{s.t.} \quad & \left(e^{-M \max_{\mathbf{p} \in \mathcal{P}_i} \sum_{i=1}^K \gamma_i^{\mathbf{p}} \delta_i^{\mathbf{p}}} \right) (1 - 2^{-b_{i,\min}}) \geq \delta_i, \forall i \\ & \sum_{j=1}^{K-2} \sigma_{ji} 2^{-b_j} \leq 1 - \frac{1}{\gamma_3}, \forall i. \end{aligned} \quad (4.10)$$

Sufficiently small throughput degradation targets δ_i , which is often the regime of interest, would ensure large optimal feedback allocations rendering the second set of convex constraints redundant. We will therefore focus only on the first set of constraints and establish their convexity. By applying a $-\log(\cdot)$ -transformation, we write the following equivalent constraint

$$-M \max_{\mathbf{p} \in \mathcal{P}_i} \sum_{i=1}^K \gamma_i^{\mathbf{p}} \delta_i^{\mathbf{p}} - \log(1 - 2^{-b_{i,\min}}) \leq -\log(\delta_i), \forall i.$$

It is well-known that for any convex function $f : \mathbb{R}^K \rightarrow \mathbb{R}$, the sub-level sets $\{\mathbf{x} : f(\mathbf{x}) \leq a\}$, $a \in \mathbb{R}$, it induces are convex. Thus, it is sufficient for us to

show that

$$h_i(\mathbf{b}) = -M \max_{\mathbf{p} \in \mathcal{P}_i} \sum_{i=1}^K \gamma_i^{\mathbf{p}} \delta_i^{\mathbf{p}} - \log(1 - 2^{-b_{i,\min}})$$

are convex for all i in order to establish that the resource allocation problem in (4.10) under the structure imposed by weighted-SNR scheduling. This follows directly from two facts. The first fact is that the set of convex functions is closed under the sum and maximum operators. The second fact is that the functions 2^{-x} , $x > 0$ and $2^{-\min_i x_i} = \max_i 2^{-x_i}$ are convex.

Once the fractional solution b_j^* , $j = 1, \dots, N$, to (4.10) is computed, we obtain the integral solution through the operation $b_j^I = \lceil b_j^* \rceil$. The increase in the feedback budget due to this operation is quantified in the following theorem.

Theorem 16. *The convex relaxation algorithm has the following approximation guarantees:*

- (i) $\sum_i \gamma_i b_i^I \leq \sum_i \gamma_i b_i^* + N\gamma_{\max}$
- (ii) $\max_i \gamma_i b_i^I \leq \min \max_i \gamma_i b_i^* + \gamma_{\max}$

where $\gamma_{\max} = \max_i \gamma_i$.

Proof. Both results follow from the fact that $b_i^I \leq b_i^* + 1$. □

It is well-known that if one uses interior point methods [144] to solve (4.7), the number of Newton steps to arrive within ε of the optimal solution scales as $\mathcal{O}\left(\sqrt{K} \log\left(\frac{K}{\varepsilon}\right)\right)$.

Next, we study feedback allocation for networks with interference. We revert back to the setting in Chapter 3 where data scheduling is performed on a slow time-scale. We show that here too, convex optimization may be used to compute efficient solutions.

4.4 Part II: Feedback allocation with interference

In this section, we focus on uplink multi-antenna networks, where the mobiles transmit using block-diagonalization, which is a well-established interference cancellation technique [139–143]. The structure induced by block-diagonalization precoding and allows us to leverage convex optimization-based techniques to solve the resulting feedback allocation problem.

Consider a wireless network of K mobiles, that have been pre-selected by some scheduling policy, and are communicating with their corresponding home base stations. The K mobiles and base stations are each equipped with $N_{t,i}$ and $N_{r,i}$ transmit and receive antennas respectively. Each mobile transmits elements of a Gaussian codeword x_i with power P_i . A transmission from mobile i passes through channels $\{g_{ij}\mathbf{H}_{ij}\}_{j \in \mathcal{N}_e(i)}$ where g_{ij} is the path-loss and \mathbf{H}_{ij} is the MIMO channel between mobile i and base station j . As in the earlier section, the path-loss coefficients changes every T_{LS} slots and we are interested in making feedback allocations on this slower time-scale. First, we study the infinite feedback case before introducing the effects of quantization. Under perfect feedback, the discrete-time equivalent sampled signal model for one channel use at baseband with perfect synchronization at receiver i can be

written as

$$\begin{aligned} \mathbf{y}_i &= \sqrt{P_i} \mathbf{G}_{ii} \mathbf{w}_i x_i + \sum_{j \in \mathcal{N}(i)} \sqrt{P_j} \mathbf{G}_{ji} \mathbf{w}_j x_j + \mathbf{n}_i \\ &= \sqrt{\alpha_{ii} P_i} \mathbf{H}_{ii} \mathbf{w}_i x_i + \sum_{j \in \mathcal{N}(i)} \sqrt{\alpha_{ji} P_j} \mathbf{H}_{ji} \mathbf{w}_j x_j + \mathbf{n}_i, \end{aligned} \quad (4.11)$$

where $\mathbf{n}_i \sim \mathcal{CN}(0, N_o \mathbf{I})$ is additive white Gaussian noise that is independent across receivers. Recall that the receiver has perfect knowledge of the channel states $\{\mathbf{H}_{ji}\}_{j \in \mathcal{N}_e(i)}$. According to the block-diagonalization approach, the precoder $\mathbf{w}_i \in \mathbb{C}^{N_{t,i} \times 1}$ is selected to satisfy

$$\mathbf{H}_{ij} \mathbf{w}_i = \mathbf{0}, \quad j \in \mathcal{N}(i) \quad (4.12)$$

thereby eliminating all interference user i generates. We assume that the number of transmit antennas at user i is $N_{t,i} > \sum_{j \in \mathcal{N}(i)} N_{r,j} + 1$ since this is required in order to cancel $\sum_{j \in \mathcal{N}(i)} N_{r,j}$ interfering dimensions. This follows from the fact that the null space of the augmented matrix $[\{\mathbf{H}_{ij}\}_{j \in \mathcal{N}(i)}]$ has dimension $N_{t,i} - \min\{\sum_{j \in \mathcal{N}(i)} N_{r,j}, N_{t,i}\}$. Thus, the maximum number of independent data streams that can be transmitted is $\min\{N_{t,i} - \min\{\sum_{j \in \mathcal{N}(i)} N_{r,j}, N_{t,i}\}, N_{r,i}\}$. We let $\bar{\mu}_i^*[\mathbf{G}[\bar{t}T_{LS}]]$ denote the rate under infinite capacity.

This technique is being actively researched in industry as a multiple-antenna interference mitigation solution on the uplink [107–111]. Furthermore, the proposed uplink interference cancellation model finds concrete application in recent deployments of distributed antenna systems, a topic of active research [113–118], by AT&T in Palo Alto, California [112] and at other locations around the continent such as Seattle, Philadelphia and San Diego to name a few [119–123]. In Palo Alto for instance, AT&T envisions putting up

small antenna units on utility poles for instance to improve capacity. These small antennas are linked to a centralized controller through high-speed backhaul. The other use case involves covering high-load areas such as stadiums and theme parks with distributed antennas [121–123]. These are real-world scenarios where it is indeed possible for a multi-antenna mobile to be interfering with many single-antenna receivers and thus falls squarely in the regime where our results are applicable, and hence our optimization algorithms can be used to efficiently compute optimal feedback allocations. Yet another potential application involves the future deployment of “lightRadios” by Alcatel-Lucent [124], which again are low-cost single antenna nodes that might receive transmissions from multi-antenna mobiles.

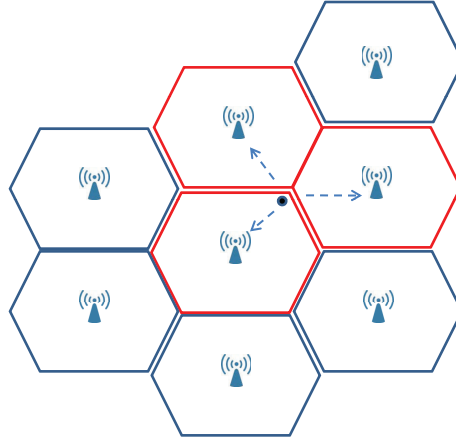


Figure 4.1: Uplink interference neighbourhood

Note that any kind of coordinated beamforming such as block-diagonalization requires the presence of control channels connecting neighbouring links. Exchange of real-time channel information through high-capacity backhaul links

is being seriously considered [131] in both major IMT Advanced candidate standards, LTE-A and IEEE 802.16m. Since feedback in realistic systems is imperfect due to limited feedback budgets, we must consider and appropriately incorporate the effects of quantization error – error that is introduced when the receiver quantizes the precoder \mathbf{w}_i using b_i bits in preparation for feedback – into our signal model in (4.11). The quantized precoder is denoted by $\hat{\mathbf{w}}_i$ and the signal model with limited feedback now becomes

$$\mathbf{y}_i = \sqrt{\alpha_{ii}P_i}\mathbf{H}_{ii}\hat{\mathbf{w}}_ix_i + \sum_{j \in \mathcal{N}(i)} \sqrt{\alpha_{ji}P_j}\mathbf{H}_{ji}\hat{\mathbf{w}}_jx_j + \mathbf{n}. \quad (4.13)$$

We let $\bar{\mu}_i[\mathbf{G}[\bar{t}T_{LS}], \mathbf{b}]$ represent the rate under feedback allocation \mathbf{b} .

Similar to the last section, we are interested in the following resource allocation problem

$$\begin{aligned} \mathbf{b}^* = \arg \min \quad & c(\mathbf{b}) \\ \text{s.t.} \quad & \bar{\mu}_i[\mathbf{G}[\bar{t}T_{LS}], \mathbf{b}] - \bar{\mu}_i^*[\mathbf{G}[\bar{t}T_{LS}]] \leq \delta, \quad \forall i \\ & b_k \in \{0, 1, \dots, \infty\}. \end{aligned} \quad (4.14)$$

where $c(\mathbf{b}) = \sum_k b_k$ or $c(\mathbf{b}) = \min \max_k b_k$. However, in contrast to the earlier section where the focus was on a multiplicative loss in throughput, here we are interested in the additive loss due to quantization. The impact of limited feedback on block-diagonalization precoding has been studied by Jindal [83] and Ravindran et al. [133]. We leverage these results in order to write down the rate loss

$$\bar{\mu}_i^*[\mathbf{G}[\bar{t}T_{LS}]] - \bar{\mu}_i[\mathbf{G}[\bar{t}T_{LS}], \mathbf{b}] \leq \delta$$

as a function of the quantization bits available. Ravindran et al. [133] and Jindal [83] bound the loss in rate due to quantization, specifically random

vector quantization, but in their model, all receivers quantize the precoders using the same budget. Since this is not the case in our setup, we re-derive their result with this minor generalization in Theorem 17 below. The proof is given in Appendix B.3.

Theorem 17. *When all users transmit one stream and maximal-ratio-combining aligned to the quantized precoder is used at the receiver, the rate loss for user i due to quantization by its receiver as well as in its neighbouring cells is given by*

$$\bar{\mu}_i^* [\mathbf{G} [\bar{t}T_{LS}]] - \bar{\mu}_i [\mathbf{G} [\bar{t}T_{LS}], \{b_j\}_{j \in \mathcal{N}(i)}] = \log_2 \left(1 + N_{t,i} \sum_{j \in \mathcal{N}(i)} g_{ji} P_j N_{r,i} \frac{\Delta_j(b_j)}{N_{t,i} - 1} \right), \quad (4.15)$$

where $\Delta_j(b_j) = 2^{-\frac{b_j}{N_{t,j}-1}}$.

From the above theorem, it becomes clear that the feedback budget is especially crucial for scenarios where users transmit using block-diagonalization. Under ideal conditions (infinite feedback capacity and a sufficient number of antennas), the interference terms would be *completely nulled* using block-diagonalization. This is as opposed to other strategies where there would be residual interference even under ideal conditions. Limited feedback however introduces an interference contribution with power that is proportional to the feedback budget.

Substituting the rate functions derived in the above theorem into (4.14), the resource allocation problems for a block-diagonalization-based MIMO sys-

tem with random vector quantization become

$$\begin{aligned} \min \quad & \sum_i c(\mathbf{b}) \\ \text{s.t.} \quad & \sum_{j \in \mathcal{N}(i)} a_{ji} \Delta_j(b_j) \leq 2^\delta - 1, \quad \forall i, \\ & b_i \in \mathbb{N}_0, \quad \forall i \end{aligned} \quad (4.16)$$

where $a_{ji} = \frac{N_{t,i} g_{ji} P_j N_{r,i}}{N_{t,i} - 1}$, $j \neq i$ when all users transmit one stream and perform maximal-ratio-combining at the receiver. Dropping the integral constraints in the above equivalent problem, we obtain the following convex programs:

$$\begin{aligned} \min \quad & -\sum_i \gamma_i \log_2 \tilde{b}_i \\ \text{s.t.} \quad & a_{ii} \tilde{b}_i + \sum_{j \in \mathcal{N}(i)} a_{ji} \tilde{b}_j \leq d_i \\ & \tilde{b}_i \in [0, 1], \quad \forall i \end{aligned} \quad (4.17)$$

and

$$\begin{aligned} \min \quad & \max_i -\gamma_i \log_2 \tilde{b}_i \\ \text{s.t.} \quad & a_{ii} \tilde{b}_i + \sum_{j \in \mathcal{N}(i)} a_{ji} \tilde{b}_j \leq d_i \\ & \tilde{b}_i \in [0, 1], \quad \forall i \end{aligned} \quad (4.18)$$

Convexity of the above problem enables us to utilize standard numerical solvers from convex optimization to solve (4.17) and (4.18). In the following theorem, we go a step further and use the Karush-Kuhn-Tucker (KKT) conditions to compute an optimal solution to (4.17) in closed form. It is less straightforward to compute the solution to (4.18) in closed form.

Theorem 18. *The solution to (4.17) is*

$$\tilde{b}_j^* = \left[\left(\frac{1}{\log 2} \right) \frac{\gamma_j}{\sum_{k \in \mathcal{N}(j) \cup \{j\}} \lambda_k^* a_{kj}} \right]_1^+, \quad (4.19)$$

where $\{\lambda_j^*\}_{j=1}^N$ is chosen to satisfy the constraints $a_{ii} \tilde{b}_i^* + \sum_{j \in \mathcal{N}(i)} a_{ji} \tilde{b}_j^* \leq d_i, \quad \forall i$.

Proof. Refer to Appendix B.4. □

Once the fractional solution $b_j^* = -\log_2 \tilde{b}_i^*$, $j = 1, \dots, N$, to (4.17) or (4.18) is computed, we obtain the integral solution through the operation $b_j^I = \lceil b_j^* \rceil$. The increase in the feedback budget due to this operation is quantified in the following theorem.

Theorem 19. *The convex relaxation algorithm has the following approximation guarantees”*

- (i) $\sum_i \gamma_i b_i^I \leq \sum_i \gamma_i b_i^* + N\gamma_{\max}$
- (ii) $\max_i \gamma_i b_i^I \leq \min \max_i \gamma_i b_i^* + \gamma_{\max}$

Proof. Both results follow from the fact that $b_i^I \leq b_i^* + 1$. □

The solution in (4.19) allow us to study the behaviour of the allocation as function of the system parameters. In (4.19), if we interpret λ_k^* as the price charged by access point k for receiving one unit of interference (from in-cell and out-of-cell), then the bit allocation for user j is inversely proportional to the ratio of the cost per feedback bit for cell k over the total price it pays for the interference it generates $\sum_{k \in \mathcal{N}(j) \cup \{j\}} \lambda_k^* a_{kj}$.

As with the feedback allocation in the last section, one may use interior point methods [144] to solve (4.17) and (4.18) with complexity $\mathcal{O}\left(\sqrt{N} \log\left(\frac{N}{\varepsilon}\right)\right)$.

4.5 Concluding remarks

In this chapter, we considered two extensions of the work in the previous chapter, where we studied feedback allocation for a single-cell OFDMA uplink network with slow data scheduling. Firstly, we developed a joint feedback allocation and fast data scheduling algorithm for a single-cell downlink OFDMA system that does not experience inter-cell interference. Secondly, we developed a feedback allocation algorithm for the uplink of a multi-antenna network with inter-cell interference. We showed that under both these network settings, convex optimization can be used to efficiently compute solutions to the respective feedback allocation problems.

Chapter 5

Exploiting Sparse Dynamics for Controlling Whitespace Networks

This chapter contains our final contribution where we examine future network architectures. In particular, we consider whitespace wireless networks where a group of secondary users operate seamlessly on the same spectrum as a set of primary transmitters or incumbents. The secondary or whitespace users are served by a whitespace base station. In this setting, we are interested in acquiring channel state information for the purposes of downlink scheduling in the whitespace network while minimizing the amount of feedback/control bandwidth consumed for this acquisition process. Of course, in addition to bandwidth efficiency, it is important to have computational efficiency as well. We propose algorithms in this chapter that achieve both bandwidth and computational efficiency.

5.1 Introduction

With the tremendous increase in wireless connectivity over the last decade, the demand for wireless spectrum has never been greater. Traditionally, a portion of spectrum is allocated or licensed for use by a specific group of

users by regulatory agencies. This inherent rigidity coupled with the growing demand for wireless applications has led to a scarcity of spectrum. However, a recent Federal Communications Commission (FCC) study [146] has revealed that large portions of spectrum, though allocated, are significantly under-utilized by the licensees. To increase spectral efficiency, the FCC recently opened up *TV whitespaces*, which essentially lie in the 54 MHz - 806 MHz range, for unlicensed use [145]. Furthermore, the ruling removes the need for spectral sensing by the unlicensed or whitespace users in order to detect the presence of interfering transmitters (TV stations, wireless microphones, etc.). Instead, each whitespace user is required to access a central database in order to determine which TV band is available at its location. The database essentially contains a list of reservations by the interfering users or incumbents and is updated on a day-to-day basis.

It follows that any whitespace network that communicates only on the TV bands that are deemed available by the database¹ through the course of the day will not interfere with the incumbents. This leaves one other major impediment to achieving high throughputs in whitespace networks and this is interference from other unlicensed users. In this chapter, we consider the design of a whitespace network that operates in the presence of other interfering unlicensed users². In other words, the downlink transmissions of the

¹The details concerning the protocols for acquisition of database information are beyond the scope of this chapter.

²While these could potentially be other non-cooperative whitespace networks, we will refer to them as interfering users to avoid confusion.

whitespace network are on the same frequency band as the transmissions of the interfering users or nodes. The objective is to control whitespace transmissions to achieve maximal throughput regions for the whitespace network. We are interested in devising scheduling algorithms to achieve near-throughput-optimality.

The MaxWeight scheduling algorithm has been studied extensively as a simple throughput optimal scheduling algorithm [154]. We refer to [156,157] for a comprehensive survey on the MaxWeight algorithm and its variations. We consider recent variants of the MaxWeight algorithm [162–164] that perform joint feedback allocation and data scheduling. This chapter can be viewed as an extension of the above work to scenarios with interference. The general setup in these papers can be described as follows: The system has a feedback bandwidth constraint of B bits. Note that the feedback constraint proposed by Ouyang et al. [163] is in terms of a total number of sub-bands in the context of an orthogonal-frequency-division-multiple-access (OFDMA) system. This model can be equivalently expressed in terms of bits. A feedback bandwidth constraint of B bits also represents a softer model than that presented by Gopalan et al. [161] as the latter precludes a variable number of feedback bits per user. Given this bandwidth constraint, the system periodically decides how to partition these feedback bits across the users in order to maximize the *expected* cumulative queue-weighted-rate through the course of the upcoming period. This expectation is in general computed over the randomness inherent in the users' channels as well as the impinging interference in a interference-

limited whitespace setting.

Such a computation requires knowledge about the interfering network's transmission process. Measuring this transmission process, however, in general requires a feedback channel whose capacity *scales linearly with the number of interfering users* and is prohibitive for most realistic networks. In our model, the transmission process is completely parametrized by a set of target rates, each corresponding to one interfering user. The key idea we exploit in this chapter is the following: while the transmission process parameter vector at a snapshot in time in general lives in some arbitrary high dimension, in most practical networks (supporting voice calls and streaming video), there is a time-scale separation of flow-level dynamics versus scheduling. In other words, network layer (TCP/IP) dynamics occur at a much slower time scale than scheduling (hundreds-of-milliseconds versus milliseconds). Thus while the transmission vector itself may not be sparse, its dynamics are. This chapter is about exploiting this sparsity in the dynamics, to obtain much more data-efficient acquisition algorithms. It should be noted that fast acquisition of the interfering process is relevant not only to the whitespace bands, but also to other unlicensed bands (e.g. military radar bands at 5.6 GHz) where the FCC ruling does not apply.

It has long been known, and recently popularized under the name of compressed sensing, that whereas N linear measurements are required to reconstruct a vector (signal) in \mathbb{R}^N , if it is S -sparse (i.e., it has S non-zero coefficients) then under appropriate conditions on the linear (non-adaptive)

measurements, $\mathcal{O}(S \log N)$ are enough [158–160]. By developing similar tools, and applying them on the dynamics (rather than the signal directly) we are able to show that with greatly reduced, and in particular, sub-linear (logarithmic) feedback rates, our algorithms perform close to the full information (linear feedback) case.

Main Contributions and Organization

To the best of our knowledge, this is the first work to exploit *sparsity in the dynamics* of a network. As this is likely much more prevalent than sparsity in the actual trajectory of the network state (of course, if the trajectory is sparse, then so are the dynamics) we expect this high-level idea to find broad application. More concretely, the main contributions in this chapter are as follows:

- (1) A first (to the best of our knowledge) application of compressed sensing³ in designing a joint learning, feedback allocation and scheduling protocol for whitespace wireless networks thereby exploiting the *naturally-sparse dynamics* of the interfering network.
- (2) A proof that path-loss matrices satisfy the *null space property* thereby allowing for efficient acquisition or sensing of the interference state using ℓ_1 -norm minimization. By efficient, we mean logarithmic scaling in

³Compressed sensing has been used to solve some problems pertaining to the wireless physical layer in the past [165]–[168].

feedback bandwidth. The proof technique is novel since path-loss matrices contain entries that have non-zero mean and are not independent, a scenario that has not been dealt with extensively in past research.

- (3) Simulation results that numerically compare the performance of the full and partial information settings. The results establish the superior quality of the joint learning, feedback allocation and scheduling algorithm.

The rest of this chapter is organized as follows. In Section 5.2, we introduce the system model for the whitespace network under consideration. We present queue-based throughput optimal feedback allocation and data scheduling algorithms in Section 5.3. In Section 5.4, we discuss the compressed sensing algorithm that enables feedback allocation using significantly-reduced control overhead. We establish the “goodness” of path-loss sensing matrices in Section 5.5. The joint learning, feedback allocation and scheduling algorithm is presented in Section 5.6. Simulation results establishing the superior performance of the algorithm are contained in Section 5.7.

5.2 System model

In this section, we define the whitespace network we consider in the chapter. We introduce the communication models employed by the whitespace and interfering networks respectively.

Whitespace network: Each whitespace receiver is dropped uniformly on a circle of radius r_p centered at the origin. There are a total of N_p whites-

pace receivers located at points $\{(r_p, \theta_{i'})\}_{i'=1}^{N_p}$ where $\theta_{i'} \sim U[0, 2\pi]$, $\forall i'$. The whitespace base station is located at $(r_{p,b}, \theta_{p,b})$ anywhere on the xy -plane.

Interfering network: There are N_s interfering transmitters are placed on a collection of many circles of radii $\{r_{s,1}, r_{s,2}, \dots, r_{s,q}\}$ where N_s is such that $\frac{N_s}{q}$ is *even*. Circle c contains $\frac{N_s}{q}$ interfering receivers located at fixed points $\{(r_{s,c}, \theta_i)\}_{i=1}^{N_s}$ that are equally-spaced $\left(\theta_i = \frac{2\pi q}{N_s}, i = 0, 1, \dots, \frac{N_s}{q} - 1\right)$ as shown in Fig. 5.1. We note that this would roughly be the case when N_s becomes large and the users are uniformly distributed.

The spatial distribution we use is overly restrictive, and we believe that our proofs could be extended to handle much broader settings, although we have not yet been able to do so. This is supported by our simulation section. Indeed, the proposed algorithms work even under more general spatial models such as when the users scattered uniformly at random on a square area.

For the sake of the analysis, we also partition the whitespace receivers according to the circle they belong to thus creating q partitions $\{\mathcal{C}_1, \mathcal{C}_2, \dots, \mathcal{C}_q\}$ such that $\bigcup_{i=1}^q \mathcal{C}_i = \{1, 2, \dots, N_s\}$ and $\mathcal{C}_i \cap \mathcal{C}_j = \emptyset$ for $i \neq j$. Within each circle, the users are numbered or ordered in diametrically opposite pairs as shown in Fig.5.1, a labelling rule that is feasible since $\frac{N_s}{q}$ is even. In other words, all pairs $(j, j+1) \in \mathcal{C}_i$, j *odd*, will correspond to a pair of diametrically opposite receivers on circle \mathcal{C}_i .

Channel gain model: There are three types of nodes in the network: interfering nodes, whitespace mobiles, and the whitespace base station. Let

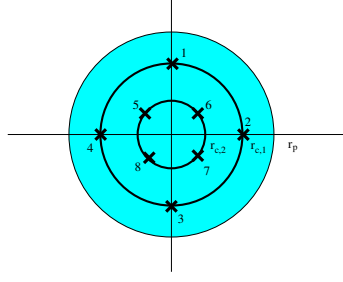


Figure 5.1: Network with interfering transmitters (not shown) uniformly distributed on the blue circle of radius r_p . There are $N_s = 8$ whitespace receivers in the network equally-divided across two circles ($q = 2$) of radii $r_{s,1}$ and $r_{s,2}$ respectively. This gives rise to partitions $\mathcal{C}_1 = \{1, 2, 3, 4\}$ and $\mathcal{C}_2 = \{5, 6, 7, 8\}$. The whitespace receivers are equally-spaced on each circle as shown.

m and n denote any two such nodes, which are located at points (r_m, θ_m) and (r_n, θ_n) respectively. The distance between these two nodes is given by

$$d_{mn} = \sqrt{r_m^2 + r_n^2 - 2r_m r_n \cos(\theta_m - \theta_n)},$$

which determines the following path-loss gain

$$\kappa_{mn} = \frac{1}{K + d_{mn}^2}, \quad K > 0. \quad (5.1)$$

between the same. This model is an approximation of the free space path loss model (with path-loss coefficient two) [170], a choice that affords us analytical tractability while compromising very little on modeling accuracy. The composite channel gain between nodes m and n is given by

$$h_{mn}(t) = g_{mn}(t) \kappa_{mn}, \quad (5.2)$$

where $g_{mn}(t) \sim \exp(1)$ models small-scale Rayleigh fading. In the sequel, all whitespace mobiles will be indexed by i , the interfering transmitters by i' , and the whitespace base station by i_s .

Power models: We assume that interfering transmitter i' has a rate target of $r_{i'}(t)$ at time t . Accordingly, the transmitter adopts a power-control policy given by $p_{i'}(h_{i'}(t), r_{i'}(t))$ at time t that essentially combats the effects of the channel $h_{i'}(t)$ to its corresponding receiver. We assume that the rate targets $\{r_{i'}(t)\}_{i'}$ change every T_I time slots and that T_I is large enough to calculate the average power expended during this period as $\bar{p}_{i'} = \mathbb{E}[p_{i'}(h_{i'}(t), r_{i'}(t))]$. Finally, we also assume that the whitespace base station transmits at power P .

Traffic model: We define $a_i(t)$ to be the number of packets associated with whitespace user i at time t . We assume these are random processes that are independent and identically distributed (i.i.d.) across time slots and users.

Information available at the base station: We assume that all interferer positions and hence $\{\kappa_{ii'}\}$ are known to the base station. While this might be idealistic in some scenarios, it is often possible to acquire this information through minimal cooperation with the interfering network. For example, if the interferers consist of cellular towers that are operating in whitespace mode, then their positions are easy to obtain.

Scheduling and feedback allocation: We assume that at each time slot, at most one whitespace user can be selected for downlink transmission. This would be the case in any OFDMA system with per-sub-band scheduling, which is known not to compromise on throughput optimality [171]. In order to decide which whitespace user to schedule, the base station must acquire information about the signal-to-interference-plus-noise ratio (SINR) at each

user as this determines the maximum supportable rate to that user. The SINR at user i is given by

$$\text{SINR}_i(t) = \frac{Ph_{i_s i}(t)\kappa_{i_s i}}{\sum_{i'=1}^{N_s} h_{i' i}(t)\kappa_{i' i}p_{i'}(h_{i'}(t), r_{i'}(t)) + N_o} \quad (5.3)$$

where N_o denotes the power of additive noise. Ideally, the base station would be able to acquire full information, i.e. $\{\text{SINR}_i(t)\}_{i=1}^K$ and then choose the user in each time slot that maximizes

$$k = \arg \max_i q_i(t) \log_2(1 + \text{SINR}_i(t)), \quad (5.4)$$

which corresponds to the popular MaxWeight data scheduling policy [154]. However, such an acquisition of full information incurs a feedback bandwidth of $\mathcal{O}(K)$. In many realistic systems, feedback bandwidth is limited as it consumes valuable uplink capacity. Thus, it may not be feasible for the feedback bandwidth to scale linearly in the number of users. In the next section, we address this issue by considering data scheduling policies that operate under limited feedback budgets.

5.3 Joint scheduling and feedback allocation with interference

Recent work [161, 163] has analysed the effects of limited feedback on the throughput of a queueing system. Through the remainder of this chapter, we adopt the feedback allocation policy proposed by Gopalan et al. [161] and subsequently generalized to multi-carrier systems by Ganapathy et al. [162] and two-time scale operation. The policy essentially chooses k out of K users

to “sample” and then performs MaxWeight using the available channel information.

The policy operates on two time-scales. Feedback allocation happens once every T_I seconds following by data scheduling. The two stages of the policy can be described in detail as follows:

- *Feedback allocation*: Let $\bar{t} = \left\lfloor \frac{t}{T_I} \right\rfloor$. Then every $\bar{t}T_I$ time slots, the feedback allocation policy solves

$$\begin{aligned} \vec{g}(\bar{t})^* = & \arg \max \mathbb{E} \left[\max_{\{i: g_i=1\}} q_i(\bar{t}T_I) \log_2(1 + \text{SINR}_i) \mid \vec{q}(\bar{t}) \right] \\ \text{s.t.} \quad & \sum_{k=1}^K g_k \leq c \\ & g_k \in \{0, 1\}, \forall k \in \{j : Q_j(\bar{t}) > 0\} \end{aligned} \quad (5.5)$$

where the expectation is computed over the direct channel *and the interfering channel*.

- *Data scheduling*: For $\bar{t}T_I \leq t \leq (\bar{t} + 1)T_I$, given some $\vec{g}(\bar{t})^*$, the users are scheduled according to MaxWeight rule

$$\max_{\{i: g_i=1\}} q_i(\bar{t}T_I) \log_2(1 + \text{SINR}_i). \quad (5.6)$$

In (5.5), we are essentially select the subset of users that maximizes the *expected* MaxWeight. Given the optimal subset, we then perform standard MaxWeight across these users in (5.6).

The rule in (5.5) is representative of a general class of resource allocation problems [161–163] where resources have to be allocated prior to being able to view the realization of the channel. In such settings, one needs to compute

the expected MaxWeight, that is function of the probability distributions of the direct channels as well as interfering channels. Ganapathy et al. [162] compute (5.5) in closed-form but do not consider the effects of interference in their system. On the other hand, Gopalan et al. gopalan and Ouyang et al. [163] do not preclude the effects of interference in their model but do not comment on how to compute (5.5). The obvious challenge to computing the expect MaxWeight is determining the distribution of the interference.

To address this challenge, we begin with a general assumption that the distribution of the interference at user i is completely parametrized by a finite set of M moments $\{m_{i1}, m_{i2}, \dots, m_{iM}\}$. Thus, in order to compute the distribution of the interference, we can turn our attention to estimating the set of moments $\mathcal{M} = \{m_{i1}, m_{i2}, \dots, m_{iM}\}$. According to (5.3), the n -th moment of the interference $Z_i = \sum_{i'=1}^{N_s} h_{i'i}(t) \kappa_{i'i} p_{i'}(h_{i'}(t), r_{i'}(t))$ at user i is

$$\mathbb{E}[Z_i^n] = \sum_{i'=1}^{N_s} \mathbb{E}[h_{i'i}^n(t)] \kappa_{i'i}^n \mathbb{E}[p_{i'}^n(h_{i'}(t), r_{i'}(t))]. \quad (5.7)$$

For simplicity, let us assume that the interference depends only on the mean (first moment, i.e., $M = 1$). The ensuing analysis can be easily extended to the more general case with $M > 1$ moments. If we define $\mathbf{I}(\bar{t}) = [Z_1 \ Z_2 \ \dots \ Z_K]^T$, \mathbf{H} with elements $\{\kappa_{i'i}\}$ and $\bar{\mathbf{p}}(\bar{t}) = [\bar{p}_1(\bar{t}) \ \bar{p}_2(\bar{t}) \ \dots \ \bar{p}_{N_s}(\bar{t})]^T$, the above relationship (5.7) can be succinctly written as

$$\mathbf{I}(\bar{t}) = \mathbf{H} \bar{\mathbf{p}}(\bar{t}) \quad (5.8)$$

where we recall that $\bar{\mathbf{p}}(t)$ is the average transmit power across T_I time slots. Our goal is to determine $\mathbf{I}(\bar{t})$ through the course of the slow time-scale as this deter-

mines the feedback allocation policy through that period. The naïve solution to determining $\mathbf{I}(\bar{t})$ would be to devote δT_I time slots to sample averaging at each of K receivers respectively and then transmit the measured values to the base station. For simplicity, through the remainder of this chapter, we assume that T_I is large enough and δ small enough to ensure that the sample averaging estimator is perfect. The above naïve solution would consume a feedback control bandwidth of $\mathcal{O}(K)$. This is clearly not justifiable since the subsequent feedback process of the SINRs only consumes a bandwidth proportional to k .

If the process $\bar{\mathbf{p}}(t)$ is completely general, there is little that can be done to remedy this problem, and partial feedback (of only a subset of $\mathbf{I}(\bar{t})$) will necessarily result in degraded performance, i.e., smaller throughput regions. However, as discussed in the introduction, for networks where the only a subset of rate targets $\{r_{i'}(t)\}$ vary every T_I slots, we show that it is possible to reduce the control bandwidth. Using ideas from subset selection and compressed sensing, the next section considers how this can be exploited in order to achieve near-optimal performance consuming a feedback bandwidth that grows only logarithmically in N_s .

5.4 Exploiting Sparse Dynamics in Learning

In this section, we propose a compressed sensing approach to efficiently learn $\bar{\mathbf{p}}(t)$ and hence $\mathbf{I}(t)$. This approach is effective when the average power transmitted by the each interfering user changes on a slower time-scale. This is indeed what one typically expects for networks that exhibit a time-scale

separation between higher-layer dynamics (for eg. TCP/IP) and scheduling dynamics. This is also trivially the case for interfering networks do not perform power control. Before we investigate how to exploit this structure, we will take a short diversion into the topic of compressed sensing.

5.4.1 Compressed Sensing

The topic of compressed sensing has received tremendous interest in the recent years [158–160]. The theory essentially states that one can recover sparse data exactly, given an under-determined system of equations. Specifically, the generic problem is the following: Given a signal $\mathbf{x} \in \mathbb{R}^p$, one receives $k \ll p$ linear, potentially noisy measurements: $\mathbf{y} = \mathbf{M}\mathbf{x} + \mathbf{w}$. Here, \mathbf{M} encodes the measurement matrix and \mathbf{w} denotes additive noise, usually of bounded norm.

For general vector $\mathbf{x} \in \mathbb{R}^p$, p independent measurements are required to hope to reconstruct \mathbf{x} . When $k < p$, the problem therefore is underdetermined. If \mathbf{x} is sparse, however, in some settings the problem is no longer underdetermined, and can be solved by considering a combinatorial optimization problem:

$$\min_{\mathbf{x} \in \mathbb{R}^p} : ||\mathbf{M}\mathbf{x} - \mathbf{y}||_2^2 - \lambda ||\mathbf{x}||_0,$$

where $||\cdot||_0$ denotes the so-called ℓ_0 norm (which is not really a norm) which counts the cardinality of the support. This approach succeeds as long as the linear equations, or measurements, satisfy a property called *Null Space Property* (NSP), which essentially amount to the statement that there are no

very sparse vectors in the null-space of the measurements.

As this problem is combinatorial, the natural convexification has been considered, where the $\|\cdot\|_0$ norm is replaced by its closest convex approximation, the $\|\cdot\|_1$ norm. This gives the so-called Lasso [177] formulation for model selection (subset selection):

$$\min_{\mathbf{x} \in \mathbb{R}^p} : \|\mathbf{M}\mathbf{x} - \mathbf{y}\|_2^2 - \lambda \|\mathbf{x}\|_1, \quad (5.9)$$

in addition to controlling the nullspace, one can control the smallest eigenvalue of submatrices, then the resulting problem is *strongly convex* around sparse solutions, and hence one can show that the convex problem given above recovers the exact solution to the combinatorial problem. Many such results have appeared in the literature, e.g., [158–160, 186]. Indeed, the results are attractive from an algorithmic perspective as well since the convex relaxation is easily solvable, with computation time that scales gracefully as the size of the problem increases, allowing the efficient solution of very large problems.

When there is no noise added, one can also solve the so-called Basis Pursuit problem [179], which is the ℓ_1 -norm minimization problem given as:

$$\begin{aligned} \min : \quad & \|\mathbf{x}\|_1 \\ & \mathbf{M}\mathbf{x} = \mathbf{y}. \end{aligned}$$

This can be reformulated as a linear program using standard techniques. The theoretical connections between Lasso and Basis Pursuit have been well-analysed by authors such as Tropp [187].

5.4.2 The feedback protocol

Returning to our problem, we define $\Delta\bar{\mathbf{p}}(t) : \Delta\bar{\mathbf{p}}(t) = \bar{\mathbf{p}}(t) - \bar{\mathbf{p}}(t-1)$ and apply the model selection paradigm outlined above, to *the dynamics vector* rather than the power vector itself: $\Delta\bar{\mathbf{p}}(t)$. We can assume that at some initial time, $\bar{\mathbf{p}}(t_0)$ is known. At time t , we can query the interference levels $\mathbf{I}(t) = \mathbf{H}\bar{\mathbf{p}}(t)$ from all or a subset of whitespace users. We can then construct the difference in measurements

$$\begin{aligned}\mathbf{z}(t) = \mathbf{I}(t) - \mathbf{I}(t-1) &= \mathbf{H}[\bar{\mathbf{p}}(t) - \bar{\mathbf{p}}(t-1)] \\ &= \mathbf{H}\Delta\bar{\mathbf{p}}(t).\end{aligned}$$

Since the left hand side, $\mathbf{z}(t)$, is known, this falls precisely into the sparse recovery paradigm developed above, and in particular, can be solved by Basis Pursuit in the noiseless case, and Lasso in the noisy case.

More concretely, let Q be the subset queried users and $k = |Q|$. Given $k = |Q|$, k even is chosen according to the following algorithm:

It is necessary for the query set Q to be selected in this way for the sake

Algorithm 2 Protocol to choose query set Q

- 1: Set $Q = \emptyset$.
 - 2: **while** $i \leq \frac{k}{2}$ **do**
 - 3: Choose any pair of diametrically opposite receivers $(j, j+1)$ from circle i , i.e., $j \in \mathcal{C}_i$, j odd.
 - 3: $Q = Q \cup \{j, j+1\}$.
 - 3: Set $\mathcal{C}_i = \mathcal{C}_i \setminus \{j, j+1\}$
 - 4: Increment $i = i + 1$.
 - 5: **end while**
-

of analytical tractability. Such a selection procedure would ensure that the number of nodes in circle \mathcal{C}_i that are selected for feedback, i.e., $|Q \cap \mathcal{C}_i|$ scales linearly in N_p . At the beginning of each scheduling instant, the whitespace base station acquires observations $\mathbf{I}_Q(t)$. It is of immediate interest to determine the smallest query size k (or feedback bandwidth) that the whitespace base station requires in order to recover $\mathcal{A}_p(t)$ reliably using

$$\begin{aligned} & \text{minimize} \quad \|\mathbf{x}\|_1 \\ & \text{subject to} \quad \mathbf{H}_{Q,r}\mathbf{x} = \mathbf{z}_Q(t) \end{aligned} \quad (5.10)$$

In this work, we do not consider the number of bits required to communicate $\mathbf{y}_I(t)$ reliably as we are interested primarily in the scaling behaviour of feedback bandwidth.

As briefly stated earlier, compressed sensing theory states that it is possible to recover any S -sparse vector if and only if the *sensing matrix* \mathbf{H} satisfies the NSP [181] of order S . This property will be defined in the next section. Furthermore, the choice of subset I is not important (only the size) for this special class of matrices. In the following section, we will show that path-loss matrices as defined in (5.1) do indeed satisfy the NSP and hence facilitate compressed sensing. In our setting, this means that we can exploit the sparsity structure induced by our wireless application and use compressed sensing techniques to conserve feedback bandwidth. We note that in our application, the sensing matrix is provided by the channel as opposed to traditional compressed sensing where the designer is allowed to choose a convenient sensing mechanism.

In the next section, we present the main result of this chapter, which states path-loss matrices \mathbf{H} make for good sensing matrices.

5.5 NSP of path-loss matrices

In this section, we establish that path-loss matrices \mathbf{H} satisfy the NSP (which will be defined shortly) when the feedback bandwidth obeys $k = \mathcal{O}(S \log N_p)$. Lemma 20, Lemma 21 along with Theorem 23 constitute the main results in this section.

5.5.1 Preliminaries

We define the null space property from Gribonval et al. [183]. Given a matrix \mathbf{M} , let $\mathcal{N}(\mathbf{M})$ denote its null space.

Definition (Null space Property): A matrix \mathbf{M} satisfies the null space property of order S if for all subsets $\mathcal{S} \subseteq \{1, 2, \dots, N\}$ with $|\mathcal{S}| \leq S$, the following holds

$$\|\mathbf{v}_{\mathcal{S}}\|_1 \leq \|\mathbf{v}_{\mathcal{S}^c}\|_1, \quad \forall \mathbf{v} \in \mathcal{N}(\mathbf{M}) \setminus \mathbf{0}.$$

where $\mathcal{S}^c = \{1, 2, \dots, N\} \setminus \mathcal{S}$. Based on this property, the following recovery result [183] has appeared both implicitly and explicitly in works such as [181, 184]. Let the support set of $\mathbf{x}(t)$ be denoted by \mathcal{S} with $|\mathcal{S}| \leq S$. A vector $\mathbf{x}(t)$ is S -sparse if $|\mathcal{S}| \leq S$.

Theorem 20. *Let $\mathbf{M} \in \mathbb{R}^{k \times N}$. Every S -sparse vector $\mathbf{x} \in \mathbb{R}^N$ is the solution to the ℓ_1 -norm minimization problem in (5.10) with $\mathbf{y} = \mathbf{M}\mathbf{s}$ iff \mathbf{M} satisfies the NSP of order S .*

□

The NSP is typically quite difficult to prove directly leading to the development of sufficient conditions that are easier to establish. One such sufficient condition is the *restricted isometry property* [186] that has become quite popular in recent years and is defined below.

Definition (Restricted Isometry Property): A $k \times N$ matrix \mathbf{M} satisfies the Restricted Isometry Property (RIP) of order p if there exists $\epsilon_p(\mathbf{M}) \in (0, 1)$ such that

$$(1 - \epsilon_p(\mathbf{M}))\|\mathbf{x}_{\mathcal{T}}\|_2^2 \leq \|\mathbf{M}_{\mathcal{T},c}\mathbf{v}_{\mathcal{T}}\|_2^2 \leq (1 + \epsilon_p(\mathbf{M}))\|\mathbf{x}_{\mathcal{T}}\|_2^2, \quad \mathbf{x} \in \mathbb{R}^N, \quad (5.11)$$

holds for all sets \mathcal{T} with $|\mathcal{T}| \leq p$.

Here, $\epsilon_p(\mathbf{M})$ is called the *restricted isometric constant* of \mathbf{M} . The RIP essentially requires that all $k \times |\mathcal{T}|$ sub-matrices of \mathbf{M} be well-conditioned. Under such a conditioning, perfect recovery of \mathbf{x} is possible as stated in the following theorem.

Theorem 21. [192, 193] *Let $\mathbf{M} \in \mathbb{R}^{k \times N}$. If \mathbf{M} satisfies the RIP with $\epsilon_{2S}(\mathbf{M}) \leq 2\frac{(3-\sqrt{2})}{7} \approx 0.4531$, then every S -sparse vector $\mathbf{x} \in \mathbb{R}^N$ is the solution to the ℓ_1 -norm minimization problem in (5.10).*

□

Thus, the RIP with a sufficiently small constant immediately implies the NSP in the context of ℓ_1 -recovery. The approach we use to prove “goodness” of path-loss matrices \mathbf{H} is motivated by the following observation. In

general, the null space of a product of two matrices \mathbf{NM} contains the null space of \mathbf{M} and therefore if \mathbf{NM} satisfies the NSP, so does \mathbf{M} . This allows us to study the class of *linearly-processed* path-loss matrices $\mathbf{A} = \mathbf{BG} = \mathbf{BWH}$ where

$$\mathbf{W} = \text{diag}\{\underbrace{\mathbf{J} \mathbf{J} \dots \mathbf{J}}_{\frac{k}{2} \text{ times}}\}, \mathbf{J} = \begin{bmatrix} 1 & -1 \\ -1 & 1 \end{bmatrix},$$

and $\text{diag}\{\cdot\}$ is the standard block-diagonal operator;

$$\mathbf{B} = \text{diag}\left\{\frac{1}{\sqrt{\text{Var}\{g_{11}\}}} \dots \frac{1}{\sqrt{\text{Var}\{g_{k1}\}}}\right\} \begin{bmatrix} \beta_1 & 0 & 0 & 0 & \cdot & \cdot & 0 & 0 & 0 \\ 0 & \beta_2 & 0 & 0 & \cdot & \cdot & 0 & 0 & 0 \\ \cdot & \cdot & \cdot & \cdot & \cdot & \cdot & \cdot & \cdot & \cdot \\ \cdot & \cdot & \cdot & \cdot & \cdot & \cdot & \cdot & \cdot & \cdot \\ 0 & 0 & 0 & 0 & \cdot & \cdot & 0 & \beta_{k-1} & 0 \\ 0 & 0 & 0 & 0 & \cdot & \cdot & 0 & 0 & \beta_k \end{bmatrix} \quad (5.12)$$

with $\beta_i \sim \text{Bernoulli}(\frac{1}{2})$, $\forall i$ and independent across i ; . The Bernoulli random variables have support $\{\pm 1\}$. We focus our attention on establishing the recovery properties of \mathbf{A} rather than \mathbf{H} . We will show that \mathbf{A} satisfies the RIP with $k = \mathcal{O}(S \log N_p)$ observations and hence the NSP. The transformation \mathbf{W} essentially subtracts rows of \mathbf{H} corresponding to *diametrically opposite* pairs of whitespace receivers in the *same* partition. Thus, the dimension of \mathbf{G} is still $k \times k$. The transformation \mathbf{B} weights and adds adjacent rows of \mathbf{G} .

According to our spatial distribution model, when conditioned on the positions of the whitespace users, the columns of \mathbf{H} become stochastically independent since each interfering transmitter is independently thrown. We will rely heavily on recent results from Vershyn [188] and Adamczyk et al. [189] that deal with sensing matrices containing independent columns. Before we

reproduce the RIP result [188, 189] for matrices with independent columns, we present a primer on sub-gaussian and sub-exponential random variables along with some useful results from non-asymptotic matrix theory.

5.5.2 Useful concentration inequalities

We refer the reader to the tutorial paper by Vershynin [188] for a great introduction to non-asymptotic matrix theory. Lemmas 17-19 below are well-known past results that are summarized in this paper [188]. The proofs are not reproduced due to lack of space.

Lemma 17. *Let z be random variable. The following properties are equivalent with parameters $K_i > 0$ differing from each other by at most an absolute constant factor.*

- (i) *Tails:* $\Pr(|z| > t) \leq \exp(1 - \frac{t^2}{K_2})$ for all $t > 0$,
- (ii) *Moments:* $(\mathbb{E}[|z|^p])^{\frac{1}{p}} \leq K_2 \sqrt{p}$ for all $p \geq 1$,
- (iii) *Super-exponential moment:* $\mathbb{E}\left[\exp\left(\frac{z^2}{K_3}\right)\right] \leq e$.

Moreover, if $\mathbb{E}[z] = 0$ then properties (i)-(iii) are also equivalent to the following one:

- (iv) *Moment generating function:* $\mathbb{E}[\exp(tz)] \leq \exp(t^2 K_4)$ for all $t \in \mathbb{R}$.

□

A random variable that satisfies the above property is called a *sub-gaussian* random variable. Such random variables are often characterized by the ψ_2 -

norm⁴, which is defined as

$$||z||_{\psi_2} = \sup_{p \geq 1} \frac{(\mathbb{E}[|z|^p])^{\frac{1}{p}}}{\sqrt{p}}. \quad (5.13)$$

It follows that if the ψ_2 -norm of z is finite, then z is a sub-gaussian random variable with $||z||_{\psi_2} = K_2$. This is the case for bounded random variables with symmetric distributions.

Lemma 18. *Let z be a symmetrically distributed, bounded random variable with $|z| \leq M$, $M > 0$. Then, \mathbf{z} is a sub-gaussian random variable with $||z||_{\psi_2} \leq cM^2$, $c > 0$.*

□

In higher dimensions, a random vector \mathbf{z} of dimension N is called sub-gaussian if $\mathbf{z}^T \mathbf{x}$ is sub-gaussian for every $\mathbf{x} \in \mathbb{R}^N$.

Lemma 19. *Let $\{z_i\}_{i=1}^M$ be a collection of independent, zero-mean, sub-gaussian random variables. Then, \mathbf{z} is a sub-gaussian random vector with $||\mathbf{z}||_{\psi_2} = C \max_i ||z_i||_{\psi_2}$.*

□

We are now ready to prove the RIP (hence NSP) for matrix \mathbf{A} . Before we move on to this task, we require one more definition. A random vector \mathbf{m} of dimension M is called *isotropic* if $\mathbb{E}[|\mathbf{m}^T \mathbf{x}|^2] = ||\mathbf{x}||^2$ for all $\mathbf{x} \in \mathbb{R}^M$.

⁴Alternate definitions of this norm have been adopted (such as in [189]) that are all equivalent to within a constant factor.

5.5.3 NSP of linearly-processed path-loss matrices \mathbf{A}

We reproduce the recent RIP (hence NSP) result [188, 189] concerning matrices with independent columns. We refer the reader to [188, 189] for the proof.

Theorem 22. *Let \mathbf{M} be an $k \times N$ random matrix whose columns are independent, isotropic and sub-gaussian with $\psi_{\max, m} = \max_i \|\mathbf{m}_i\|_{\psi_2}$. Furthermore, let the columns satisfy $\|\mathbf{m}_i\|^2 = k$ almost surely. Then, the normalized matrix $\frac{1}{\sqrt{k}}\mathbf{M}$ is such that if $k \geq C_{\psi_{\max, m}} \varepsilon^{-2} S \log\left(\frac{eN}{S}\right)$, then*

$$\varepsilon_p \left(\frac{1}{\sqrt{k}} \mathbf{M} \right) \leq \varepsilon \quad (5.14)$$

with probability at least $1 - 2\exp(-c_{\psi_{\max, m}} \varepsilon^2 k)$. Here, $c_{\psi_{\max, m}}$ and $C_{\psi_{\max, m}}$ depend only the worst-case sub-gaussian norm $\psi_{\max, m}$.

□

As mentioned earlier, the channel matrix \mathbf{H} contains independent columns since the positions of the whitespace users are fixed. However, each column contains entries that are not centered, not isotropic and that are highly coupled. This is because all entries in \mathbf{h}_i are completely determined by the position of the interfering transmitter i . For this reason, it is not immediately clear whether the columns are sub-gaussian.

To prove the NSP of \mathbf{H} , our approach will be to suitably left-multiply the channel matrix \mathbf{H} by carefully-chosen matrices so as to meet the sufficient conditions in Theorem 22. The following lemmas and theorem constitutes the main results of this chapter.

Lemma 20. *The matrix $\mathbf{A} = \mathbf{BWH}$ of size $k \times N$ contains independent, isotropic, centered, sub-gaussian columns.*

Proof. See Appendix C.1. \square

Lemma 21. *For matrix $\mathbf{A} = \mathbf{BWH}$ of size $k \times N$, we have that $\|\mathbf{a}_i\|^2 = k$ almost surely.*

Proof. See Appendix C.2. \square

Theorem 23. *\mathbf{H} satisfies NSP of order S almost surely when $k = \mathcal{O}(S \log N_p)$.*

Proof. The result follows from Lemma 20, Lemma 21 and Theorem 22. \square

We discuss in the next section, how this sparse recovery algorithm is integrated with scheduling. In particular, since we are estimating dynamics rather than the signal itself, the real possibility of *error propagation* arises. This has not been heretofore addressed in the literature, to the best of our knowledge. In the next section, the algorithm introduces an explicit step to control this. The simulations in Section 5.7 demonstrate the effectiveness of our approach.

5.6 Joint Learning, Feedback Allocation and Scheduling

The essential conclusion of the previous section is that the average power vector $\bar{\mathbf{p}}(\bar{t})$ can be recovered by acquiring $\log N_p$ measurements (from $\log N_p$ whitespace users) if the dynamics of $\bar{\mathbf{p}}(\bar{t})$ are sparse.

The complete learning, feedback allocation and scheduling is presented in Algorithm 3.

We have the following remarks:

- The l_1 -minimization in Step 4 is to recover $\Delta\bar{\mathbf{p}}(\bar{t})$. The recovery can be almost surely accurate when $\Delta\bar{\mathbf{p}}(\bar{t})$ is sparse.
- The purpose of Step 6 is to verify the accuracy of $\Delta\bar{\mathbf{p}}(\bar{t})$. We add this step because $\Delta\bar{\mathbf{p}}(\bar{t})$ may not be always sparse, and even it is sparse, the learning algorithm is not perfect. We introduce Step 6 to detect the errors in learning and to protect the interfering network. The constant ϵ is the error cap, a small positive number.
- The goal of Step 10 is to recover $\Delta\bar{\mathbf{p}}(\bar{t})$ an error is detected in Step 6. We acquire all N_s whitespace users and use this to directly construct the average transmission power vector. If this reconstruction also fails, then the whitespace base station keeps silent in that time slot.
- For interfering networks that do not employ power control, we can set $\delta = \frac{1}{T_I}$. In other words, we only need one slot to recover the average power vector.

Algorithm 3 Joint learning, feedback allocation and scheduling in whitespace radio networks

- 1: **for** each t **do**
- 2: During time slots $nT_I \leq t < \delta T_I$, each whitespace user (say the whitespace user at micro-cell i) measures the interference from the interfering network and sample average the realizations to find $\mathbf{I}_i(t)$, which is the i^{th} entry of vector $\mathbf{H}\tilde{\mathbf{p}}(t)$.
- 3: The whitespace base station randomly queries $M = \Theta(\log N)$ micro-cells containing whitespace users and acquires the change of interference levels $\Delta\mathbf{I}_i(t) = \mathbf{I}_i(t) - \mathbf{I}_i(t-1)$. We index the queried micro-cells using j ($1 \leq j \leq M$), and let i_j denote the cell index of the j^{th} queried cell.
- 4: In time slot $t = \delta T_I + 1$, the whitespace base station estimates the change of the average interfering powers $\Delta\tilde{\mathbf{p}}(t)$ by solving the following optimization problem:

$$\Delta\tilde{\mathbf{p}}(t) = \arg \min \|\tilde{\mathbf{p}}\|_1 \quad (5.15)$$

$$\text{subject to} \quad \mathbf{H}\tilde{\mathbf{p}} = \mathbf{y}(t). \quad (5.16)$$

In the equations above, $\tilde{\mathbf{p}}$ is the optimization variable, $\mathbf{y}(t)$ is M -vector with $\mathbf{y}_j(t) = \Delta\mathbf{I}_{i_j}(t)$, and $\tilde{\mathbf{H}}$ is a $N \times M$ matrix where the j^{th} row is the i_j^{th} row of \mathbf{H} .

- 5: The whitespace base station sets $\tilde{\mathbf{p}}(t) = \tilde{\mathbf{p}}(t-1) + \Delta\tilde{\mathbf{p}}(t)$.
- 6: The whitespace base station acquires additional M' cell containing whitespace users and acquire their interference levels. We index the queried micro-cells using j' ($1 \leq j' \leq M'$), and let $i_{j'}$ denote the cell index of the j'^{th} queried cell. Then the whitespace base station computes

$$e = \frac{1}{|M'|} \|\mathbf{H}'\tilde{\mathbf{p}} - \mathbf{y}'(t)\|,$$

where $\mathbf{y}'(t)$ is M' -vector with $\mathbf{y}'_{j'}(t) = \Delta\mathbf{I}_{i_{j'}}(t)$, and \mathbf{H}' is a $N \times M'$ matrix where the j'^{th} row is the $i_{j'}^{\text{th}}$ row of \mathbf{H} .

- 7: **if** the estimate is accurate (i.e., if $e \leq \epsilon$) **then**
 - 8: Perform feedback allocation at time $t = \delta T_I + 1$ by solving (5.5) and obtain $g^*(t)$.
 - 9: Through time slots $\delta T_I + 1 \leq t < \bar{t}T_I$, use the above-computed allocation $g^*(\delta T_I + 1)$ and perform MaxWeight scheduling according to (5.6) to select a downlink whitespace.
 - 10: **else**
 - 11: The whitespace base station queries the uplink interference levels from all whitespace users. The whitespace base station uses $N_s - M'$ of measurements to recover $\tilde{\mathbf{p}}(t)$ (by solving a l_1 minimization problem similar to Step 4) and M' of them to verify the accuracy of the estimated value $\tilde{\mathbf{p}}(t)$ (similar to Step 6).
 - 12: **if** the estimate is accurate **then**
 - 13: go to Step 8.
 - 14: **else**
 - 15: No whitespace downlink transmission is scheduled.
 - 16: **end if**
 - 17: **end if**
 - 18: **end for**
-

5.7 Simulations

In this section, as we are primarily interested in the performance of the learning component of our joint algorithm – the recovery of sparse dynamics – we evaluate the performance of the algorithm under a simplified setting. We compare the throughput of the joint algorithm with the scheduling algorithm with complete knowledge of the interfering network and another one without any knowledge of the interfering network. We set $T_I = 1$, $\delta = \frac{1}{T_I}$, $g_{i'i} = g_{i_s i} = 1, \forall i', i$. This means that there is no feedback allocation, assume that the channels are determined only by path-loss and are interested in learning the instantaneous values of interference. This follows from the fact that, in the absence of fading, (5.8) represents the instantaneous interference powers. The simulation setting is described in detail in the following.

We consider a square cell with side length 1 kilometer, which is the size of a typical urban network [147]. We partition this square area into $N = 49$ micro-cells, each micro-cell is $20(m) \times 20(m)$ square area, which is sufficiently small to ensure at most one user in a micro-cell in an urban network. We index the micro-cells by i ($1 \leq i \leq N$), counted column-wise as shown in Figure 5.2. The interfering base-station is positioned at the center of the unit square. Each cell contains one *potential* interfering user that communicates with the interfering base station. The user is located at the center of the square cell. The whitespace users are positioned *uniformly at random* in 26 distinct micro-cells. At most one whitespace user is allowed in a micro-cell. The whitespace base is co-located with the interfering base station at the center of the square

cell.

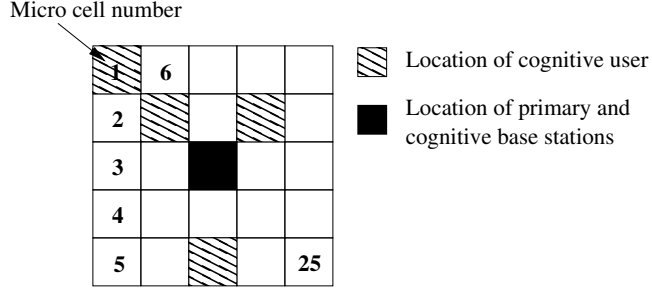


Figure 5.2: Illustrative example of grid model used in simulations with $N = 25$ and $N_s = 4$.

Current wireless standards such as 3GPP Long-Term-Evolution (LTE) can support rates of more than 25Mbps on the uplink with 200 users per cell on 20MHz of spectrum [147]. We set the transmit powers according to the popular channel inversion power control algorithm. Assume that the power-rate function is $\bar{p}_i = \frac{(2^R - 1)(1 + \varepsilon)}{h_{i'}}$ (Watts) where $R = \frac{25}{20}$ bits/s/Hz is the desired spectral efficiency and the interference compensation coefficient is $\varepsilon = 0.05$. We further assume that the maximum transmit power of whitespace users $p^{\max} = 50$.

The activity of each interfering node is modeled as a Markovian ON-OFF process where the transition probabilities from OFF to ON is $\eta_0 = 0.05$ and from ON to OFF is $\eta_1 = 0.95$. The probability that a interfering user changes his/her state from one scheduling instant to the next is

$$\frac{2\eta_0\eta_1}{(\eta_0 + \eta_1)^2} = \frac{2 \times 0.05 \times 0.95}{(0.95 + 0.05)^2} = 0.05.$$

So on average $49 \times 0.05 \approx 2.5$ users change their states, which reflects the

sparse dynamics. We initialize the system at $\gamma_i(0) = 0$ for all i . The arrival processes to whitespace users are assumed to be deterministic, i.e., a fixed number of packets arrive at a whitespace user at the beginning of each time slot. In our simulation, the arrival rates are symmetric to all whitespace users, and denoted by λ (bits/second).

In the simulations, we compare the performance of the joint learning and scheduling algorithm with the following two algorithms.

1. Scheduling with perfect knowledge of $\bar{\mathbf{p}}(t)$.
2. MaxWeight downlink scheduling only when $\bar{\mathbf{p}}(t) = \emptyset$. In this case, the whitespace base station transmits with a power that guarantees limited interference (ϵ_d) to all micro-cells in the network.

The joint algorithm queries 10 whitespace users at each time slot to recover $\Delta\mathcal{A}_p(t)$. We set the penalty parameter ξ to be 0.0005 in the Lasso (5.9). Recall that $\bar{\mathbf{p}}(t)$ may not be always sparse due to the randomness of the activity processes, and the estimation errors may propagate over time. Steps 6 to 8 in Algorithm 3 are in place to counter this phenomenon. The number of additional whitespace users queried for error estimation is set to be $\tilde{M} = 4$ and the error threshold is set to be 0.5.

In Figure 5.3, we plot the average maximum queue lengths under the two cases. We observe that the per-user throughput under the joint learning and scheduling algorithm is close to 2.5 (Mbits/second), which is 60% of the

throughput under the complete knowledge case where the throughput is 4 (Mbits/second). This demonstrates the competitive performance of the joint learning and scheduling approach.

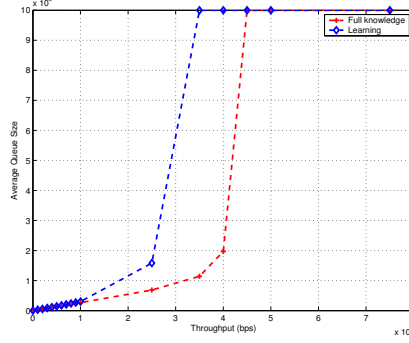


Figure 5.3: The average maximum queue lengths under the two different cases

5.8 Conclusion

In this chapter, we exploited the *naturally-sparse dynamics* of the interfering network's transmission processes to develop a joint learning and scheduling algorithm for whitespace radio networks. The learning algorithm is a first (to the best of our knowledge) application of compressed sensing to whitespace networks. The simulation results established the superior quality of the joint learning and scheduling algorithm.

Appendices

Appendix A

Appendix for Chapter 3

A.1 Proof of Theorem 10

The proof is essentially the same as in [48] with some minor modifications. It uses Foster's theorem to prove positive recurrence of the queue state process $\mathbf{q}[t]$. We define a quadratic potential function $V(\mathbf{x}) = \frac{1}{2} \sum_i x_i^2$. The standard Lyapunov drift function can be computed and bounded as

$$\begin{aligned}
 d(\mathbf{q}) &= \mathbb{E}[V(\mathbf{q}[t+1]) - V(\mathbf{q}[t]) \mid \mathbf{q}[t] = \mathbf{q}] \\
 &= \frac{1}{2} \sum_{k=1}^K \mathbb{E}[q_k^2[t+1] - q_k^2[t] \mid q_k[t] = q_k] \\
 &= \frac{1}{2} \sum_{k=1}^K \mathbb{E}\left[\left([q_k[t] + a_k[t+1] - d_k[t+1]]^+\right)^2 - q_k^2[t] \mid q_k[t] = q_k\right] \\
 &\leq \frac{1}{2} \sum_{k=1}^K \mathbb{E}\left[(a_k[t+1] - d_k[t+1])^2 + 2q_k[t](a_k[t+1] - d_k[t+1]) \mid q_k[t] = q_k\right] \text{ since } [x]^+ \leq x \\
 &\leq \frac{1}{2} \sum_{k=1}^K \mathbb{E}[a_k^2[t+1]] + \mathbb{E}[d_k^2[t+1]] + 2\mathbb{E}[q_k[t](a_k[t+1] - d_k[t+1]) \mid q_k[t] = q_k].
 \end{aligned} \tag{A.1}$$

As is standard in the literature, we assume that the arrival and departure processes have bounded second moments, i.e., $\mathbb{E}[a_k^2[t+1]] + \mathbb{E}[d_k^2[t+1]] \leq c_k$, for some $c_k > 0, \forall k$. For Part (i), we can continue to bound the drift as

$$\begin{aligned}
 d(\mathbf{q}) &\leq \frac{1}{2} \sum_{k=1}^K c_k + 2\mathbb{E}[q_k[t](a_k[t+1] - d_k[t+1]) \mid q_k[t] = q_k] \\
 &= \frac{1}{2} \sum_{k=1}^K c_k + 2q_k(\mathbb{E}[a_k[t+1]] - \mathbb{E}[d_k[t+1] \mid q_k[t] = q_k]) \\
 &= \frac{1}{2} \sum_{k=1}^K c_k + 2q_k(\lambda_k - \beta\nu_k(\vec{\phi}) + \beta\nu_k(\vec{\phi}) - \mathbb{E}[d_k[t+1] \mid q_k[t] = q_k]) \\
 &= \left(\frac{1}{2} \sum_{k=1}^K c_k\right) + \mathbf{q}^T(\boldsymbol{\lambda} - \beta\nu(\vec{\phi})) \\
 &\quad + \mathbf{q}^T(\beta \sum_{\mathbf{m} \in \mathcal{M}} \pi_m \sum_{\mathbf{b} \in \mathcal{B}} \phi_{\mathbf{mb}} \boldsymbol{\mu}(\mathbf{m}, \mathbf{b}) - \mathbb{E}[\mathbf{d}[t+1] \mid \mathbf{q}[t] = \mathbf{q}]) \\
 &= \left(\frac{1}{2} \sum_{k=1}^K c_k\right) + \mathbf{q}^T(\boldsymbol{\lambda} - \beta\nu(\vec{\phi})) + \beta \sum_{\mathbf{m} \in \mathcal{M}} \pi_m \sum_{\mathbf{b} \in \mathcal{B}} \phi_{\mathbf{mb}} (\mathbf{q}^T \boldsymbol{\mu}(\mathbf{m}[t], \mathbf{b})) \\
 &\quad - \mathbb{E}[\mathbf{q}^T \mathbf{d}[t+1] \mid \mathbf{q}[t] = \mathbf{q}]
 \end{aligned} \tag{A.2}$$

Since $\mathbf{q}^T (\boldsymbol{\lambda} - \beta \boldsymbol{\nu}(\bar{\phi})) < 0$ by the conditions of the theorem, we need to show that

$$\beta \sum_{\mathbf{m} \in \mathcal{M}} \pi_m \sum_{\mathbf{b} \in \mathcal{B}} \phi_{\mathbf{mb}} (\mathbf{q}^T \boldsymbol{\mu}(\mathbf{m}, \mathbf{b})) - \mathbb{E} [\mathbf{q}^T \mathbf{d}[t+1] \mid \mathbf{q}[t] = \mathbf{q}] \leq 0, \quad (\text{A.3})$$

in order to prove positive recurrence or stability according to Foster's Theorem. To this end, we define $\chi_{\mathbf{mb}}[t+1] \in \{0, 1\}$, to be random variables that represent the scheduling decision at time $t+1$; $\chi_{\mathbf{mb}}[t+1] = 1$ if bit allocation $\bar{\mathbf{b}}$ is selected at time $t+1$ and $\chi_{\mathbf{mb}}[t+1] = 0$ otherwise. Since only one bit allocation can be selected at each time, we have the constraint $\sum_{\mathbf{b} \in \mathcal{B}} \chi_{\mathbf{mb}}[t+1] = 1$.

We re-write (A.3) using these newly introduced scheduling variables as

$$\begin{aligned} & \beta \sum_{\mathbf{m} \in \mathcal{M}} \pi_m \sum_{\mathbf{b} \in \mathcal{B}} \phi_{\mathbf{mb}} (\mathbf{q}^T \boldsymbol{\mu}(\mathbf{m}, \mathbf{b})) - \mathbb{E} [\mathbf{q}^T \mathbf{d}[t+1] \mid \mathbf{q}[t] = \mathbf{q}] \\ = & \beta \sum_{\mathbf{m} \in \mathcal{M}} \pi_m \sum_{\mathbf{b} \in \mathcal{B}} \phi_{\mathbf{mb}} [\mathbf{q}^T \boldsymbol{\mu}(\mathbf{m}, \mathbf{b})] \\ & - \sum_{\mathbf{m} \in \mathcal{M}} \pi_m \mathbb{E} [\sum_{\mathbf{b} \in \mathcal{B}} \chi_{\mathbf{mb}}[t+1] \mathbf{q}^T \mathbf{d}[t+1] \mid \mathbf{q}[t] = \mathbf{q}, \mathbf{m}[t] = \mathbf{m}] \\ = & \beta \sum_{\mathbf{m} \in \mathcal{M}} \pi_m \sum_{\mathbf{b} \in \mathcal{B}} \phi_{\mathbf{mb}} [\mathbf{q}^T \boldsymbol{\mu}(\mathbf{m}, \mathbf{b})] \\ & - \sum_{\mathbf{m} \in \mathcal{M}} \pi_m \sum_{\mathbf{b} \in \mathcal{B}} \chi_{\mathbf{mb}}[t+1] \mathbf{q}^T \mathbb{E} [\boldsymbol{\mu}(\mathbf{m}[t+1], \mathbf{b}) \mid \mathbf{q}[t] = \mathbf{q}, \mathbf{m}[t+1] = \mathbf{m}] \\ & \text{since given } \mathbf{q}[t] = \mathbf{q} \text{ and } \mathbf{m}[t+1] = \mathbf{m}, \text{ the scheduling variables } \chi_{\mathbf{mb}}[t+1], \\ & \forall \mathbf{m}, \mathbf{b}, \text{ are no longer random} \\ = & \beta \sum_{\mathbf{m} \in \mathcal{M}} \pi_m \sum_{\mathbf{b} \in \mathcal{B}} \phi_{\mathbf{mb}} (\mathbf{q}^T \boldsymbol{\mu}(\mathbf{m}, \mathbf{b})) - \sum_{\mathbf{m} \in \mathcal{M}} \pi_m \sum_{\mathbf{b} \in \mathcal{B}} \chi_{\mathbf{mb}}[t+1] \mathbf{q}^T \boldsymbol{\mu}(\mathbf{m}, \mathbf{b}) \\ = & \beta \sum_{\mathbf{m} \in \mathcal{M}} \pi_m \sum_{\mathbf{b} \in \mathcal{B}} \phi_{\mathbf{mb}} (\mathbf{q}^T \boldsymbol{\mu}(\mathbf{m}, \mathbf{b})) - \sum_{\mathbf{m} \in \mathcal{M}} \pi_m (\mathbf{q}^T \boldsymbol{\mu}(\mathbf{m}, \bar{\mathbf{b}})) \\ & \text{for some } \bar{\mathbf{b}} \in \mathcal{B} \\ \leq & \beta \sum_{\mathbf{m} \in \mathcal{M}} \pi_m \sum_{\mathbf{b} \in \mathcal{B}} \phi_{\mathbf{mb}} (\mathbf{q}^T \boldsymbol{\mu}(\mathbf{m}, \mathbf{b})) - \beta \sum_{\mathbf{m} \in \mathcal{M}} \pi_m [\max_{\mathbf{b} \in \mathcal{B}} \mathbf{q}^T \boldsymbol{\mu}(\mathbf{m}, \mathbf{b})]. \end{aligned} \quad (\text{A.4})$$

The last inequality follows since our scheduling rule dictates that we choose allocation $\bar{\mathbf{b}}$ such that $\mathbf{q}^T \boldsymbol{\mu}(\mathbf{m}, \bar{\mathbf{b}}) \geq \beta \max_{\mathbf{b} \in \mathcal{B}} \mathbf{q}^T \boldsymbol{\mu}(\mathbf{m}, \mathbf{b})$. Finally, it is straightforward to see that

$$\begin{aligned} \max & \quad [\beta \sum_{\mathbf{m} \in \mathcal{M}} \pi_m \sum_{\mathbf{b} \in \mathcal{B}} \phi_{\mathbf{mb}} \mathbf{q}^T \boldsymbol{\mu}(\mathbf{m}, \mathbf{b})] = \beta \sum_{\mathbf{m} \in \mathcal{M}} \pi_m [\max_{\mathbf{b} \in \mathcal{B}} \mathbf{q}^T \boldsymbol{\mu}(\mathbf{m}, \mathbf{b})] \\ \text{s.t} & \quad \sum_{\mathbf{b} \in \mathcal{B}} \phi_{\mathbf{mb}} = 1, \forall \mathbf{m} \in \mathcal{M} \\ & \quad \phi_{\mathbf{mb}} \in [0, 1], \forall \mathbf{m} \in \mathcal{M}, \mathbf{b} \in \mathcal{B} \end{aligned} \quad (\text{A.5})$$

Thus, the drift $d(\mathbf{q})$ is strictly negative for q_k sufficiently large which proves stability.

For Part (ii), as done in the earlier proof, we bound the drift as

$$\begin{aligned} d(\mathbf{q}) &\leq \frac{1}{2} \sum_{k=1}^K c_k + 2\mathbb{E}[q_k[t](a_k[t+1] - d_k[t+1]) \mid q_k[t] = q_k] \\ &= \left(\frac{1}{2} \sum_{k=1}^K c_k\right) + \mathbf{q}^T (\boldsymbol{\lambda} - \boldsymbol{\nu}(\bar{\boldsymbol{\phi}})) + \sum_{\mathbf{m} \in \mathcal{M}} \pi_m \sum_{\mathbf{b} \in \mathcal{B}} \phi_{\mathbf{mb}} (\mathbf{q}^T \boldsymbol{\mu}(\mathbf{m}[t], \mathbf{b})) \\ &\quad - \mathbb{E}[\mathbf{q}^T \mathbf{d}[t+1] \mid \mathbf{q}[t] = \mathbf{q}]. \end{aligned} \quad (\text{A.6})$$

We now show that

$$\beta \sum_{\mathbf{m} \in \mathcal{M}} \pi_m \sum_{\mathbf{b} \in \mathcal{B}} \phi_{\mathbf{mb}} (\mathbf{q}^T \boldsymbol{\mu}(\mathbf{m}, \mathbf{b})) - \mathbb{E}[\mathbf{q}^T \mathbf{d}[t+1] \mid \mathbf{q}[t] = \mathbf{q}] \leq \mathbf{q}^T \boldsymbol{\beta}. \quad (\text{A.7})$$

We define $\chi_{\mathbf{mb}}[t+1] \in \{0, 1\}$, to be random variables that represent the scheduling decision at time $t+1$; $\chi_{\mathbf{mb}}[t+1] = 1$ if bit allocation $\bar{\mathbf{b}}$ is selected at time $t+1$ and $\chi_{\mathbf{mb}}[t+1] = 0$ otherwise. Since only one bit allocation can be selected at each time, we have the constraint $\sum_{\mathbf{b} \in \mathcal{B}} \chi_{\mathbf{mb}}[t+1] = 1$. We re-write (A.3) using these newly introduced scheduling variables as

$$\begin{aligned} &\sum_{\mathbf{m} \in \mathcal{M}} \pi_m \sum_{\mathbf{b} \in \mathcal{B}} \phi_{\mathbf{mb}} (\mathbf{q}^T \boldsymbol{\mu}(\mathbf{m}, \mathbf{b})) - \mathbb{E}[\mathbf{q}^T \mathbf{d}[t+1] \mid \mathbf{q}[t] = \mathbf{q}] \\ &= \sum_{\mathbf{m} \in \mathcal{M}} \pi_m \sum_{\mathbf{b} \in \mathcal{B}} \phi_{\mathbf{mb}} [\mathbf{q}^T \boldsymbol{\mu}(\mathbf{m}, \mathbf{b})] \\ &\quad - \sum_{\mathbf{m} \in \mathcal{M}} \pi_m \mathbb{E}[\sum_{\mathbf{b} \in \mathcal{B}} \chi_{\mathbf{mb}}[t+1] \mathbf{q}^T \mathbf{d}[t+1] \mid \mathbf{q}[t] = \mathbf{q}, \mathbf{m}[t] = \mathbf{m}] \\ &= \sum_{\mathbf{m} \in \mathcal{M}} \pi_m \sum_{\mathbf{b} \in \mathcal{B}} \phi_{\mathbf{mb}} [\mathbf{q}^T \boldsymbol{\mu}(\mathbf{m}, \mathbf{b})] \\ &\quad - \sum_{\mathbf{m} \in \mathcal{M}} \pi_m \sum_{\mathbf{b} \in \mathcal{B}} \chi_{\mathbf{mb}}[t+1] \mathbf{q}^T \mathbb{E}[\boldsymbol{\mu}(\mathbf{m}[t+1], \mathbf{b}) \mid \mathbf{q}[t] = \mathbf{q}, \mathbf{m}[t+1] = \mathbf{m}] \\ &\quad \text{since given } \mathbf{q}[t] = \mathbf{q} \text{ and } \mathbf{m}[t+1] = \mathbf{m}, \text{ the scheduling variables } \chi_{\mathbf{mb}}[t+1], \\ &\quad \forall \mathbf{m}, \mathbf{b}, \text{ are no longer random} \\ &= \sum_{\mathbf{m} \in \mathcal{M}} \pi_m \sum_{\mathbf{b} \in \mathcal{B}} \phi_{\mathbf{mb}} (\mathbf{q}^T \boldsymbol{\mu}(\mathbf{m}, \mathbf{b})) - \sum_{\mathbf{m} \in \mathcal{M}} \pi_m \sum_{\mathbf{b} \in \mathcal{B}} \chi_{\mathbf{mb}}[t+1] \mathbf{q}^T \boldsymbol{\mu}(\mathbf{m}, \mathbf{b}) \\ &= \sum_{\mathbf{m} \in \mathcal{M}} \pi_m \sum_{\mathbf{b} \in \mathcal{B}} \phi_{\mathbf{mb}} (\mathbf{q}^T \boldsymbol{\mu}(\mathbf{m}, \mathbf{b})) - \sum_{\mathbf{m} \in \mathcal{M}} \pi_m \sum_{\mathbf{b} \in \mathcal{B}} \mathbf{q}^T \boldsymbol{\mu}(\mathbf{m}, \bar{\mathbf{b}}) \\ &\leq \sum_{\mathbf{m} \in \mathcal{M}} \pi_m \sum_{\mathbf{b} \in \mathcal{B}} \phi_{\mathbf{mb}} (\mathbf{q}^T \boldsymbol{\mu}(\mathbf{m}, \mathbf{b})) - \sum_{\mathbf{m} \in \mathcal{M}} \pi_m [\mathbf{q}^T \boldsymbol{\mu}(\mathbf{m}, \mathbf{b}^*) - \mathbf{q}^T \boldsymbol{\beta}] \\ &\quad \text{since } \bar{\mathbf{b}} \text{ satisfies } \mathbf{q}^T \boldsymbol{\mu}(\mathbf{m}, \bar{\mathbf{b}}) \geq \mathbf{q}^T \boldsymbol{\mu}(\mathbf{m}, \mathbf{b}^*) - \mathbf{q}^T \boldsymbol{\beta}. \\ &\leq \mathbf{q}^T \boldsymbol{\beta} \text{ by the argument in (A.5)} \end{aligned} \quad (\text{A.8})$$

The proof is complete from the fact that $\mathbf{q}^T (\boldsymbol{\lambda} + \boldsymbol{\beta} - \boldsymbol{\nu}(\bar{\boldsymbol{\phi}})) < 0$ by the conditions of the theorem.

A.2 Proof of Theorem 1

Firstly, we present an alternate characterization of sub-modular functions from Nemhauser et al. [70] that is useful for the proof. For any two disjoint subsets S and $T = \{t_1, \dots, t_N\}$, $S, T \subseteq E$, we can write

$$F(S \cup T) = \left[\sum_{i=2}^N F(S \cup \{t_1, \dots, t_i\}) - F(S \cup \{t_1, \dots, t_{i-1}\}) \right] + (F(S \cup \{t_1\}) - F(S)) + F(S) \quad (\text{A.9})$$

through telescoping. By the sub-modularity of F , we have

$$\begin{aligned} F(S \cup T) &\leq \left[\sum_{i=1}^N F(S \cup t_i) - F(S) \right] + F(S) \\ &= F(S) + \sum_{i=1}^N \rho_{t_i}(S) \end{aligned} \quad (\text{A.10})$$

and furthermore, for $S \subseteq T$, this simplifies to

$$F(T) \leq F(S) + \sum_{t \in T \setminus S} \rho_t(S). \quad (\text{A.11})$$

Now, let S^* and S_g be the optimal solution and the solution generated by the greedy algorithm respectively; ρ_i represents the incremental value that is obtained during the i -th iteration of the greedy algorithm. Then, by setting $S = S_{g,0} = \emptyset$ in (A.11) and noting that $|S^*| \leq k$ since it is a uniform matroid, we calculate

$$F^* \leq \sum_{e \in T} F(\{e\}) \leq k\rho_1 = k \max_{e \in E} F(\{e\}). \quad (\text{A.12})$$

Recalling that $F(S_{g,0}) = 0$ due to normalization and applying (A.11) to set $S_{g,j}$ generated by the greedy algorithm after j iterations, we have

$$\begin{aligned} F^* &\leq F(S_{g,j}) + \sum_{t \in T \setminus S_{g,j}} \rho_t(S_{g,j}) \\ &= \sum_{i=1}^j (F(S_{g,i}) - F(S_{g,i-1})) + \sum_{t \in T \setminus S_{g,j}} \rho_t(S_{g,j}) \\ &\leq \sum_{i=1}^j \rho_i + k\rho_{j+1}. \end{aligned} \quad (\text{A.13})$$

By dividing both sides by k , re-arranging and adding $\sum_{i=1}^j \rho_i$ to both sides, we get

$$\sum_{i=1}^{j+1} \rho_i \geq \frac{1}{k} F^* + \frac{k-1}{k} \sum_{i=1}^j \rho_i. \quad (\text{A.14})$$

The following result is proved through induction in order to solve the recursion.

$$\sum_{i=1}^j \rho_i \geq \left(\frac{k^j - (k-1)^j}{k^j} \right) F^*. \quad (\text{A.15})$$

For $j = 1$, we get $\rho_1 \geq \frac{F^*}{k}$, which is true since, for $S^* = \{s_1^*, s_2^*, \dots, s_K^*\}$, we have

$$\begin{aligned} F^* &= F(S^*) \\ &= \sum_{i=2}^k \left[F(\{s_1^*, s_2^*, \dots, s_i^*\}) - F(\{s_1^*, s_2^*, \dots, s_{i-1}^*\}) \right] + F(\{s_1^*\}) \\ &\leq (k-1)F(\{s_1^*\}) + F(\{s_1^*\}) \\ &= kF(\{s_1^*\}). \end{aligned} \quad (\text{A.16})$$

Assuming the statement holds true for $(j-1)$, and substituting it in (A.14), we get

$$\begin{aligned} \sum_{i=1}^j \rho_i &\geq \frac{1}{k} F^* + \frac{k-1}{k} \left(\frac{k^{j-1} - (k-1)^{j-1}}{k^{j-1}} \right) F^* \\ &= \frac{1}{k} F^* + (k-1) \left(\frac{k^{j-1} - (k-1)^{j-1}}{k^j} \right) F^* \\ &= \frac{k^{j-1} + (k-1)(k^{j-1} - (k-1)^{j-1})}{k^j} F^* \\ &= \left(\frac{k^j - (k-1)^j}{k^j} \right) F^*, \end{aligned} \quad (\text{A.17})$$

which proves the claim. Now, by setting $j = k$, we calculate

$$F_g = \sum_{i=1}^k \rho_i \geq \left(\frac{k^k - (k-1)^k}{k^k} \right) F^*, \quad (\text{A.18})$$

or in other words,

$$\frac{F_g}{F^*} \geq \left(\frac{k^k - (k-1)^k}{k^k} \right) = 1 - \left(1 - \frac{1}{k} \right)^k. \quad (\text{A.19})$$

The result follows since $\lim_{k \rightarrow \infty} \left(1 - \frac{1}{k} \right)^k = \frac{1}{e}$ and the fact that $\left(1 - \frac{1}{k} \right)^k$ is increasing in k .

A.3 Proof of Theorems 12-14

A.3.1 Proof of Theorem 12

With $\Delta(b_k) = \mathbb{E}[\sigma^2] (1 - c_1(N_t, N_r) 2^{-c_2(N_t, N_r)b_k})$, the objective function (omitting dependence on t) becomes

$$\text{minimize}_{b \in \mathcal{B}} \quad - \sum_{k=1}^K w_k \log_2 (1 + a_k \mathbb{E}[\sigma^2] (1 - c_1(N_t, N_r) 2^{-c_2(N_t, N_r)b_k})) \quad . \quad (\text{A.20})$$

The objective function is clearly convex since $2^{-c_2(N_t, N_r)b_k}$ is convex. By studying (A.20) closely, we can also say that b_k^* is such that $\sum_{k=1}^K b_k^* = B$ since if this not true, we can increase the bit allocation for at least one user thereby decreasing the objective function. Since $B > 0$, $b_k = 0, \forall k$ is in the interior of our constraint set \mathcal{B} which implies that Slater's constraint qualification condition holds. Consequently, the Karush-Kuhn-Tucker (KKT) conditions become sufficient in nature. The Lagrangian cost function can be written as

$$\begin{aligned} \mathcal{L}(b_k, \lambda_k, \eta) = & - \sum_{k=1}^K w_k \log_2 (1 + a_k \mathbb{E}[\sigma^2] (1 - c_1(N_t, N_r) 2^{-c_2(N_t, N_r)b_k})) \\ & - \lambda_k b_k + \eta (\sum_k b_k - B) \end{aligned} \quad (\text{A.21})$$

for which the KKT conditions are

$$\begin{aligned} b_k^* &\geq 0, & \lambda_k^* &\geq 0, & b_k^* \lambda_k^* &= 0, \\ \eta^* &= \frac{a_k \mathbb{E}[\sigma^2] c_1(N_t, N_r) c_2(N_t, N_r) (\log 2)}{(1 + a_k \mathbb{E}[\sigma^2]) 2^{c_2(N_t, N_r)b_k} - \mathbb{E}[\sigma^2] c_1(N_t, N_r)} + \lambda_k^*, \end{aligned} \quad (\text{A.22})$$

Since $\frac{a_k \mathbb{E}[\sigma^2] c_1(N_t, N_r) c_2(N_t, N_r) (\log 2)}{(1 + a_k \mathbb{E}[\sigma^2]) 2^{c_2(N_t, N_r)b_k} - \mathbb{E}[\sigma^2] c_1(N_t, N_r)}$ is a decreasing function in b_k , if $\eta^* \leq \frac{a_k \mathbb{E}[\sigma^2] c_1(N_t, N_r) c_2(N_t, N_r) (\log 2)}{(1 + \mathbb{E}[\sigma^2]) (a_k - c_1(N_t, N_r))}$, then $\lambda_k^* = 0$ and

$$b_k^* = \frac{1}{c_2(N_t, N_r)} \log_2 \left(\frac{\mathbb{E}[\sigma^2] c_1(N_t, N_r)}{(1 + a_k \mathbb{E}[\sigma^2])} \left(\frac{a_k c_2(N_t, N_r) (\log 2)}{\eta^*} + 1 \right) \right) \quad (\text{A.23})$$

is a valid solution to (A.20). If $\eta^* > \frac{a_k \mathbb{E}[\sigma^2] c_1(N_t, N_r) c_2(N_t, N_r) (\log 2)}{(1 + \mathbb{E}[\sigma^2])(a_k - c_1(N_t, N_r))}$, $\lambda_k^* = \eta^* - \frac{a_k \mathbb{E}[\sigma^2] c_1(N_t, N_r) c_2(N_t, N_r) (\log 2)}{(1 + \mathbb{E}[\sigma^2])(a_k - c_1(N_t, N_r))}$ and $b_k^* = 0$. Hence, we can write the solution as

$$b_k^* = \left[\frac{1}{c_2(N_t, N_r)} \log_2 \left(\frac{\mathbb{E}[\sigma^2] c_1(N_t, N_r)}{(1 + a_k \mathbb{E}[\sigma^2])} \left(\frac{a_k c_2(N_t, N_r) (\log 2)}{\eta^*} + 1 \right) \right) \right]^+ \quad (\text{A.24})$$

where η^* is chosen such that $\sum_k b_k^* = B$.

A.3.2 Proof of Theorem 13

In order to compute (3.26), we first need to sort

$$\left\{ \frac{a_k \mathbb{E}[\sigma^2] c_1(N_t, N_r) c_2(N_t, N_r) (\log 2)}{(1 + \mathbb{E}[\sigma^2])(a_k - c_1(N_t, N_r))} \right\}$$

in ascending order, which has complexity $\mathcal{O}(K \log_2 K)$. Call this sorted set

$$\left\{ \frac{a_m \mathbb{E}[\sigma^2] c_1(N_t, N_r) c_2(N_t, N_r) (\log 2)}{(1 + \mathbb{E}[\sigma^2])(a_m - c_1(N_t, N_r))} \right\}. \text{ Once sorted, we need to set}$$

$$\eta^* = \frac{a_m \mathbb{E}[\sigma^2] c_1(N_t, N_r) c_2(N_t, N_r) (\log 2)}{(1 + \mathbb{E}[\sigma^2])(a_m - c_1(N_t, N_r))}$$

for each m and test feasibility. Testing feasibility incurs $\mathcal{O}(K)$, as it is a K -term addition and scanning through each $\frac{a_m \mathbb{E}[\sigma^2] c_1(N_t, N_r) c_2(N_t, N_r) (\log 2)}{(1 + \mathbb{E}[\sigma^2])(a_m - c_1(N_t, N_r))}$ incurs $\mathcal{O}(\log_2 K)$ through the use of binary search. As we increase η^* , more b_m^* terms are set to zero. Once we locate m_1 and m_2 such that

$$\eta^* = \frac{a_{m_1} \mathbb{E}[\sigma^2] c_1(N_t, N_r) c_2(N_t, N_r) (\log 2)}{(1 + \mathbb{E}[\sigma^2])(a_{m_1} - c_1(N_t, N_r))}$$

is infeasible while $\eta^* = \frac{a_{m_2} \mathbb{E}[\sigma^2] c_1(N_t, N_r) c_2(N_t, N_r) (\log 2)}{(1 + \mathbb{E}[\sigma^2])(a_{m_2} - c_1(N_t, N_r))}$ is feasible, we can compute

η^* in closed-form since it satisfies $\sum_{m \geq m_2} b_m^* = B$. Hence, the total complexity is $\mathcal{O}(K \log_2 K) + \mathcal{O}(K \log_2 K) = \mathcal{O}(K \log_2 K)$.

A.3.3 Proof of Theorem 14

Firstly, we have that

$$b_{k,INT}^* \geq \begin{cases} b_k^* - 1, & b_k^* \geq 1 \\ 0, & b_k^* < 1 \end{cases}. \quad (\text{A.25})$$

From (A.25), we can bound what essentially is the quantization noise as

$$\begin{aligned} & \frac{1 - c_1(N_t, N_r) 2^{-c_2(N_t, N_r) b_k^*}}{1 - c_1(N_t, N_r) 2^{-c_2(N_t, N_r) b_{k,INT}^*}} \\ & \leq \max \left\{ \frac{1}{1 - c_1(N_t, N_r) 2^{c_2(N_t, N_r)}}, \frac{1}{1 - c_1(N_t, N_r)} \right\}. \end{aligned} \quad (\text{A.26})$$

Now, we can bound the loss in weighted-sum-rate as follows

$$\begin{aligned} & \sum_{k=1}^K w_k \log_2 (1 + a_k \mathbb{E}[\sigma^2] (1 - c_1(N_t, N_r) 2^{-c_2(N_t, N_r) b_k^*})) \\ & - \sum_{k=1}^K w_k \log_2 (1 + a_k \mathbb{E}[\sigma^2] (1 - c_1(N_t, N_r) 2^{-c_2(N_t, N_r) b_{k,INT}^*})) \\ & \leq \sum_{k=1}^K w_k \log_2 \left(\frac{1 + a_k \mathbb{E}[\sigma^2] (1 - c_1(N_t, N_r) 2^{-c_2(N_t, N_r) b_k^*})}{1 + a_k \mathbb{E}[\sigma^2] (1 - c_1(N_t, N_r) 2^{-c_2(N_t, N_r) b_{k,INT}^*})} \right) \\ & \leq \sum_{k=1}^K w_k \log_2 \left(1 + \frac{1 - c_1(N_t, N_r) 2^{-c_2(N_t, N_r) b_k^*}}{1 - c_1(N_t, N_r) 2^{-c_2(N_t, N_r) b_{k,INT}^*}} \right) \\ & \leq \log_2 \left(1 + \max \left\{ \frac{1}{1 - c_1(N_t, N_r) 2^{c_2(N_t, N_r)}}, \frac{1}{1 - c_1(N_t, N_r)} \right\} \right) \left(\sum_{k=1}^K w_k \right) \text{ from (A.26)} \\ & \quad (\text{A.27}) \end{aligned}$$

to get the result.

Appendix B

Appendix for Chapter 4

B.1 Proofs of Lemmas

B.1.1 Proof of Lemma 13

The proof is based on induction on the variable N . For $N = 2$, the result holds true because

$$\int_{x_2 \kappa_2} e^{-w} dw = e^{-x_2 \kappa_2} \quad (\text{B.1})$$

We will assume then that the hypothesis is true for $N = k$, i.e.,

$$\begin{aligned} & \int_{x_k \kappa_N} \int_{x_{k-1} \kappa_{k-1}} \cdots \int_{x_2 \kappa_2} e^{-w} \prod_{i=2}^{k-1} e^{-x_i} dw dx_2 dx_3 \cdots dx_{k-1} \\ &= \left[\prod_{i=1}^{k-1} \frac{1}{\delta_i} \right] e^{-\delta_{k-1} \kappa_k x_k}. \end{aligned} \quad (\text{B.2})$$

Then for $N = k + 1$, we have that

$$\begin{aligned} & \int_{x_{k+1} \kappa_N} \int_{x_k \kappa_{k-2}} \cdots \int_{x_2 \kappa_2} e^{-w} \prod_{i=2}^k e^{-x_i} dw dx_2 dx_3 \cdots dx_k \\ &= \int_{x_{k+1} \kappa_N} \left[\int_{x_k \kappa_{k-2}} \cdots \int_{x_2 \kappa_2} e^{-w} \prod_{i=2}^{k-1} e^{-x_i} dw dx_2 dx_3 \cdots dx_{k-1} \right] e^{-x_k} dx_k \\ &= \int_{x_{k+1} \kappa_{k+1}} \left[\prod_{i=1}^{k-1} \frac{1}{\delta_i} \right] e^{-\delta_{k-1} \kappa_k x_k} e^{-x_k} dx_k \\ &= \left[\prod_{i=1}^{k-1} \frac{1}{\delta_i} \right] \int_{x_{k+1} \kappa_{k+1}} e^{-(\delta_{k-1} \kappa_k + 1) x_k} dx_k \\ &= \left[\prod_{i=1}^k \frac{1}{\delta_i} \right] e^{-\delta_k \kappa_{k+1} x_{k+1}}. \end{aligned} \quad (\text{B.3})$$

This concludes the proof.

B.1.2 Proof of Lemma 23

The proof is based on induction on the variable N . For $N = 2$, the result holds true because

$$\begin{aligned} \int_{x_2 \kappa_{2i}}^M e^{-w} dw &= e^{-x_2 \kappa_{2i}} - e^M, \forall i \\ &\doteq e^{-x_2 \kappa_{2i}}, \forall i. \end{aligned} \quad (\text{B.4})$$

We will assume then that the hypothesis is true for $N = k$, i.e.,

$$\begin{aligned} &\int_{x_k \kappa_{ki}}^{\frac{M}{\kappa_{(k-1)i}}} \int_{x_{k-1} \kappa_{(k-1)i}}^{\frac{M}{\kappa_{(k-2)i}}} \dots \int_{x_2 \kappa_{2i}}^M e^{-w} \prod_{i=2}^{k-1} e^{-x_i} dw dx_2 dx_3 \dots dx_{k-1} \\ &\geq \left[\prod_{j=1}^{k-1} \frac{1}{\delta_j^i} \right] e^{-x_k \kappa_{ki} \delta_{k-1}^i}, \forall i \end{aligned} \quad (\text{B.5})$$

Then for $N = k + 1$, we have that

$$\begin{aligned} &\int_{x_{k+1} \kappa_{(k+1)i}}^{\frac{M}{\kappa_{ki}}} \int_{x_k \kappa_{ki}}^{\frac{M}{\kappa_{(k-1)i}}} \dots \int_{x_2 \kappa_{2i}}^M e^{-w} \prod_{i=2}^k e^{-x_i} dw dx_2 dx_3 \dots dx_k \\ &= \int_{x_{k+1} \kappa_{(k+1)i}}^{\frac{M}{\kappa_{ki}}} \left[\int_{x_k \kappa_{ki}}^{\frac{M}{\kappa_{(k-1)i}}} \dots \int_{x_2 \kappa_{2i}}^M e^{-w} \prod_{i=2}^{k-1} e^{-x_i} dw dx_2 dx_3 \dots dx_{k-1} \right] e^{-x_k} dx_k \\ &\geq \int_{x_{k+1} \kappa_{(k+1)i}}^{\frac{M}{\kappa_{ki}}} \left[\prod_{j=1}^{k-1} \frac{1}{\delta_j^i} \right] e^{-x_k \kappa_{ki} \delta_{k-1}^i} e^{-x_k} dx_k \\ &= \left[\prod_{j=1}^{k-1} \frac{1}{\delta_j^i} \right] \int_{x_{k+1} \kappa_{(k+1)i}}^{\frac{M}{\kappa_{ki}}} e^{-x_k (\kappa_{ki} \delta_{k-1}^i + 1)} dx_k \\ &= \left[\prod_{j=1}^k \frac{1}{\delta_j^i} \right] \left[e^{-x_{k+1} \kappa_{(k+1)i} \delta_k^i} - e^{-x_{k+1} \frac{M}{\kappa_{ki}}} \right] \\ &\geq \left[\prod_{j=1}^k \frac{1}{\delta_j^i} \right] e^{-x_{k+1} \kappa_{(k+1)i} \delta_k^i}. \end{aligned} \quad (\text{B.6})$$

B.1.3 Proof of Lemma 14

It is straightforward to see the following implication on events

$$\{\beta_k h_{kk} \geq \beta_{i_2} h_{i_2 i_2} \geq \dots \beta_{i_K} h_{i_K i_K}\} \rightarrow \{k = \arg \max_j \beta_j h_{jj}\}. \quad (\text{B.7})$$

Furthermore, for any two permutations $(k, i_2, \dots, i_K) \in \mathcal{P}_k$ and $(k, j_2, \dots, j_K) \in \mathcal{P}_k$, $j_1 = k$, the corresponding events $\{\beta_k h_{kk} \geq \beta_{i_2} h_{i_2 i_2} \geq \dots \beta_{i_K} h_{i_K i_K}\}$ and

$\{\beta_k h_{kk} \geq \beta_{j_2} h_{j_2 j_2} \geq \dots \beta_{j_K} h_{j_K j_K}\}$ are mutually exclusive. Thus, it follows that $\{\cup_{(i_1, i_2, \dots, i_K) \in \mathcal{P}_k, i_1=k} \{\beta_{i_1} h_{i_1 i_1} \geq \beta_{i_2} h_{i_2 i_2} \geq \dots \beta_{i_K} h_{i_K i_K}\}\}$ and $\{k = \arg \max_j \beta_j h_{jj}\}$ are equivalent events and the probability of the latter event occurring can be expressed as

$$\begin{aligned} & \Pr(k = \arg \max_j \beta_j h_{jj}) \\ &= \sum_{(i_1, i_2, \dots, i_K) \in \mathcal{P}_k, i_1=k} \Pr(\beta_{i_1} h_{i_1 i_1} \geq \beta_{i_2} h_{i_2 i_2} \geq \dots \beta_{i_K} h_{i_K i_K}). \end{aligned} \quad (\text{B.8})$$

By (B.8), we can now focus on computing $\Pr(\beta_{i_1} h_{i_1 i_1} \geq \beta_{i_2} h_{i_2 i_2} \geq \dots \beta_{i_K} h_{i_K i_K})$ for any arbitrary permutation $(i_1, i_2, \dots, i_K) \in \mathcal{P}_k, i_1 = k$. For ease in notation, we set $k = 1$ and $\mathbf{p}^* = [1 \ 2 \dots K]^T$ as the user and permutation of interest without loss of generality. This probability can be computed from first principles as follows

$$\begin{aligned} & \Pr(\beta_1 h_{11} \geq \beta_2 h_{22} \geq \dots \beta_K h_{KK}) \\ &= \Pr(h_{11} \geq \sigma_{21} h_{22} \geq \dots \sigma_{K1} h_{KK}) \\ &= \int_0^\infty \int_{\sigma_{K1} x_K}^\infty \int_{\sigma_{(K-1)1} x_{K-1}}^\infty \dots \int_{\sigma_{21} x_2}^\infty e^{-w} \prod_{i=2}^{K-1} e^{-x_i} dw dx_2 dx_3 \dots dx_K \end{aligned} \quad (\text{B.9})$$

We proceed by applying the result in Lemma 13 to get

$$\begin{aligned} \Pr(\beta_1 h_{11} \geq \beta_2 h_{22} \geq \dots \beta_K h_{KK}) &= \left[\prod_{j=1}^{K-1} \frac{1}{\delta_j^{\mathbf{p}^*}} \right] \int_0^\infty e^{-\delta_{K-1}^{\mathbf{p}^*} \kappa_K x_K} e^{-x_K} dx_K \\ &= \prod_{j=1}^K \frac{1}{\delta_j^{\mathbf{p}^*}}. \end{aligned} \quad (\text{B.10})$$

The result follows by substituting (B.10) into (B.8).

B.1.4 Proof of Lemma 15

Using similar arguments as in the proof of Lemma 15, we get the following

$$\begin{aligned} & \Pr(k = \arg \max_j \beta_j [h_{jj}]_{b_j}) \\ &= \sum_{(i_1, i_2, \dots, i_K) \in \mathcal{P}_k, i_1=k} \Pr(\beta_{i_1} [h_{i_1 i_1}]_{b_{i_1}} \geq \beta_{i_2} [h_{i_2 i_2}]_{b_{i_2}} \geq \dots \beta_{i_K} [h_{i_K i_K}]_{b_{i_K}}). \end{aligned} \quad (\text{B.11})$$

The following lemma, which relates h_{ii} and $[h_{ii}]_{b_i}$, is useful later in the proof.

Lemma 22. *If $h_{ii} \in [0, M]$, then $h_{ii} - \frac{M}{2^{b_i}} \leq [h_{ii}]_{b_i} \leq h_{ii}$.*

Proof. The proof follows from the definition of $[h_{ii}]_{b_i}$ in (4.5) along with the property $\lfloor x \rfloor \geq x - 1$ for any $x \geq 0$. \square

We focus again on the case $k = 1$ without loss of generality. From the above result followed by a little algebra, we establish that the following event

$$\{h_{11} \geq \sigma_{21}h_{22} + M2^{-b_1} \geq \sigma_{31}h_{33} + M2^{-b_1} + \sigma_{21}M2^{-b_2} \geq \dots \geq \sigma_{K1}h_{KK} + \left[\sum_{j=1}^{K-1} \sigma_{j1}M2^{-b_j} \right]\} \cap \{h_{ii} \in [0, M], \forall i\} \quad (\text{B.12})$$

implies the event $\{\beta_1[h_{11}]_{b_1} \geq \beta_2[h_{22}]_{b_2} \geq \dots \beta_K[h_{KK}]_{b_K}\}$. Thus, the probability of the event (B.12) can be used to form a lower bound on

$$\Pr \left(k = \arg \max_j \beta_j [h_{jj}]_{b_j} \right)$$

and can be computed from first principles as follows

$$\begin{aligned} & \Pr \{ \{h_{11} \geq \sigma_{21}h_{22} + M\gamma_1 \geq \sigma_{31}h_{33} + M\gamma_2 \geq \dots \geq \sigma_{K1}h_{KK} + M\gamma_{K-1}\} \\ & \cap \{h_{ii} \in [0, M], \forall i\} \} \\ = & \int_0^{\frac{M}{\sigma_{K1}}(1-\gamma_{K-1})} \dots \int_{\sigma_{(K-1)1}x_{K-1} + M\gamma_{K-2}}^{\frac{M}{\sigma_{(K-2)1}}(1-\gamma_{K-3})} \dots \int_{\sigma_{21}x_2 + M\gamma_1}^M e^{-w} \prod_{i=2}^{K-1} e^{-x_i} dw dx_2 dx_3 \dots dx_K \end{aligned} \quad (\text{B.13})$$

where $\gamma_p = \sum_{j=1}^{p-1} \sigma_{j1}2^{-b_j}$. The above expression can be bounded in closed-form by using the following lemma.

Lemma 23. *Given any set of ratios $\{\sigma_{ij}\}_{i,j=1}^N$, $N \geq 2$ and if M is selected according to (4.4), the following relationship holds when \mathbf{b} satisfies the constraints $\{\sum_{j=1}^{K-2} \sigma_{ji}2^{-b_j} \leq 1 - \frac{1}{\gamma_3}, \forall i\}$*

$$\begin{aligned} & \int_{\sigma_{K1}x_K + M\gamma_{K-1}}^{\frac{M}{\sigma_{(K-1)1}}(1-\gamma_{K-2})} \int_{\sigma_{(K-1)1}x_{K-1} + M\gamma_{K-2}}^{\frac{M}{\sigma_{(K-2)1}}(1-\gamma_{K-3})} \dots \int_{\sigma_{21}x_2 + M\gamma_1}^M \prod_{i=1}^{K-1} e^{-x_i} dx_1 dx_2 dx_3 \dots dx_{K-1} \\ = & \left[\prod_{i=1}^{K-1} \frac{e^{-M\gamma_i \delta_i}}{\delta_i} \right] e^{x_K \delta_{K-1} \sigma_{K1}} \end{aligned} \quad (\text{B.14})$$

where $\delta_j^i = \delta_{j-1}^i \kappa_{ji} + 1$ and $\delta_1^i = 1$, $\forall i$.

Proof. The proof is based on induction on the variable N . For $N = 2$, the result holds true because

$$\begin{aligned}
& \int_0^{\frac{M}{\sigma_{21}}(1-\gamma_1)} \int_{\sigma_{21}x_2+M\gamma_1}^M e^{-x_1} e^{-x_2} dx_1 dx_2 \\
&= \int_0^{\frac{M}{\sigma_{21}}(1-\gamma_1)} e^{-x_2} \left[e^{-(\sigma_{21}x_2+M\gamma_1)} - e^{-M} \right] dx_1 \\
&\doteq e^{-M\gamma_1} \int_0^{\frac{M}{\sigma_{21}}(1-\gamma_1)} \left[e^{-\delta_2 x_2} \right] dx_2 \\
&= \frac{e^{-M\gamma_1}}{\delta_2} - e^{-\delta_2 \frac{M}{\sigma_{21}}(1-\gamma_1)} \\
&\geq \frac{e^{-M\gamma_1}}{\delta_2} - e^{-\frac{M}{\gamma_3 \sigma_{\max}}} \\
&\doteq \frac{e^{-M\gamma_1}}{\delta_2}
\end{aligned} \tag{B.15}$$

We will assume then that the hypothesis is true for $N = k$, i.e.,

$$\begin{aligned}
& \int_{\sigma_{k1}x_k+M\gamma_{k-1}}^{\frac{M}{\sigma_{(k-1)1}}(1-\gamma_{k-2})} \int_{\sigma_{(k-1)1}x_{k-1}+M\gamma_{k-2}}^{\frac{M}{\sigma_{(k-2)1}}(1-\gamma_{k-3})} \cdots \int_{\sigma_{21}x_2+M\gamma_1}^M \prod_{i=1}^{k-1} e^{-x_i} dx_1 dx_2 dx_3 \cdots dx_{k-1} \\
&\doteq \left[\prod_{i=1}^{k-1} \frac{e^{-M\gamma_i \delta_i}}{\delta_i} \right] e^{x_k \delta_{k-1} \sigma_{k1}}.
\end{aligned} \tag{B.16}$$

Then for $N = k + 1$, we have that

$$\begin{aligned}
& \int_{\sigma_{(k+1)1}x_{(k+1)}+M\gamma_k}^{\frac{M}{\sigma_{k1}}(1-\gamma_{k-1})} \int_{\sigma_{k1}x_k+M\gamma_{k-1}}^{\frac{M}{\sigma_{(k-1)1}}(1-\gamma_{k-2})} \cdots \int_{\sigma_{21}x_2+M\gamma_1}^M \prod_{i=1}^k e^{-x_i} dx_1 dx_2 dx_3 \cdots dx_k \\
&= \int_{\sigma_{(k+1)1}x_{(k+1)}+M\gamma_k}^{\frac{M}{\sigma_{k1}}(1-\gamma_{k-1})} \left[\int_{\sigma_{k1}x_k+M\gamma_{k-1}}^{\frac{M}{\sigma_{(k-1)1}}(1-\gamma_{k-2})} \cdots \int_{\sigma_{21}x_2+M\gamma_1}^M \prod_{i=1}^{k-1} e^{-x_i} dx_1 dx_2 dx_3 \cdots dx_{k-1} \right] e^{-x_k} \\
&\doteq \left[\prod_{i=1}^{k-1} \frac{e^{-M\gamma_i \delta_i}}{\delta_i} \right] \int_{\sigma_{k1}x_k+M\gamma_{k-1}}^{\frac{M}{\sigma_{(k-1)1}}(1-\gamma_{k-2})} e^{-x_k(\delta_{k-1}\sigma_{k1}+1)} \\
&= \left[\prod_{i=1}^{k-1} \frac{e^{-M\gamma_i \delta_i}}{\delta_i} \right] \int_{\sigma_{(k+1)1}x_{(k+1)}+M\gamma_k}^{\frac{M}{\sigma_{k1}}(1-\gamma_{k-1})} e^{-x_k \delta_k} \\
&= \left[\prod_{i=1}^k \frac{e^{-M\gamma_i \delta_i}}{\delta_i} \right] \left[e^{-\sigma_{(k+1)1}x_{(k+1)}\delta_k} - e^{-\frac{M}{\sigma_{k1}}(1-\gamma_{k-1})\delta_k} \right] \\
&\geq \left[\prod_{i=1}^k \frac{e^{-M\gamma_i \delta_i}}{\delta_i} \right] \left[e^{-\sigma_{(k+1)1}x_{(k+1)}\delta_k} - e^{-\frac{M}{\gamma_3 \sigma_{\max}}} \right] \\
&\doteq \left[\prod_{i=1}^k \frac{e^{-M\gamma_i \delta_i}}{\delta_i} \right] e^{-\sigma_{(k+1)1}x_{(k+1)}\delta_k}.
\end{aligned} \tag{B.17}$$

□

We continue the derivation in (B.13) by applying the result in the above

lemma

$$\begin{aligned}
& \Pr(\{h_{11} \geq \sigma_{21}h_{22} + M\gamma_1 \geq \sigma_{31}h_{33} + M\gamma_2 \geq \dots \geq \sigma_{K1}h_{KK} + M\gamma_{K-1}\} \\
& \cap \{h_{ii} \in [0, M], \forall i\}) \\
&= \int_0^{\frac{M}{\sigma_{K1}}(1-\gamma_{K-1})} \dots \int_{\sigma_{(K-1)1}x_{K-1}+M\gamma_{K-2}}^{\frac{M}{\sigma_{(K-2)1}}(1-\gamma_{K-3})} \dots \int_{\sigma_{21}x_2+M\gamma_1}^M e^{-w} \prod_{i=2}^{K-1} e^{-x_i} dw dx_2 dx_3 \dots dx_K \\
&\doteq \left[\prod_{i=1}^{k-1} \frac{e^{-M\gamma_i \delta_i}}{\delta_i} \right] \int_0^{\frac{M}{\sigma_{K1}}(1-\gamma_{K-1})} e^{-x_k(\delta_{k-1}\sigma_{k1}+1)} dx_k \\
&\geq \prod_{i=1}^k \frac{e^{-M\gamma_i \delta_i}}{\delta_i}
\end{aligned} \tag{B.18}$$

to obtain the main result.

B.1.5 Proof of Lemma 16

The event $\{i = \arg \max_j \beta_j[h_{jj}]_{b_j}\}$ can be equivalently expressed as $\{\beta_i[h_{ii}]_{b_i} \geq \max_{j \neq i} \beta_j[h_{jj}]_{b_j}\}$. Consider the case when the user of interest has highest priority, i.e., $i^* = \arg \max_j \beta_j$. For $i \neq i^*$, the expectation of interest can be expressed as

$$\begin{aligned}
& \mathbb{E}_{\mathbf{h}} \left[\log_2 \left(1 + \frac{Pg_{ii}h_{ii}}{N_o} \right) \middle| i = \arg \max_j \beta_j[h_{jj}]_{b_j} \right] \\
&= \mathbb{E}_{\mathbf{h}} \left[\log_2 \left(1 + \frac{Pg_{ii}[h_{ii}]_{b_i}}{N_o} \right) \middle| \beta_i[h_{ii}]_{b_i} \geq \max_{j \neq i} \beta_j[h_{jj}]_{b_j} \right] \\
&= \mathbb{E}_{\{h_j\}_{j \neq i}} \left[\mathbb{E}_{h_i} \left[\log_2 \left(1 + \frac{Pg_{ii}[h_{ii}]_{b_i}}{N_o} \right) \middle| \beta_i[h_{ii}]_{b_i} \geq \max_{j \neq i} \beta_j[h_{jj}]_{b_j}, \{h_{jj}\}_{j \neq i} \right] \right] \\
&\geq \mathbb{E}_{\{h_j\}_{j \neq i}} \left[\log_2 \left(1 + \frac{Pg_{ii} \max_{j \neq i} \sigma_{ji}[h_{jj}]_{b_j}}{N_o} \right) \right].
\end{aligned} \tag{B.19}$$

Now, substituting the result in Lemma 22 into (B.19), we get

$$\begin{aligned}
& \mathbb{E}_{\mathbf{h}} \left[\log_2 \left(1 + \frac{Pg_{ii}h_{ii}}{N_o} \right) \mid i = \arg \max_j \beta_j[h_{jj}]_{b_j} \right] \\
& \geq \mathbb{E}_{\{h_j\}_{j \neq i}} \left[\log_2 \left(1 + \frac{Pg_{ii} \max_{j \neq i} \sigma_{ji}[h_{jj}]_{b_j}}{N_o} \right) \right] \\
& \geq \Pr \left(h_{jj} \in \left[\frac{M}{2^{b_j}}, M \right], \forall j \neq i \right) \mathbb{E}_{\{h_j\}_{j \neq i}} \left[\log_2 \left(1 + \frac{Pg_{ii} \max_{j \neq i} \sigma_{ji}(1-2^{-b_j})h_{jj}}{N_o} \right) \mid \right. \\
& \quad \left. h_{jj} \in \left[\frac{M}{2^{b_j}}, M \right], \forall j \neq i \right] \\
& = \left(e^{-\frac{M}{2^{b_j}}} - e^{-M} \right)^{K-1} \mathbb{E}_{\{h_j\}_{j \neq i}} \left[\log_2 \left(1 + \frac{Pg_{ii} \max_{j \neq i} \sigma_{ji}(1-2^{-b_j})h_{jj}}{N_o} \right) \mid \right. \\
& \quad \left. h_{jj} \in \left[\frac{M}{2^{b_j}}, M \right], \forall j \neq i \right].
\end{aligned} \tag{B.20}$$

Since it is true that $\max_{j \neq i} \sigma_{ji}(1-2^{-b_j})h_{jj} \geq \sigma_{ki}(1-2^{-b_k})h_{kk}$, $\forall k \neq i$, we have that

$$\begin{aligned}
& \mathbb{E}_{\{h_{jj}\}_{j \neq i}} \left[\log_2 \left(1 + \frac{Pg_{ii} \max_{j \neq i} \sigma_{ji}(1-2^{-b_j})h_{jj}}{N_o} \right) \mid h_{jj} \in \left[\frac{M}{2^{b_j}}, M \right], \forall j \neq i \right] \\
& \geq \mathbb{E}_{h_{kk}} \left[\log_2 \left(1 + \frac{Pg_{ii}\sigma_{ki}(1-2^{-b_k})h_{kk}}{N_o} \right) \mid h_{jj} \in \left[\frac{M}{2^{b_j}}, M \right], \forall j \neq i \right], \forall k \neq i,
\end{aligned} \tag{B.21}$$

and thus, for all users $i \neq i^*$, the result can be obtained as follows

$$\begin{aligned}
& \mathbb{E}_{\mathbf{h}} \left[\log_2 \left(1 + \frac{Pg_{ii}h_{ii}}{N_o} \right) \mid i = \arg \max_j \beta_j[h_{jj}]_{b_j} \right] \\
& \geq (1-2^{-b_k}) \mathbb{E}_{h_{kk}} \left[\log_2 \left(1 + \frac{Pg_{ii}\sigma_{ki}h_{kk}}{N_o} \right) \mid h_{kk} \in \left[\frac{M}{2^{b_j}}, M \right] \right], \forall k \neq i \\
& \quad \text{by Jensen's inequality} \\
& \geq (1-2^{-b_{i,\min}}) \mathbb{E}_{h_{kk}} \left[\log_2 \left(1 + \frac{Pg_{ii}\sigma_i^*h_{kk}}{N_o} \right) \mid h_{kk} \in \left[\frac{M}{2^{b_j}}, M \right] \right].
\end{aligned} \tag{B.22}$$

Now consider the user $i^* = \arg \max_j \beta_j$ with highest priority. Then, for this user, it follows that $\sigma_{i^*}^* = \max_{k \neq i^*} \sigma_{ki^*} \leq 1$ and hence, the event $\{[h_{i^*i^*}]_{b_i^*} \geq \max_{j \neq i^*} [h_{jj}]_{b_j}\}$ implies the event $\{\beta_{i^*}[h_{i^*i^*}]_{b_i^*} \geq \max_{j \neq i^*} \beta_j[h_{jj}]_{b_j}\}$. Again, through the Law of Total Probability, one can express the expectation of in-

terest as

$$\begin{aligned}
& \mathbb{E}_{\mathbf{h}} \left[\log_2 \left(1 + \frac{Pg_{i^*i^*}h_{i^*i^*}}{N_o} \right) \middle| i^* = \arg \max_j \beta_j [h_{jj}]_{b_j} \right] \\
\geq & \mathbb{E}_{\mathbf{h}} \left[\log_2 \left(1 + \frac{Pg_{i^*i^*}h_{i^*i^*}}{N_o} \right) \middle| i^* = \arg \max_j [h_{jj}]_{b_j} \right] \\
= & \mathbb{E}_{\mathbf{h}} \left[\log_2 \left(1 + \frac{Pg_{i^*i^*}[h_{i^*i^*}]_{b_{i^*}}}{N_o} \right) \middle| [h_{i^*i^*}]_{b_{i^*}} \geq \max_{j \neq i^*} [h_{jj}]_{b_j} \right] \\
= & \mathbb{E}_{\{h_j\}_{j \neq i^*}} \left[\mathbb{E}_{h_{i^*}} \left[\log_2 \left(1 + \frac{Pg_{i^*i^*}[h_{i^*i^*}]_{b_{i^*}}}{N_o} \right) \middle| [h_{i^*i^*}]_{b_{i^*}} \geq \max_{j \neq i^*} [h_{jj}]_{b_j}, \{h_{jj}\}_{j \neq i^*} \right] \right] \\
\geq & \mathbb{E}_{\{h_j\}_{j \neq i^*}} \left[\log_2 \left(1 + \frac{Pg_{i^*i^*} \max_{j \neq i^*} [h_{jj}]_{b_j}}{N_o} \right) \right].
\end{aligned} \tag{B.23}$$

and using similar arguments as earlier, we get

$$\begin{aligned}
& \mathbb{E}_{\mathbf{h}} \left[\log_2 \left(1 + \frac{Pg_{i^*i^*}h_{i^*i^*}}{N_o} \right) \middle| i^* = \arg \max_j \beta_j [h_{jj}]_{b_j} \right] \\
\geq & \left(e^{-\frac{M}{2^{b_j}}} - e^{-M} \right)^{K-1} (1 - 2^{-b_{i,\min}}) \mathbb{E}_{h_{kk}} \left[\log_2 \left(1 + \frac{Pg_{ii}h_{kk}}{N_o} \right) \middle| h_{kk} \in \left[\frac{M}{2^{b_j}}, M \right] \right], \\
& \text{where } b_{i,\min} = \min_{j \neq i} b_j.
\end{aligned} \tag{B.24}$$

to obtain the result.

B.2 Proof of Theorem 23

We start with the definitions obtained through conditioning

$$\frac{\bar{\mu}_i[\mathbf{w}, \mathbf{G}[tT_{LS}], \mathbf{b}]}{\bar{\mu}_i^*[\mathbf{w}, \mathbf{G}[tT_{LS}]]} = \frac{\Pr(i = \arg \max_j \beta_j [h_{jj}]_{b_j})}{\Pr(i = \arg \max_j \beta_j h_{jj})} \frac{\mathbb{E}_{\mathbf{h}} \left[\log_2 \left(1 + \frac{Pg_{ii}[h_{ii}]_{b_i}}{N_o} \right) \middle| i = \arg \max_j \beta_j [h_{jj}]_{b_j} \right]}{\mathbb{E}_{\mathbf{h}} \left[\log_2 \left(1 + \frac{Pg_{ii}h_{ii}}{N_o} \right) \middle| i = \arg \max_j \beta_j h_{jj} \right]} \tag{B.25}$$

By substituting the results in Lemmas 14 and 15, we proceed to obtain

$$\begin{aligned}
& \frac{\bar{\mu}_i[\mathbf{w}, \mathbf{G}[\bar{t}T_{LS}], \mathbf{b}]}{\bar{\mu}_i^*[\mathbf{w}, \mathbf{G}[\bar{t}T_{LS}]]} \\
& \geq \left(e^{-M \max_{\mathbf{p} \in \mathcal{P}_i} \sum_{i=1}^K \gamma_i^{\mathbf{p}} \delta_i^{\mathbf{p}}} \right) \frac{\mathbb{E}_{\mathbf{h}} \left[\log_2 \left(1 + \frac{Pg_{ii}[h_{ii}]b_i}{N_o} \right) \middle| i = \arg \max_j \beta_j [h_{jj}]_{b_j} \right]}{\mathbb{E}_{\mathbf{h}} \left[\log_2 \left(1 + \frac{Pg_{ii}h_{ii}}{N_o} \right) \middle| i = \arg \max_j \beta_j h_{jj} \right]} \\
& \geq \left(e^{-M \max_{\mathbf{p} \in \mathcal{P}_i} \sum_{i=1}^K \gamma_i^{\mathbf{p}} \delta_i^{\mathbf{p}}} \right) \mathbb{E}_{\mathbf{h}} \left[\log_2 \left(1 + \frac{Pg_{ii}[h_{ii}]b_i}{N_o} \right) \middle| i = \arg \max_j \beta_j [h_{jj}]_{b_j} \right] \times \\
& \quad \left(\Pr(h_{ii} \in [\frac{M}{2^{b_i}}, M]) \mathbb{E}_{\mathbf{h}} \left[\log_2 \left(1 + \frac{Pg_{ii}h_{ii}}{N_o} \right) \middle| h_{ii} \in [\frac{M}{2^{b_i}}, M] \right] + \Pr(h_{ii} \in [M, \infty)) \right. \\
& \quad \mathbb{E}_{\mathbf{h}} \left[\log_2 \left(1 + \frac{Pg_{ii}h_{ii}}{N_o} \right) \middle| h_{ii} \in [M, \infty) \right] + \Pr(h_{ii} \in [0, \frac{M}{2^{b_i}}]) \mathbb{E}_{\mathbf{h}} \left[\log_2 \left(1 + \frac{Pg_{ii}h_{ii}}{N_o} \right) \middle| \right. \\
& \quad \left. \left. h_{ii} \in [0, \frac{M}{2^{b_i}}] \right] \right)^{-1} \\
& \geq \frac{\left(e^{-M \max_{\mathbf{p} \in \mathcal{P}_i} \sum_{i=1}^K \gamma_i^{\mathbf{p}} \delta_i^{\mathbf{p}}} \right) \mathbb{E}_{\mathbf{h}} \left[\log_2 \left(1 + \frac{Pg_{ii}[h_{ii}]b_i}{N_o} \right) \middle| i = \arg \max_j \beta_j [h_{jj}]_{b_j} \right]}{\Pr(h_{ii} \in [\frac{M}{2^{b_i}}, M]) \mathbb{E}_{\mathbf{h}} \left[\log_2 \left(1 + \frac{Pg_{ii}h_{ii}}{N_o} \right) \middle| h_{ii} \in [\frac{M}{2^{b_i}}, M] \right] + e^{-M} \mathbb{E}_{\mathbf{h}} \left[\log_2 \left(1 + \frac{Pg_{ii}h_{ii}}{N_o} \right) \middle| h_{ii} \in [M, \infty) \right]} \times \\
& = \left(e^{-M \max_{\mathbf{p} \in \mathcal{P}_i} \sum_{i=1}^K \gamma_i^{\mathbf{p}} \delta_i^{\mathbf{p}}} \right) \frac{\mathbb{E}_{\mathbf{h}} \left[\log_2 \left(1 + \frac{Pg_{ii}[h_{ii}]b_i}{N_o} \right) \middle| i = \arg \max_j \beta_j [h_{jj}]_{b_j} \right]}{\Pr(h_{ii} \in [\frac{M}{2^{b_i}}, M]) \mathbb{E}_{\mathbf{h}} \left[\log_2 \left(1 + \frac{Pg_{ii}h_{ii}}{N_o} \right) \middle| h_{ii} \in [\frac{M}{2^{b_i}}, M] \right]}
\end{aligned} \tag{B.26}$$

where the last step follows from the fact that

$$\mathbb{E}_{\mathbf{h}} \left[\log_2 \left(1 + \frac{Pg_{ii}h_{ii}}{N_o} \right) \middle| i = \arg \max_j \beta_j h_{jj} \right] \leq \mathbb{E}_{\mathbf{h}} \left[\log_2 \left(1 + \frac{Pg_{ii}h_{ii}}{N_o} \right) \right]$$

along with the application of the Law of Total Probability. Thus we obtain

$$\begin{aligned}
& \frac{\bar{\mu}_i[\mathbf{w}, \mathbf{G}[\bar{t}T_{LS}], \mathbf{b}]}{\bar{\mu}_i^*[\mathbf{w}, \mathbf{G}[\bar{t}T_{LS}]]} \\
& \geq \left(e^{-M \max_{\mathbf{p} \in \mathcal{P}_i} \sum_{i=1}^K \gamma_i^{\mathbf{p}} \delta_i^{\mathbf{p}}} \right) \frac{\mathbb{E}_{\mathbf{h}} \left[\log_2 \left(1 + \frac{Pg_{ii}[h_{ii}]b_i}{N_o} \right) \middle| i = \arg \max_j \beta_j [h_{jj}]_{b_j} \right]}{\Pr(h_{ii} \in [\frac{M}{2^{b_i}}, M]) \mathbb{E}_{\mathbf{h}} \left[\log_2 \left(1 + \frac{Pg_{ii}h_{ii}}{N_o} \right) \middle| h_{ii} \in [\frac{M}{2^{b_i}}, M] \right]} \\
& = \left(e^{-M \max_{\mathbf{p} \in \mathcal{P}_i} \sum_{i=1}^K \gamma_i^{\mathbf{p}} \delta_i^{\mathbf{p}}} \right) \frac{\mathbb{E}_{\mathbf{h}} \left[\log_2 \left(1 + \frac{Pg_{ii}[h_{ii}]b_i}{N_o} \right) \middle| i = \arg \max_j \beta_j [h_{jj}]_{b_j} \right]}{\Pr(h_{ii} \in [\frac{M}{2^{b_i}}, M]) \mathbb{E}_{\mathbf{h}} \left[\log_2 \left(1 + \frac{Pg_{ii}h_{ii}}{N_o} \right) \middle| h_{ii} \in [\frac{M}{2^{b_i}}, M] \right]} \\
& \geq \left(e^{-M \max_{\mathbf{p} \in \mathcal{P}_i} \sum_{i=1}^K \gamma_i^{\mathbf{p}} \delta_i^{\mathbf{p}}} \right) \frac{\mathbb{E}_{\mathbf{h}} \left[\log_2 \left(1 + \frac{Pg_{ii}[h_{ii}]b_i}{N_o} \right) \middle| i = \arg \max_j \beta_j [h_{jj}]_{b_j}, h_{ii} \in [\frac{M}{2^{b_i}}, M] \right]}{\mathbb{E}_{\mathbf{h}} \left[\log_2 \left(1 + \frac{Pg_{ii}h_{ii}}{N_o} \right) \middle| h_{ii} \in [\frac{M}{2^{b_i}}, M] \right]}.
\end{aligned} \tag{B.27}$$

For $i \neq i^* = \arg \max_j \beta_j$, we substitute the result from Lemma 16 to get

$$\begin{aligned}
& \frac{\bar{\mu}_i[\mathbf{w}, \mathbf{G}[\bar{\ell}T_{LS}], \mathbf{b}]}{\bar{\mu}_i^*[\mathbf{w}, \mathbf{G}[\ell T_{LS}]]} \\
& \geq \left(e^{-M \max_{\mathbf{p} \in \mathcal{P}_i} \sum_{i=1}^K \gamma_i^{\mathbf{p}} \delta_i^{\mathbf{p}}} \right) \frac{\mathbb{E}_{\mathbf{h}} \left[\log_2 \left(1 + \frac{Pg_{ii}[h_{ii}]b_i}{N_o} \right) \middle| i = \arg \max_j \beta_j [h_{jj}]_{b_j}, h_{ii} \in \left[\frac{M}{2^{b_i}}, M \right] \right]}{\mathbb{E}_{\mathbf{h}} \left[\log_2 \left(1 + \frac{Pg_{ii}h_{ii}}{N_o} \right) \middle| h_{ii} \in \left[\frac{M}{2^{b_i}}, M \right] \right]} \\
& \doteq (1 - 2^{-b_{i,\min}}).
\end{aligned} \tag{B.28}$$

For the remaining users, we get

$$\begin{aligned}
& \frac{\bar{\mu}_i[\mathbf{w}, \mathbf{G}[\bar{\ell}T_{LS}], \mathbf{b}]}{\bar{\mu}_i^*[\mathbf{w}, \mathbf{G}[\ell T_{LS}]]} \\
& \geq \left(e^{-M \max_{\mathbf{p} \in \mathcal{P}_i} \sum_{i=1}^K \gamma_i^{\mathbf{p}} \delta_i^{\mathbf{p}}} \right) \frac{\mathbb{E}_{\mathbf{h}} \left[\log_2 \left(1 + \frac{Pg_{ii}[h_{ii}]b_i}{N_o} \right) \middle| i = \arg \max_j \beta_j [h_{jj}]_{b_j}, h_{ii} \in \left[\frac{M}{2^{b_i}}, M \right] \right]}{\mathbb{E}_{\mathbf{h}} \left[\log_2 \left(1 + \frac{Pg_{ii}h_{ii}}{N_o} \right) \middle| h_{ii} \in \left[\frac{M}{2^{b_i}}, M \right] \right]} \\
& \doteq \left(e^{-M \max_{\mathbf{p} \in \mathcal{P}_i} \sum_{i=1}^K \gamma_i^{\mathbf{p}} \delta_i^{\mathbf{p}}} \right) (1 - 2^{-b_{i,\min}}) \frac{\mathbb{E}_{h_{kk}} \left[\log_2 \left(1 + \frac{Pg_{ii}\sigma_i^* h_{kk}}{N_o} \right) \middle| h_{kk} \in \left[\frac{M}{2^{b_j}}, M \right] \right]}{\mathbb{E}_{\mathbf{h}} \left[\log_2 \left(1 + \frac{Pg_{ii}h_{ii}}{N_o} \right) \middle| h_{ii} \in \left[\frac{M}{2^{b_i}}, M \right] \right]} \\
& \doteq \left(e^{-M \max_{\mathbf{p} \in \mathcal{P}_i} \sum_{i=1}^K \gamma_i^{\mathbf{p}} \delta_i^{\mathbf{p}}} \right) (1 - 2^{-b_{i,\min}}) \frac{\mathbb{E}_{h_{kk}} \left[\log_2 \left(1 + \frac{Pg_{ii}\sigma_i^* h_{kk}}{N_o} \right) \middle| h_{kk} \in \left[\frac{M}{2^{b_j}}, M \right] \right]}{\mathbb{E}_{\mathbf{h}} \left[\log_2 \left(1 + \frac{Pg_{ii}r_i^* h_{ii}}{N_o} \right) \middle| h_{ii} \in \left[\frac{M}{2^{b_i}}, M \right] \right]} \\
& \doteq \left(e^{-M \max_{\mathbf{p} \in \mathcal{P}_i} \sum_{i=1}^K \gamma_i^{\mathbf{p}} \delta_i^{\mathbf{p}}} \right) (1 - 2^{-b_{i,\min}}),
\end{aligned} \tag{B.29}$$

where the second last step follows from the fact that $\sigma_i^* = \max_j \sigma_{ji} \geq 1$.

B.3 Proof of Theorem 17

Excluding minor generalizations, the proof is a reproduction from Ravindran et al. [133] and Jindal [83]. Based on the signal model in (4.11), when the receiver employs maximal-ratio-combining matched to the quantized beam-

former $\hat{\mathbf{w}}_i$, we can write

$$\begin{aligned}
& R_i(\infty) - R_i(\{b_j\}_{j \in \mathcal{N}_e(i)}) \\
&= \mathbb{E} \left[\log_2 \left(1 + \frac{\alpha_{ii} P_i}{N_{t,i}} \frac{\|\mathbf{H}_{ii} \mathbf{w}_i\|^2}{N_o} \right) \right] - \mathbb{E} \left[\log_2 \left(1 + \frac{\alpha_{ii} P_i}{N_{t,i}} \frac{\|\mathbf{H}_{ii} \hat{\mathbf{w}}_i\|^2}{\sum_{j \in \mathcal{N}(i)} \frac{\alpha_{ii} P_i}{N_{t,i}} |\hat{\mathbf{w}}_i^\dagger \mathbf{H}_{ii}^\dagger \mathbf{H}_{ji} \mathbf{w}_j|^2 + N_o} \right) \right] \\
&= \mathbb{E} \left[\log_2 \left(1 + \frac{\alpha_{ii} P_i}{N_{t,i}} \frac{\|\mathbf{H}_{ii} \mathbf{w}_i\|^2}{N_o} \right) \right] - \mathbb{E} \left[\log_2 \left(1 + \sum_{j \in \mathcal{N}_e(i)} \frac{\alpha_{ji} P_j}{N_{t,i}} |\hat{\mathbf{w}}_i^\dagger \mathbf{H}_{ii}^\dagger \mathbf{H}_{ji} \mathbf{w}_j|^2 + N_o \right) \right] \\
&\quad + \mathbb{E} \left[\log_2 \left(1 + \sum_{j \in \mathcal{N}(i)} \frac{\alpha_{ji} P_j}{N_{t,j}} |\hat{\mathbf{w}}_i^\dagger \mathbf{H}_{ii}^\dagger \mathbf{H}_{ji} \hat{\mathbf{w}}_j|^2 + 1 \right) \right] \\
&\leq \mathbb{E} \left[\log_2 \left(1 + \frac{\alpha_{ii} P_i}{N_{t,i}} \frac{\|\mathbf{H}_{ii} \mathbf{w}_i\|^2}{N_o} \right) \right] - \mathbb{E} \left[\log_2 \left(1 + \frac{\alpha_{ii} P_i}{N_{t,i}} \|\mathbf{H}_{ji} \hat{\mathbf{w}}_i\|^2 \right) \right] \\
&\quad + \mathbb{E} \left[\log_2 \left(1 + \sum_{j \in \mathcal{N}(i)} \frac{\alpha_{ji} P_j}{N_{t,j}} |\hat{\mathbf{w}}_i^\dagger \mathbf{H}_{ii}^\dagger \mathbf{H}_{ji} \hat{\mathbf{w}}_j|^2 \right) \right] \text{ by dropping some positive terms} \\
&= \mathbb{E} \left[\log_2 \left(1 + \sum_{j \in \mathcal{N}(i)} \frac{\alpha_{ji} P_j}{N_{t,j}} |\hat{\mathbf{w}}_i^\dagger \mathbf{H}_{ii}^\dagger \mathbf{H}_{ji} \hat{\mathbf{w}}_j|^2 \right) \right] \\
&\leq \log_2 \left(1 + \sum_{j \in \mathcal{N}(i)} \frac{\alpha_{ji} P_j}{N_{t,j}} \mathbb{E} [\|\mathbf{H}_{ii} \hat{\mathbf{w}}_i\|^2] \mathbb{E} [\|\mathbf{H}_{ji} \hat{\mathbf{w}}_j\|^2] \right) \text{ by Jensen's and} \\
&\quad \text{the Cauchy-Schwartz inequality} \\
&\leq \log_2 \left(1 + \sum_{j \in \mathcal{N}(i)} \frac{\alpha_{ji} P_j}{N_{t,j}} N_{r,i} N_{t,i} \sum_{k=1}^{N_{r,j}} \mathbb{E} [|\mathbf{h}_{k,j}^\dagger \hat{\mathbf{w}}_j|^2] \right) \text{ where } \mathbf{h}_{k,j} \text{ is} \\
&\quad \text{the } k\text{-th column of } \mathbf{H}_{ji}^\dagger
\end{aligned} \tag{B.30}$$

In [83], the author shows that $\mathbb{E} [|\mathbf{h}_{k,j}^\dagger \hat{\mathbf{w}}_j|^2] = \frac{N_{t,j}}{N_{t,i}-1} \Delta_j(b_j)$ where $\Delta_j(b_j) = 2^{-\frac{b_j}{N_{t,j}-1}}$. The result follows.

B.4 Proof of Theorem 5

The Lagrangian cost function for Part (i) can be written as

$$\begin{aligned}
\mathcal{L}(b_i, \lambda_i, \eta_i, \nu_i) &= -\sum_i \gamma_i \log_2 \tilde{b}_i - \sum_i \eta_i \tilde{b}_i + \sum_i \lambda_i \left(a_{ii} \tilde{b}_i + \sum_{j \in \mathcal{N}(i)} a_{ji} \tilde{b}_j - d_i \right) \\
&\quad + \sum_i \nu_i (\tilde{b}_i - 1)
\end{aligned} \tag{B.31}$$

for which the KKT conditions are

$$\begin{aligned}
& \tilde{b}_i^* \geq 0, \quad \eta_i^* \geq 0, \quad \tilde{b}_i^* \eta_i^* = 0, \\
& \nu_i^* (\tilde{b}_i^* - 1) = 0, \quad \lambda_i \in \mathbb{R}, \quad a_{ii} \tilde{b}_i^* + \sum_{j \in \mathcal{N}(i)} a_{ji} \tilde{b}_j^* \leq d_i, \quad \forall i
\end{aligned} \tag{B.32}$$

and

$$\frac{d}{d\tilde{b}_j} \mathcal{L}(b_i^*, \lambda_i^*, \eta_i^*, \nu_i^*) = - \left(\frac{1}{\log 2} \right) \frac{\gamma_j}{\tilde{b}_j} - \eta_j^* + \left(\sum_{k \in \mathcal{N}(j) \cup \{j\}} \lambda_k^* a_{kj} \right) + \nu_j^* = 0. \quad (\text{B.33})$$

We observe that $\tilde{b}_i^* \neq 0$ implying that $\eta_i^* = 0$ from (B.32), which when substituted in (B.33) yields

$$\left(\sum_{k \in \mathcal{N}(j) \cup \{j\}} \lambda_k^* a_{kj} \right) = \left(\frac{1}{\log 2} \right) \frac{\gamma_j}{\tilde{b}_j} - \nu_j^*. \quad (\text{B.34})$$

This means that if $\left(\sum_{k \in \mathcal{N}(j) \cup \{j\}} \lambda_k^* a_{kj} \right) \leq \left(\frac{1}{\log 2} \right) \frac{\gamma_j}{\tilde{b}_j}$, then $\tilde{b}_j^* = 1$ and $\nu_j^* > 0$; else

$$\tilde{b}_j^* = \left[\left(\frac{1}{\log 2} \right) \frac{\gamma_j}{\sum_{k \in \mathcal{N}(j) \cup \{j\}} \lambda_k^* a_{kj}} \right]_1^+. \quad (\text{B.35})$$

The result follows.

Appendix C

Appendix for Chapter 5

C.1 Proof of Lemma 20

In this proof, we use the j instead of i' to index the primary transmitters, i.e. the (i, j) -th entry \mathbf{H} denotes the channel from primary transmitter j to cognitive receiver i .

Recall that $\mathbf{H}_{\mathcal{C}_{i,r}}$ represent the sub-matrix of \mathbf{H} containing the rows specified in \mathcal{C}_i . Then, the entries $\{h_{ij}\}$ of sub-matrix $\mathbf{H}_{\mathcal{C}_{i,r}}$ are identically distributed. This follows from the observation that any two cognitive receivers on the circle of radius $r_{s,i}$ will perceive the same distribution of primary transmitters since the latter nodes are distributed on a circle. Recall that the transformation $\mathbf{G} = \mathbf{W}\mathbf{H}$ essentially subtracts rows of \mathbf{H} corresponding to diametrically opposite users on each circle.

Thus, the columns of \mathbf{G} are independent and all entries are centered. The next step is to show that the entries $g_{ij} = h_{ij} - h_{(i+1)j}$ are symmetric. This does not follow immediately from the fact that h_{ij} and $h_{(i+1)j}$ are identically distributed when indices i and $i + 1$ come from the same partition since they are not independent. Hence, we will need to employ the concept of exchangeable random variables defined below for the specific case of a pair of random

variables.

Definition (Exchangeability): Two random variables X and Y are called *exchangeable* if their joint cumulative distribution function (cdf) is symmetric, i.e. if $F_{X,Y}(x, y) = F_{X,Y}(y, x)$.

It is known the difference of two identically distributed, exchangeable random variables is indeed symmetric [191]. We only need to establish this fact for the case when h_{ij} and $h_{(i+1)j}$ come from the same circle, say \mathcal{C}_c , since the definition of \mathbf{G} in (5.5.1) precludes any other possibility. To establish that h_{ij} and $h_{(i+1)j}$ are exchangeable, we compute the cdf $F_{h_{ij}, h_{(i+1)j}}(x, y)$ as follows

$$\begin{aligned}
& F_{h_{ij}, h_{(i+1)j}}(x, y) \\
&= \Pr(h_{ij} \leq x, h_{(i+1)j} \leq y) \\
&= \Pr(d_{ij} \geq \frac{1}{x} - K, d_{(i+1)j} \geq \frac{1}{y} - K) \\
&= \Pr(d_{ij} \geq \left[\frac{1}{x} - K\right]_+, d_{(i+1)j} \geq \left[\frac{1}{y} - K\right]_+) \text{ where } [u]_+ = \max\{u, 0\} \\
&= \Pr\left(\sqrt{r_{s,c}^2 + r_p^2 - 2r_{s,c}r_p\cos(\theta_j - \theta_i)} \geq \left[\frac{1}{x} - K\right]_+, \right. \\
&\quad \left. \sqrt{r_{s,c}^2 + r_p^2 - 2r_{s,c}r_p\cos(\theta_j - \theta_i - \frac{2\pi q}{N_c})} \geq \left[\frac{1}{y} - K\right]_+ \right) \\
&= \frac{1}{2\pi} V(\mathcal{R}(r_p, \theta_j, r_{s,c}, \theta_i, x, y))
\end{aligned}$$

where

$$\begin{aligned}
\mathcal{R}(r_p, \theta_j, r_{s,c}, \theta_i, x, y) = & \left\{ \theta_j : \sqrt{r_{s,c}^2 + r_p^2 - 2r_{s,c}r_p\cos(\theta_j - \theta_i)} \geq \left[\frac{1}{x} - K\right]_+, \right. \\
& \left. \sqrt{r_{s,c}^2 + r_p^2 - 2r_{s,c}r_p\cos(\theta_j - \theta_i - \frac{2\pi q}{N_c})} \geq \left[\frac{1}{y} - K\right]_+ \right\}
\end{aligned}$$

and $V(\mathcal{A})$ denotes the volume of the set \mathcal{A} . The volume of set

$$\mathcal{R}(r_p, \theta_j, r_{s,c}, \theta_i, x, y)$$

can be expressed as a sum of the volumes corresponding to smaller sets. To that effect, we define

$$\mathcal{R}_s(r_{s,c}, \theta, a) = \left\{ \theta_j : \sqrt{r_{s,c}^2 + r_p^2 - 2r_{s,c}r_p \cos(\theta_j - \theta)} \leq \left[\frac{1}{a} - K \right]_+ \right\}$$

and can thus write

$$\begin{aligned} & \mathcal{V}(\mathcal{R}(r_p, \theta_j, r_{s,c}, \theta_i, x, y)) \\ &= 2\pi r_p - \left[\mathcal{V}(\mathcal{R}_s(r_{s,c}, \theta_i, x)) + \mathcal{V}\left(\mathcal{R}_s\left(r_{s,c}, \theta_i + \frac{2\pi q}{N_s}, y\right)\right) - \right. \\ & \quad \left. \mathcal{V}\left(\mathcal{R}_s(r_{s,c}, \theta_i, x) \cap \mathcal{R}_s\left(r_{s,c}, \theta_i + \frac{2\pi q}{N_s}, y\right)\right) \right]. \end{aligned} \quad (\text{C.1})$$

From this characterization, we can immediately conclude that

$$\mathcal{V}(\mathcal{R}(r_p, \theta_j, r_{s,c}, \theta_i, x, y)) = \mathcal{V}(\mathcal{R}(r_p, \theta_j, r_{s,c}, \theta_i, y, x)),$$

which gives us the desired result that h_{ij} and $h_{(i+1)j}$ are exchangeable implying that the entries $g_{ij} = h_{ij} - h_{(i+1)j}$ are symmetric for all (i, j) . It is clear from the above arguments that exchangeability essentially follows due to the uniform distribution of the primary transmitter.

The symmetry of g_{ij} is crucial for our next step where we argue that columns of $\mathbf{A} = \mathbf{B}\mathbf{G}$ remain independent. By definition, $a_{ij} = \frac{1}{\sqrt{\text{Var}\{g_{i1}\}}} \beta_i g_{ij}$. Thus, to prove that the columns of \mathbf{A} are independent, we need to show that $a_{ij} \perp \mathbf{a}_k$ for any arbitrary i, j and $k \neq j$. Since the Bernoulli random variables are independent across rows and since $g_{ij} \perp g_{mk}$, $k \neq j$, $m \neq i$, we clearly have that $a_{ij} \perp a_{mk}$, $k \neq j$, $m \neq i$. Thus, we only need to establish that $a_{ij} \perp a_{ik}$ for $k \neq j$ or equivalently that $\beta_i g_{ij} \perp \beta_i g_{ik}$. But this follows from the symmetry of g_{ij} which means that knowledge of $\beta_i g_{ij}$ reveals no information about the random variable β_i . Thus, the columns of \mathbf{A} are independent. In

addition, there are identically distributed and hence we can now focus on studying the properties of column \mathbf{a}_1 without loss of generality.

The random vector \mathbf{a}_1 is isotropic since

$$\begin{aligned}\mathbb{E}[a_{i1}^2] &= \frac{1}{\mathbb{E}[g_{i1}^2]} \mathbb{E}[g_{i1}^2] \\ &= 1,\end{aligned}\tag{C.2}$$

and $\mathbb{E}[a_{i1}a_{k1}] = \frac{1}{\sqrt{\mathbb{E}[g_{i1}^2]}} \frac{1}{\sqrt{\mathbb{E}[g_{k1}^2]}} \mathbb{E}[\beta_i \beta_k g_{i1} g_{k1}] = \frac{1}{\sqrt{\mathbb{E}[g_{i1}^2]}} \frac{1}{\sqrt{\mathbb{E}[g_{k1}^2]}} \mathbb{E}[\beta_i \beta_k] \mathbb{E}[g_{i1} g_{k1}] = 0$ for $i \neq k$, implying that

$$\begin{aligned}\mathbb{E}[|\mathbf{a}_1^T \mathbf{x}|^2] &= \sum_i \mathbb{E}[a_{i1}^2] x_i^2 + \sum_{i \neq k} \mathbb{E}[a_{i1} a_{k1}] x_i x_k \\ &= \|\mathbf{x}\|^2.\end{aligned}\tag{C.3}$$

To prove that \mathbf{a}_1 is sub-gaussian, we will first condition on the position of the first primary user (r_p, θ_1) . This will allow us to apply Lemma 17 and Lemma 18 since g_{i1} is now completely known thereby making \mathbf{a}_{i1} a collection of independent random variables. The elements a_{i1} are symmetric and bounded with $|a_{i1}| \leq \frac{|g_{i1}|}{\sqrt{\mathbb{E}[g_{i1}^2]}}$ when conditioned on (r_p, θ_1) .

Lemma 24. *There exists $M_p > 0$, $p = 0, 2, \dots, q-1$ such that*

$$\mathbb{E}[g_{i1}^2] = M_p, \text{ for } p \frac{N_s}{q} < i \leq (p+1) \frac{N_s}{q} \text{ and for all } k.\tag{C.4}$$

Proof: By definition, the distribution of g_{i1} for $p \frac{N_s}{q} < i \leq (p+1) \frac{N_s}{q}$ depends on the distance between the corresponding diametrically opposite users on circle $(p+1)$ along with the distribution of the first primary user. Since this distance always remains the same independent of i and k , the result follows. \square

Hence, by Lemma 18 and since $|g_{i1}| \leq 1$, a_{i1} is sub-gaussian with $\|a_{i1}\|_{\psi_2(r_p, \theta_1)} \leq \frac{1}{M_*^2}$ where $M_* = \min_{p=1, \dots, q} M_p$. Here, we have introduced notation $\|\cdot\|_{\psi_2(r_p, \theta_1)}$ to indicate explicitly that we have conditioned on the location of the first primary user. Now, from Lemma 17, we conclude that \mathbf{a}_1 is a sub-gaussian vector when conditioned on the location of the first primary user with $\|\mathbf{a}_1\|_{\psi_2(r_p, \theta_1)} \leq 2C$, $C > 0$. However, since the sub-gaussian norm $\|\mathbf{a}_1\|_{\psi_2(r_p, \theta_1)}$ computed above is independent of (r_p, θ_1) , this implies that \mathbf{a}_1 is a sub-gaussian vector with $\|\mathbf{a}_1\|_{\psi_2} \leq 2C$. This can be seen by applying the Law of Total Probability to the definition of sub-gaussianity in Lemma 17.

C.2 Proof of Lemma 21

To show almost-sure convergence of the norm of \mathbf{a}_1 , we would like to prove that $\exists c^* > 0$ such that

$$\Pr \left(\lim_{k \rightarrow \infty} \left| \frac{1}{k} \sum_{i=1}^k a_{i1}^2 - c^* \right| = 0 \right) = \Pr \left(\lim_{k \rightarrow \infty} \left| \frac{1}{k} \sum_{i=1}^k g_{i1}^2 - c^* \right| = 0 \right) = 1. \quad (\text{C.5})$$

where the probability is computed over the random location (r_p, θ) , $\theta \sim U[0, 2\pi]$. We will instead prove the following more general statement that $\exists c^* > 0$ such that

$$\lim_{k \rightarrow \infty} \left| \frac{1}{k} \sum_{i=1}^k \frac{g_{i1}^2}{\mathbb{E}[g_{i1}^2]} - c^* \right| = 0 \text{ for all } (r_p, \theta), \theta \in [0, 2\pi]. \quad (\text{C.6})$$

Note that (C.6) is a completely deterministic convergence statement in contrast to (C.5). From the proposed feedback protocol in Algorithm 2, we see that the number of receivers selected for feedback is a monotonically increasing

function of k for all circles. This mean that we can study the convergence of the norm for any one circle (a sub-vector of \mathbf{a}_1) and draw conclusions about the norm concentration of the entire vector \mathbf{a}_1 . Consider the first partition of cognitive receivers \mathcal{C}_1 and let the size of this partition be $\alpha(k)$ where $\alpha(k) \rightarrow \infty$ as $k \rightarrow \infty$. Due to the above argument, we shift our focus to studying the quantity

$$\lim_{k \rightarrow \infty} \left| \frac{1}{\alpha(k)} \sum_{i=1}^{\alpha(k)} \frac{g_{i1}^2}{\mathbb{E}[g_{i1}^2]} - c^* \right| = 0 \text{ for all } (r_p, \theta), \theta \in [0, 2\pi]. \quad (\text{C.7})$$

Recall that the squared-distance between the first primary transmitter located at (r_p, θ) and cognitive receiver i on \mathcal{C}_1 is given by

$$d^2(\theta_i, \theta) = r_{s,1}^2 + r_p^2 - 2r_p r_{s,1} \cos(\theta_i - \theta), \quad i = 1, 2, \dots, \alpha(k), \quad (\text{C.8})$$

where $\theta_i = \frac{2\pi i q}{k}$. Here, we have modified the distance notation to reflect an explicit dependence on the position of first primary transmitter. Now let $f(x, y) = \left(\frac{1}{x} - \frac{1}{y}\right)^2$, $x, y > 0$. Then, for $i \in \mathcal{C}_1$, $g_{i1}^2 = f(d^2(\theta_i, \theta), d^2(\theta_i + \frac{\pi}{2}, \theta))$. We prove that $c^* = 1$ for \mathcal{C}_1 thereby ensuring that the norm of the entire vector \mathbf{g}_1 is well-behaved by the above argument. We essentially need to show that

$$\lim_{k \rightarrow \infty} \left| \frac{1}{\alpha(k)} \sum_{i=1}^{\alpha(k)} \frac{g_{i1}^2}{\mathbb{E}[g_{i1}^2]} - 1 \right| = 0 \text{ for all } (r_p, \theta_1). \quad (\text{C.9})$$

This can be shown by observing that

$$\begin{aligned} \lim_{k \rightarrow \infty} \frac{1}{\alpha(k)} \sum_{i=1}^{\alpha(k)} g_{i1}^2 &= \lim_{k \rightarrow \infty} \frac{1}{\alpha(k)} \sum_{i=1}^{\alpha(k)} f(d^2(\theta_i, \theta), d^2(\theta_i + \frac{2\pi q}{k}, \theta)) \\ &= \frac{1}{2\pi} \int_0^{2\pi} f(d^2(\theta_i, \theta), d^2(\theta_i + \frac{\pi}{2}, \theta)) d\theta_i. \end{aligned} \quad (\text{C.10})$$

This claim follows from that fact that the expression on the left is essentially the Riemann sum of the integral on the right. This means that for any given $\varepsilon > 0$, we can find k_ε such that when $k \geq k_\varepsilon$, we have that

$$\left| \frac{1}{\alpha(k_\varepsilon)} \sum_{i=1}^{\alpha(k_\varepsilon)} g_{i1}^2 - \frac{1}{2\pi} \int_0^{2\pi} f\left(d^2(\theta_i, \theta), d^2\left(\theta_i + \frac{\pi}{2}, \theta\right)\right) d\theta_i \right| < \varepsilon \quad (\text{C.11})$$

Then, we can proceed by calculating

$$\mathbb{E}[g_{i1}^2] = \frac{1}{2\pi} \int_0^{2\pi} f\left(d^2(\theta_i, \theta), d^2\left(\theta_i + \frac{\pi}{2}, \theta\right)\right) d\theta. \quad (\text{C.12})$$

By substituting (C.8) in (C.10) and (C.12), we see that

$$\begin{aligned} \mathbb{E}[g_{i1}^2] &= \frac{1}{2\pi} \int_0^{2\pi} f\left(d^2(\theta_i, \theta), d^2\left(\theta_i + \frac{\pi}{2}, \theta\right)\right) d\theta \\ &= \frac{1}{2\pi} \int_0^{2\pi} f\left(d^2(\theta_i, \theta), d^2\left(\theta_i + \frac{\pi}{2}, \theta\right)\right) d\theta_i. \end{aligned} \quad (\text{C.13})$$

We can then establish convergence through

$$\begin{aligned} & \left| \frac{1}{\alpha(k)} \sum_{i=1}^{\alpha(k)} \frac{g_{i1}^2}{\mathbb{E}[g_{i1}^2]} - 1 \right| \\ &= \frac{1}{\mathbb{E}[g_{i1}^2]} \left| \frac{1}{\alpha(k)} \sum_{i=1}^{\alpha(k)} g_{i1}^2 - \mathbb{E}[g_{i1}^2] \right| \\ &= \frac{1}{\mathbb{E}[g_{i1}^2]} \left| \frac{1}{\alpha(k)} \sum_{i=1}^{\alpha(k)} g_{i1}^2 - \frac{1}{2\pi} \int_0^{2\pi} f\left(d^2(\theta_i, \theta), d^2\left(\theta_i + \frac{\pi}{2}, \theta\right)\right) d\theta_i \right| \text{ from (C.13)} \\ &< \frac{\varepsilon}{\mathbb{E}[g_{i1}^2]} \text{ when } k \geq k_\varepsilon. \end{aligned}$$

The result follows since $\mathbb{E}[g_{i1}^2]$ is bounded below by Lemma 24.

Bibliography

- [1] R. Bellman, “Dynamic programming”, *Princeton University Press*, Princeton, NJ, 1957.
- [2] D. Bertsekas, “Dynamic programming and optimal control”, *Athena Scientific*, Belmont, MA, 1995.
- [3] M. L. Puterman, “Dynamic programming and its applications”, *Academic Press*, 1978.
- [4] J. Kleinberg and E. Tardos, “Algorithm Design”, *Addison Wesley*, 2006.
- [5] R. Diestel, *Graph Theory (3rd ed.)*, Springer, ISBN 3-540-26182-6, <http://www.math.uni-hamburg.de/home/diestel/books/graph.theory/>.
- [6] S. Arnborg and A. Proskurowski, “Linear time algorithms for NP-hard problems restricted to partial k -trees”, *Discrete Appl. Math*, vol. 23, pp. 1124, 1989.
- [7] M. Shamiah, S. Banerjee and H. Vikalo, “Greedy sensor selection: Leveraging sub-modularity”, *IEEE Conf. on Decision and Control CDC 2010*, Atlanta, GA, Dec. 2010.
- [8] S. Foucart and M.-J. Lai, “Sparsest solutions of underdetermined linear systems via ℓ_q minimization for $0 < q \leq 1$ ”, *submitted to Applied and Computational Harmonic Analysis*, 2008.
- [9] M. E. Davies, and R. Gribonval, “Restricted Isometry Constants where ℓ^p sparse recovery can fail for $0 < p \leq 1$ ”, *IEEE Trans. Inform. Theory*, pp. 2203-2214, vol. 55, May. 2009.
- [10] D. Donoho, “Compressed sensing”, *IEEE Trans. Inf. Theory*, vol. 52, pp. 1289-1306, Apr. 2006.
- [11] E. Candès and T. Tao, “Near optimal signal recovery from random projections: Universal encoding strategies?”, *IEEE Trans. Inform. Theory*, vol. 52, no. 12, pp. 5406-5425, Dec. 2006.

- [12] R. Baraniuk, M. Davenport, R. DeVore, and M. Wakin, “A simple proof of the restricted isometry property for random matrices”, submitted for publication.
- [13] M. Rudelson and R. Vershynin, “On sparse reconstruction from Fourier and Gaussian measurements”, submitted for publication.
- [14] S. Mendelson, A. Pajor, and N. Tomczak-Jaegermann, “Uniform uncertainty principle for Bernoulli and sub-gaussian ensembles”, *preprint*, 2006.
- [15] G. Raskutti, M. J. Wainwright and B. Yu, “Restricted eigenvalue properties for correlated gaussian designs”, vol. 11, pp. 2241-2259, Aug. 2010.
- [16] S. Zhou, “Restricted eigenvalue conditions on subgaussian random matrices”, *Technical report*, Department of Mathematics, ETH Zurich, December 2009.
- [17] H. Rauhut, “Compressive sensing and structured random matrices”, in *Theoretical Foundations and Numerical Methods for Sparse Recovery*, ser. *Radon Series Comp. Appl. Math.* deGruyter, in preparation.
- [18] S. Mendelson and A. Pajor, “On singular values of matrices with independent rows”, *Bernoulli*, vol. 12(5), pp. 761-773, 2006.
- [19] R. Adamczak, A. E. Litvak, A. Pajor and N. Tomczak-Jaegermann, “Restricted isometry property of matrices with independent columns and neighborly polytopes by random sampling”, available from: [arXiv:0904.4723v1](https://arxiv.org/abs/0904.4723v1), 2009.
- [20] R. Vershynin, “Introduction to the non-asymptotic analysis of random matrices”, In *Compressed sensing: theory and applications*, Y. Eldar and G. Kutyniok, editors, Cambridge University Press, Submitted.
- [21] D. Achlioptas, “Database-friendly random projections”, *Proceedings of the Twentieth ACM SIGMOD-SIGACT-SIGART symposium on principles of database systems*, pp. 274-281, Santa Barbara, CA, 2001.
- [22] V. de la Peña and E. Gine, “Decoupling. From dependence to independence. Randomly stopped processes. U-statistics and processes. Martingales and beyond.”, New York: Springer-Verlag, 1999.
- [23] J. A. Tropp and A. C. Gilbert, “Signal recovery from partial information via orthogonal matching pursuit”, *IEEE Trans. Inform. Theory*, vol. 53, pp. 4655-4666, 2007.

- [24] J. A. Tropp, “Just relax: Convex programming methods for identifying sparse signals”, *IEEE Trans. Info. Theory*, vol. 51, pp. 1030-1051, Mar. 2006.
- [25] R. Tibshirani, “Regression shrinkage and selection via the lasso”, *J. Roy. Statist. Soc. Ser. B*, pp. 267-288, 1996.
- [26] M. Sharif and B. Hassibi, “A comparison of time-sharing, beamforming and DPC for MIMO broadcast channels with many users”, *IEEE Trans. Commun.*, vol. 55, pp. 11-15, Jan. 2007.
- [27] J. Huang, V. Subramanian, R. Agrawal, and R. Berry, “Joint scheduling and resource allocation in uplink OFDM Systems for broadband wireless access networks”, *IEEE Journ. Sel. Areas Commun.*, vol. 27, pp- 226-234, Feb. 2009.
- [28] D. J. Love, R. W. Heath Jr., V. K. N. Lau, D. Gesbert, B. D. Rao and M. Andrews, “An overview of limited feedback in wireless communication systems”, *IEEE Journ. Sel. Areas Commun.*, vol. 26, pp. 1341-1365, Oct. 2008.
- [29] D. J. Love, R. W. Heath Jr. and T. Strohmer, “Grassmannian beamforming for multiple-input-multiple-output wireless systems”, *IEEE Trans. Info. Theory*, vol. 49, pp. 2735-2747, Oct. 2003.
- [30] W. Santipach and M. L. Honig, “Asymptotic performance of mimo wireless channels with limited feedback”, in *Proc. IEEE MILCOM 2003*, vol. 1, pp. 141-146, Boston, MA, Oct. 2003.
- [31] —, “Asymptotic capacity of beamforming with limited feedback”, in *Proc. IEEE ISIT 2004*, p. 290, Chicago, IL, June 2004.
- [32] W. Dai, Y. Liu and B. Rider, “Quantization bounds on Grassmann manifolds and applications to MIMO communications”, *IEEE Trans. Inform. Theory*, vol. 54, pp. 1108-1123, Mar. 2008.
- [33] B. Mondal and R. Heath, “Performance analysis of quantized beamforming MIMO systems”, *IEEE Trans. Sig. Proc.*, vol. 54, pp. 4753-4766, Dec. 2006.
- [34] V. Raghavan, M. L. Honig, V. V. Veeravalli, “Performance analysis of RVQ-based limited feedback beamforming codebooks”, *Proc. IEEE ISIT 2009*, pp. 2437-2441, Seoul, Korea, June 2009.
- [35] K. K. Mukkavilli, A. Sabharwal, E. Erkip, and B. Aazhang, “On beamforming with finite rate feedback in multiple antenna systems”, *IEEE Trans. Inform. Theory*, vol. 49, pp. 2562-2579, Oct. 2003.

- [36] A. D. Dabbagh and D. J. Love, "Feedback rate-capacity loss tradeoff for limited feedback MIMO Systems", *IEEE Trans. Inform. Theory*, vol. 52, pp. 2190-2202, May 2006.
- [37] C. K. Au-Yeung and D. J. Love, "On the performance of random vector quantization limited feedback beamforming in a MISO System", *IEEE Trans. Wireless Commun.*, vol. 6, pp. 458-462, Feb. 2007.
- [38] J. Chen, R. Berry and M. Honig, "Limited feedback schemes for downlink OFDMA", *IEEE Journ. Sel. Areas Commun.*, vol. 26, pp. 1451-1461, Oct. 2008.
- [39] R. Agarwal, V. Majjigi, Z. Han, R. Vannithamby and J. Cioffi, "Low complexity resource allocation with opportunistic feedback over downlink OFDMA networks", *IEEE Journ. Sel. Areas Commun.*, vol. 26, pp. 1462-1472, Oct. 2008.
- [40] S. Sanayei and A. Nosratinia, "Opportunistic downlink transmission with limited feedback", *IEEE Trans. Info. Theory*, vol. 53, pp. 4363-4372, Nov. 2007.
- [41] N. Jindal, "MIMO broadcast channels with finite-rate feedback," *IEEE Trans. Info. Theory*, vol. 52, pp. 5045-5060, Nov. 2006.
- [42] K. Huang, J. G. Andrews, R. W. Heath, Jr., "Performance of Orthogonal Beamforming for SDMA with Limited Feedback", *IEEE Trans. Veh. Tech.*, vol. 58, pp. 152-164, Jan. 2009.
- [43] W. Dai, B. Rider, and Y. Lui, "Multi-access MIMO systems with finite rate channel state feedback", *Proceedings of the Allerton Conference on Communication, Control, and Computing*, Monticello, IN, Oct. 2005.
- [44] E. Jorswieck, A. Sezgin, B. Ottersten and A. Paulraj, "Feedback reduction in uplink MIMO OFDM systems by chunk optimization", *EURASIP Journal on Advances in Sig. Proc.*, article no. 59, Jan. 2008.
- [45] R. Zakhour and D. Gesbert, "Adaptive feedback rate control in MIMO broadcast systems", *IEEE Information Theory Workshop*, Porto, Portugal, May 2008.
- [46] R. Zakhour and D. Gesbert, "Adaptive feedback rate control in MIMO broadcast systems with user scheduling", *Information Theory and Applications Workshop*, San Diego, CA, Jan. 2008.

- [47] M. Ouyang and L. Ying, "On scheduling in multi-channel wireless downlink networks with limited feedback", *Proceedings of the Allerton Conference on Communication, Control, and Computing*, Monticello, IN, Oct. 2009.
- [48] L. Tassiulas and A. Ephremides, "Stability properties of constrained queueing systems and scheduling policies for maximum throughput in multihop radio networks", *IEEE Trans. Automatic Control*, Vol. 37, pp. 1936-1949, Dec. 1992.
- [49] C. Joo, X. Lin, and N. B. Shroff, "Greedy maximal matching: Performance limits for arbitrary network graphs under the node-exclusive interference Model", *IEEE Trans. Auto. Control*, vol. 54, no. 12, pp. 2734-2744, Dec. 2009.
- [50] A. Gupta, X. Lin and R. Srikant, "Low-complexity distributed scheduling algorithms for wireless networks", *IEEE/ACM Trans. Networking*, vol. 17, pp. 1846-1859, Dec. 2009.
- [51] M. Neely, "Dynamic power allocation and routing for satellite and wireless networks with time varying channels", *Ph.D. Thesis*, Massachusetts Institute of Technology, 2003.
- [52] M. Andrews, K. Kumaran, K. Ramanan, A. Stolyar, R. Vijayakumar and P. Whiting, "Scheduling in a queueing system with asynchronously varying service rates", *Probability in the Engineering and Informational Sciences*, vol. 18, pp. 191-217, Apr. 2004.
- [53] A. L. Stolyar, "On the asymptotic optimality of the gradient scheduling algorithm for multiuser throughput allocation", *INFORMS*, Vol. 53, Issue 1, pp. 12-25, Jan. 2005.
- [54] E. Dahlman, A. Furuskär, Y. Jading, M. Lindström and S. Parkvall, "Key features of the LTE radio interface", *Ericsson Review*, www.ericsson.com/ericsson/corpinfo/publications, No. 2, Feb. 2008.
- [55] H. Holma and A. Toskala, "LTE for UMTS : OFDMA and SC-FDMA based radio access", *Chichester : John Wiley and Sons, Ltd.*, 2009.
- [56] S. Sesia, I. Toufik and M. Baker, "LTE, The UMTS Long Term Evolution : From theory to practice", *Chichester : John Wiley and Sons, Ltd.*, 2009.
- [57] D. Gesbert, M. Kountouris, R. W. Heath Jr., C. B. Chae, and T. Salzer, "From single user to multiuser communications: Shifting the MIMO paradigm", *IEEE Sig. Proc. Magazine*, 2007.

- [58] T. Abe, “3GPP self-evaluation methodology and results”, http://www.3gpp.org/ftp/workshop/2009-12-17_ITU-R_IMT-Adv_eval/docs/REV-090008-r1.zip.
- [59] A. El Gamal, J. Mammen, B. Prabhakar and D. Shah, “Optimal throughput-delay scaling in wireless networks: part I: the fluid model”, *IEEE/ACM Trans. Networking*, vol. 14, pp. 2568-2592, June 2006.
- [60] S. Toumpis and A. Goldsmith, “Large wireless networks under fading, mobility, and delay constraints”, *Proc. of IEEE INFOCOM 2004*, vol. 1, pp. 619, Hong Kong, Mar. 2004.
- [61] D. Park and G. Caire, “Hard fairness versus proportional fairness in wireless communications: The multiple-cell case”, *arXiv:0802.2975v1 [cs.IT]*, Feb. 2008.
- [62] V. K. N. Lau, W. K. Ng, and D. S. Wing, “Asymptotic tradeoff between cross-layer goodput gain and outage diversity in OFDMA systems with slow fading and delayed CSIT”, *IEEE Trans. Wireless Commun.*, vol 7, pp. 2732-2739, July 2009.
- [63] D. Tse and P. Vishwanath, “Fundamentals of wireless communication”, *Cambridge University Press*, 2005.
- [64] T. K. Y. Lo, “Maximum ratio transmission,” *IEEE Trans. Commun.*, vol. 47, pp. 1458-1461, Oct. 1999.
- [65] D. Gesbert, M. Shafi, D.-S. Shiu, P. J. Smith, and A. Naguib, “From theory to practice: an overview of MIMO space-time coded wireless systems,” *IEEE Journ. Sel. Areas Commun.*, vol. 21, no. 3, pp. 281-302, 2003.
- [66] H. Holma and A. Toskala, “WCDMA for UMTS: Radio access for third generation mobile communications”, *Revised Edition. New York: John Wiley & Sons*, 2001.
- [67] P. R. Goundan and A. S. Schulz, “Revisiting the greedy approach to submodular set function maximization”, Jan. 2009.
- [68] G. Calinescu, C. Chekuri, M. Pal, J. Vondrak, “Maximizing a submodular set function subject to a matroid constraint (Extended Abstract)”, *Lecture Notes In Computer Science, Proc. 12th Intern. Conf. Integer Prog. and Comb. Optimization*, vol. 4513, pp. 182 - 196, Ithaca, NY, 2007

- [69] J. Vondrák, “Submodularity in combinatorial optimization”, *Ph.D. thesis*, Charles University, Prague, 2007.
- [70] G. L. Nemhauser and L. A. Wolsey, “Best algorithms for approximating the maximum of a submodular set function”, *INFORMS*, vol. 3, pp. 177-188, Aug. 1978.
- [71] “LTE-Advanced Physical Layer”, http://ftp.3gpp.org/workshop/2009-12-17_ITU-R_IMT-Adv_eval/docs/pdf/REV-090003-r1.pdf, Dec. 2009.
- [72] Alcatel-Lucent white paper, “Technologies for LTE-Advanced”, http://www.3g4g.co.uk/LteA/LteA_Pres_0810_ALU.pdf, Oct. 2008.
- [73] “Overview of 3GPP Release 10V0.0.5(2009 – 12)”, http://www.3gpp.org/ftp/Information/WORK_PLAN/Description_Releases, Dec. 2009.
- [74] Q. Li, X. Lin, J. Zhang and W. Roh, “Advancement of MIMO technology in WiMAX: from IEEE 802.16d/e/j to 802.16m”, *IEEE Comm. Magazine*, vol. 47, pp. 100-107, June 2009.
- [75] “802.16m System description document”, <http://www.ieee802.org/16/tgm/>.
- [76] D. J. Love, R. W. Heath Jr. and T. Strohmer, “Grassmannian beamforming for multiple-input-multiple-output wireless systems”, *IEEE Trans. Info. Theory*, vol. 49, pp. 2735-2747, Oct. 2003.
- [77] B. Mondal and R. Heath, “Performance analysis of quantized beamforming MIMO systems”, *IEEE Trans. Sig. Proc.*, vol. 54, pp. 4753-4766, Dec. 2006.
- [78] W. Dai, Y. Liu and B. Rider, “Quantization bounds on Grassmann manifolds and applications to MIMO communications”, *IEEE Trans. Inform. Theory*, vol. 54, pp. 1108-1123, Mar. 2008.
- [79] D. J. Love, R. W. Heath Jr., V. K. N. Lau, D. Gesbert, B. D. Rao and M. Andrews, “An overview of limited feedback in wireless communication systems”, *IEEE Journ. Sel. Areas Commun.*, vol. 26, pp. 1341-1365, Oct. 2008.
- [80] J. Chen, R. Berry and M. Honig, “Limited feedback schemes for downlink OFDMA”, *IEEE Journ. Sel. Areas Commun.*, vol. 26, pp. 1451-1461, Oct. 2008.

- [81] R. Agarwal, V. Majjigi, Z. Han, R. Vannithamby and J. Cioffi, "Low complexity resource allocation with opportunistic feedback over downlink OFDMA networks", *IEEE Journ. Sel. Areas Commun.*, vol. 26, pp. 1462-1472, Oct. 2008.
- [82] S. Sanayei and A. Nosratinia, "Opportunistic downlink transmission with limited feedback", *IEEE Trans. Info. Theory*, vol. 53, pp. 4363-4372, Nov. 2007.
- [83] N. Jindal, "MIMO broadcast channels with finite-rate feedback", *IEEE Trans. Info. Theory*, vol. 52, pp. 5045-5060, Nov. 2006.
- [84] K. Huang, J. G. Andrews, R. W. Heath, Jr., "Performance of orthogonal beamforming for SDMA with limited feedback", *IEEE Trans. Veh. Tech.*, vol. 58, pp. 152-164, Jan. 2009.
- [85] W. Dai, B. Rider, and Y. Lui, "Multi-access MIMO systems with finite rate channel state feedback", *Proceedings of the Allerton Conference on Communication, Control, and Computing*, Monticello, IN, Oct. 2005.
- [86] E. Jorswieck, A. Sezgin, B. Ottersten and A. Paulraj, "Feedback reduction in uplink MIMO OFDM systems by chunk optimization", *EURASIP Journal on Advances in Sig. Proc.*, article no. 59, Jan. 2008.
- [87] J. Perez, J. Ibez, J. Via and I. Santamara, "Performance analysis of SNR-based scheduling policies in asymmetric broadcast ergodic fading channels", in *EURASIP Journal on Wireless Communications and Networking - Special issue on fairness in radio resource management for wireless networks*, vol. 2009, Jan. 2009.
- [88] Y. Ma, A. Leith, M.-S. Alouini and X. Shen, "Weighted-SNR-based fair scheduling for uplink OFDMA", *Proc. IEEE GLOBECOM 2009*, Honolulu, Hawaii, USA, Dec. 2009.
- [89] T. Girici, O. Ozel, and E. Uysal-Biyikoglu, "Buffer sharing on an OFDMA downlink", In *Proc. of IEEE PIMRC 2010*, pp. 1162-1167, Istanbul, Turkey, Sep. 2010.
- [90] G. Song and Y. Li, "Asymptotic throughput analysis for channel-aware scheduling", *IEEE Trans. Commun.*, vol. 54, pp. 1827-1834, Oct. 2006.

- [91] L. Yang, M. Kang, and M.-S. Alouini, "On the capacity-fairness tradeoff in multiuser diversity systems", *IEEE Trans. Veh. Tech.*, vol. 56, pp. 1901-1907, July 2007.
- [92] M. Torabi, W. Ajib, and D. Haccoun, "Performance analysis of rate-adaptive scheduling in MIMO systems with antenna selection", in *Proc. IEEE PIMRC 2008*, pp.1-6, Cannes, France, Sep. 2008.
- [93] F. Berggren and R. Jantti, "Asymptotically fair transmission scheduling over fading channels", *IEEE Trans. Wireless Commun.*, vol. 3, pp. 3263-36, Jan. 2004.
- [94] A. Senst, P. Schulz-Rittich, G. Ascheid and H. Meyr, "On the throughput of proportional fair scheduling with opportunistic beamforming for continuous fading states", *IEEE VTC2004-Fall*, pp. 300-304, Los Angeles, CA, Sept. 2004.
- [95] M. Kang, Y. J. Sang, H. G. Hwang, H. Y. Lee, K. S. Kim, "Performance analysis of proportional fair scheduling with partial feedback information for multiuser multicarrier systems", *IEEE VTC Spring 2009*, Barcelona, Spain, Apr. 2009.
- [96] G. Hwang and F. Ishizaki, "Design of a fair scheduler exploiting multiuser diversity with feedback information reduction", *IEEE Commun. Lett.*, vol. 12, pp. 124-126, Feb. 2008.
- [97] F. Ishizaki and H. U. Gang, "Throughput performance of quantized proportional fair scheduling with adaptive modulation and coding", *IEEE WTS 2009*, Prague, Apr. 2009.
- [98] D. Gesbert and M.-S. Alouini, "How much feedback is multi-user diversity really worth?", in *Proc. IEEE ICC 2004*, pp. 2342-38, Paris, France, Jun. 2004.
- [99] A. Gopalan, C. Caramanis, and S. Shakkottai, "On wireless scheduling with partial channel-state information", *Proc. of the Allerton Conf. on Communication, Control, and Computing*, Monticello, IN, Sep. 2007.
- [100] M. Ouyang and L. Ying, "On scheduling in multi-channel wireless downlink networks with limited feedback", *Proceedings of the Allerton Conference on Communication, Control, and Computing*, Monticello, IN, Oct. 2009.

- [101] K. Huang and V. K. N. Lau, "Stability and delay of zero-forcing SDMA with limited feedback", *submitted to IEEE Trans. Inform. Theory*, Feb. 2009.
- [102] H. Ganapathy, S. Banerjee, N. Dimitrov and C. Caramanis, "Optimal feedback allocation algorithms for multi-user uplink", *Proceedings of the Allerton Conference on Communication, Control, and Computing*, Monticello, IN, Oct. 2009.
- [103] O. Oteri, and A. Paulraj, "Multicell optimization for diversity and interference mitigation", *IEEE Trans. Sig. Proc.*, May 2008.
- [104] "Interference mitigation for uplink", *Doc. no.: IEEE C802.16m-08/667*, July 2008.
- [105] L. Ying and S. Shakkottai, "On throughput-optimal scheduling with delayed channel state feedback", *In Proc. 2008 Information Theory and Applications Workshop*, pp. 339 - 344, San Diego, CA, Feb. 2008.
- [106] M. Andrews and L. Zhang, "Scheduling algorithms for multicarrier wireless data systems", *IEEE/ACM Trans. Networking*, vol. 19, pp. 447 - 455, Apr. 2011.
- [107] X. Huang, "Smart antennas for intelligent transportation systems", *Proc. 6th Intern. Conference on Telecom.*, Chengdu, China, June 2006.
- [108] ArrayComm LLC white paper, "IntelliCell: A fully adaptive approach to smart antennas".
- [109] ArrayComm LLC white paper, "Leveraging MIMO in wide-area networks".
- [110] ArrayComm LLC white paper, "Navigating the harsh realities of broadband wireless network economics".
- [111] ArrayComm LLC white paper, "ArrayComm A-MAS technology overview".
- [112] "Building Palo Alto's wireless infrastructure", <http://wireless4paloalto.att.com/>.
- [113] A. A. M. Saleh, A. J. Rustako, and R. S. Roman, "Distributed antennas for indoor radio communications", *IEEE Trans. on Communications*, vol. 35, pp. 1245-1251, Dec. 1987.

- [114] H. Yanikomeroglu and E. S. Sousa, "CDMA distributed antenna system for indoor wireless communications", in *Proc. IEEE Int. Conf. on Universal Personal Commun.*, Ottawa, Canada, Oct. 1993, pp. 990994.
- [115] W. Roh and A. Paulraj, "MIMO channel capacity for the distributed antenna", in *Proc. IEEE Veh. Tech. Conf.*, Sept. 2002, pp. 706709.
- [116] W. Choi and J. G. Andrews, "Downlink performance and capacity of distributed antenna systems in a multicell environment", *IEEE Trans. Wireless Commun.*, vol. 6, pp. 69-73, Jan. 2007.
- [117] H. Hu, Y. Zhang, and J. Luo (eds), *Distributed Antenna Systems: Open Architecture for Future Wireless Communications*. CRC Press, 2007.
- [118] J. Zhang and J. Andrews, "Distributed antenna systems with randomness", *IEEE Trans. Wireless Commun.*, vol. 7, pp. 3636 - 3646, 2008.
- [119] AT&T Press Release, "AT&T improves coverage in CTA subways", http://communications.wireless.att.com/ILWI_Network_Newsletter/news_release.pdf.
- [120] AT&T Press Release, "AT&T Building Most Advanced Mobile Broadband Experience in Seattle, Announces 2011 Network Upgrade Plans", <http://www.att.com/gen/press-room?pid=2943>.
- [121] AT&T Press Release, "AT&T building most advanced mobile broadband experience in greater Orlando, announces 2011 network upgrade plans", <http://www.att.com/gen/press-room?pid=2943>.
- [122] AT&T Press Release, "AT&T building most advanced mobile broadband experience in San Diego, announces 2011 network upgrade plans", <http://www.att.com/gen/press-room?pid=2943>.
- [123] AT&T Press Release, "AT&T building most advanced mobile broadband experience in Philadelphia, announces 2011 network upgrade plans", <http://www.att.com/gen/press-room?pid=2943>.
- [124] "lightRadio portfolio: Economic analysis", Whitepaper, http://www.alcatel-lucent.com/features/light_radio/index.html
- [125] E. Larsson and E. Jorswieck, "Competition versus cooperation on the MISO interference channel", *IEEE Journ. Sel. Areas Commun.*, vol. 26, pp. 1059-1069, Sep. 2008.

- [126] E. Jorswieck and E. Larsson, "Complete characterization of the Pareto boundary for the MISO interference channel", *IEEE Trans. Sig. Proc.*, vol. 56, pp. 5292-5296, Oct. 2008.
- [127] R. Zakhour and D. Gesbert, "Coordination on the MISO interference channel using the virtual SINR framework", *Proc. ITG/IEEE Workshop on Smart Antennas (WSA 2009)*, Feb. 2009.
- [128] K. M. Ho and D. Gesbert, "Spectrum sharing in multiple antenna channels: A distributed cooperative game theoretic approach", *Proc. IEEE Intern. Symp. on Personal, Indoor, Mobile Radio Communications (PIMRC)*, Cannes, 15-18 Sept. 2008.
- [129] R. Zakhour, Z. K. M. Ho, and D. Gesbert, "Distributed beamforming coordination in multicell MIMO channels", *Proc. of IEEE Veh. Tech. Conference*, Barcelona, Spain, Apr. 2009.
- [130] G. J. Foschini, Z. Miljanic, "A simple distributed autonomous power control algorithm and its convergence", *IEEE Trans. Veh. Tech.*, vol. 42, pp. 641-646, Apr. 1993.
- [131] "Nomor Research Newsletter: The way of LTE towards 4G", <http://www.nomor-research.com/home/technology/3gpp-newsletter/2009-12-the-way-of-lte-towards-4g>, Dec. 2009.
- [132] A. Gersho and R. M. Gray, *Vector quantization and signal compression*, Boston: Kluwer, 1992.
- [133] N. Ravindran and N. Jindal, "Limited feedback-based block diagonalization for the MIMO broadcast channel", *Submitted to IEEE Journ. Sel. Areas Commun.*, Nov. 2007.
- [134] I. Hicks, A. Koster, and E. Kolotoglu, "Branch and tree decomposition techniques for discrete optimization", *Tutorials in Operation Research: INFORMS*, pp. 1-29, New Orleans, 2005.
- [135] E. Amir, "Efficient approximations for triangulation of minimum treewidth", *Proc. of 17th Conf. on Uncertainty in Artificial Intelligence*, pp. 7-15, 2001.
- [136] V. Bouchitte, D. Kratsch, H. Muller, and I. Todinca, "On treewidth approximations", *Disc. Appl. Math.*, vol. 136, pp. 183-196, 2004.

- [137] M. I. Jordan, “Graphical models”, *Statistical Science (Special Issue on Bayesian Statistics)*, vol. 19, pp. 140-155, 2004.
- [138] M. I. Jordan, “Learning in graphical models”, *Cambridge MA: MIT Press*, 1999.
- [139] Q. H. Spencer, A. L. Swindlehurst, and M. Haardt, “Zero-forcing methods for downlink spatial multiplexing in multiuser MIMO channels”, *IEEE Trans. Sig. Proc.*, vol. 52, pp. 461-471, 2004.
- [140] L. U. Choi and R. D. Murch, “A transmit preprocessing technique for multiuser MIMO Systems using a decomposition approach”, *IEEE Trans. Wireless Commun.*, vol. 3, pp. 2024, Jan. 2004.
- [141] K. K. Wong, R. D. Murch and K. B. Letaief, “A joint-channel diagonalization for multiuser MIMO antenna Systems”, *IEEE Trans. Wireless Commun.*, vol. 2, pp. 773786, Jul. 2003.
- [142] Z. Pan, K. K. Wong, and T. S. Ng, “Generalized multiuser orthogonal space-division multiplexing”, *IEEE Trans. Wireless Commun.*, vol. 3, pp. 19691973, Nov. 2004.
- [143] Z. Shen, R. Chen, J. G. Andrews, R. W. Heath, Jr., and B. L. Evans, “Low complexity user selection algorithms for multiuser MIMO Systems with block diagonalization”, *IEEE Trans. Sig. Proc.*, vol. 54, pp. 3658-3663, Sep. 2006.
- [144] S. Boyd and L. Vandenberghe, “Convex Optimization”, *Cambridge Univ. Press*, Cambridge, U.K., 2004.
- [145] “FCC frees up vacant TV airwaves for ‘Super-Wi-Fi’ technologies”, Federal Communications Commission, www.fcc.gov.
- [146] National Telecommunications and Information Administration (NTIA), “FCC frequency allocation chart”, 2003. Download available at www.ntia.doc.gov/osmhome/allochrt.pdf.
- [147] White PAPER - 3G/UMTS “Towards global mobile broadband, standardising the future of mobile communications with LTE (Long Term Evolution)”, <http://www.umts-forum.org/>, 2008.
- [148] J. Mitola and G. Q. Maguire, “whitespace radios: making software radios more personal”, *IEEE Personal Communications.*, vol. 6, pp. 1318, Aug. 1999.

- [149] Federal Communications Commission Spectrum Policy Task Force, “Report of the Spectrum Efficiency Working Group”, Technical Report 02-135, Nov. 2002.
- [150] A. Goldsmith, S. A. Jafar, I. Maric, and S. Srinivasa, “Breaking spectrum gridlock with whitespace radios: an information theoretic perspective”, *Proc. of the IEEE*, vol. 97, pp. 894-914, May 2009.
- [151] A. Attar, M. Reza Nakhai and A. H. Aghvami, “whitespace radio game: a framework for efficiency, fairness and QoS guarantee”, *Proc. of IEEE ICC 2008*, pp. 4170 - 4174, 2008.
- [152] N. Gatsis, A. G. Marques and G.B. Giannakis, “Utility based power control for peer-to peer whitespace radio networks with heterogeneous constraints”, *IEEE ICASSP 2008*, Las Vegas, NV, Apr. 2008.
- [153] L. Le and E. Hossain, “Resource allocation for spectrum underlay in whitespace radio networks”, *IEEE Trans. Wireless Commun.*, vol. 7, pp. 1–11, Dec. 2008.
- [154] L. Tassiulas and A. Ephremides, “Stability properties of constrained queueing systems and scheduling policies for maximum throughput in multihop radio networks,” *IEEE Trans. Automat. Contr.*, vol. 4, pp. 1936–1948, Dec. 1992.
- [155] L. Tassiulas and A. Ephremides, “Dynamic server allocation to parallel queues with randomly varying connectivity”, *IEEE Trans. Inform. Theory*, vol. 39, pp. 466–478, March 1993.
- [156] X. Lin, N. Shroff, and R. Srikant, “A tutorial on cross-layer optimization in wireless networks”, *IEEE J. Sel. Areas Commun.*, vol. 24, no. 8, pp. 1452–1463, Aug. 2006.
- [157] L. Georgiadis, M. J. Neely and L. Tassiulas, “Resource allocation and cross-layer control in wireless networks”, *Foundations and Trends in Networking*, vol. 1, no. 1, pp.1-144, Apr. 2006.
- [158] E. Candes and M. Wakin, “An introduction to compressive sampling”, *IEEE Sig. Proc. Magazine*, vol. 25, pp. 21 - 30, Mar. 2008.
- [159] R. Baraniuk, “Compressive sensing”, *IEEE Sig. Proc. Magazine*, vol. 24, pp. 118-121, July 2007.

- [160] D. Donoho, "Compressed sensing", *IEEE Trans. Inform. Theory*, vol. 52, pp. 1289-1306, Apr. 2006.
- [161] A. Gopalan, C. Caramanis and S. Shakkotai, "On wireless scheduling with partial channel-state information", *Proc. of the Allerton Conf. on Communication, Control, and Computing*, Monticello, IN, Oct. 2007.
- [162] H. Ganapathy and C. Caramanis, "Queue-based sub-carrier grouping for feedback reduction in OFDMA systems", *in preparation*.
- [163] M. Ouyang and L. Ying, "On scheduling in multi-channel wireless downlink networks with limited feedback", *Proc. of the Allerton Conference on Communication, Control, and Computing*, Monticello, IN, Oct. 2009.
- [164] H. Ganapathy, S. Banerjee, N. Dimitrov and C. Caramanis, "Optimal feedback allocation algorithms for multi-user uplink", *Proceedings of the Allerton Conference on Communication, Control, and Computing*, Monticello, IN, Oct. 2009.
- [165] N. Kalouptsidis, G. Mileounis, B. Babadi, V. Tarokh, "Adaptive algorithms for sparse nonlinear channel estimation", *Proc. IEEE Workshop on Statistical Signal Processing*, Cardiff, Wales, Sep. 2009.
- [166] S. F. Cotter and B. D. Rao, "Sparse channel estimation via matching pursuit with application to equalization", *IEEE Trans. Commun.*, vol. 50, pp. 374-377, Mar. 2002.
- [167] W. U. Bajwa, A. M. Sayeed, and R. Nowak, "Learning sparse doubly-selective channels", *Proc. Allerton Conf. on Communication, Control, and Computing*, Monticello, IL, Sep. 2008.
- [168] T. Yücek and H. Arslan, "A survey of spectrum sensing algorithms for whitespace radio applications", *IEEE Comm. Surveys And Tutorials*, vol. 11, First Quarter 2009.
- [169] J. G. Andrews, A. Ghosh, and R. Muhamed, "Fundamentals of WiMAX: Understanding broadband wireless networking", *Prentice Hall*, 2007.
- [170] Rappaport, S. T., "Wireless communications principles and practice", *Prentice-hall*, Chp. 4, pp. 138-139, 2002.
- [171] M. Andrews and L. Zhang, "Scheduling algorithms for multicarrier wireless data systems", *IEEE/ACM Trans. Networking*, vol. 19, pp. 447 - 455, Apr. 2011.

- [172] L. Lovasz and S. Vempala, “Fast Algorithms for Logconcave Functions: Sampling, Rounding, Integration and Optimization”, *Proc. of the 47th IEEE Symposium on Foundations of Computer Science (FOCS '06)*, Berkeley, CA, Oct. 2006.
- [173] R. Adamczak, A.E. Litvak, A. Pajor and N. Tomczak-Jaegermann, “Restricted isometry property of matrices with independent columns and neighborly polytopes by random sampling”, available from: [arXiv:0904.4723v1](https://arxiv.org/abs/0904.4723v1), 2009.
- [174] S. Mendelson and A. Pajor, “On singular values of matrices with independent rows”, *Bernoulli*, vol. 12(5), pp. 761-773, 2006.
- [175] J. A. Tropp and A.C. Gilbert, “Signal recovery from partial information via orthogonal matching pursuit”, *IEEE Trans. Inform. Theory*, vol. 53, pp. 4655-4666, 2007.
- [176] J. A. Tropp, “Just relax: Convex programming methods for identifying sparse signals”, *IEEE Trans. Info. Theory*, vol. 51, pp. 1030-1051, Mar. 2006.
- [177] R. Tibshirani, “Regression shrinkage and selection via the lasso”, *J. Roy. Statist. Soc. Ser. B*, pp. 267-288, 1996.
- [178] E. Candès and T. Tao, “The Dantzig selector: Statistical estimation when p is much larger than n ”, *Ann. Statist.*, pp. 2313-2351, Dec. 2007.
- [179] S. S. Chen, D. L. Donoho, and M. A. Saunders, “Atomic decomposition by basis pursuit”, *SIAM Journal Scientific Computing*, vol. 20, pp. 33-61, 1998.
- [180] H. Rauhut, “Compressive sensing and structured random matrices”, in *Theoretical Foundations and Numerical Methods for Sparse Recovery*, ser. Radon Series Comp. Appl. Math. deGruyter, in preparation.
- [181] A. Cohen, W. Dahmen and R. DeVore, “Compressed sensing and best k -term approximation”, *J. Amer. Math. Soc.*, vol. 22, pp. 211-231, 2009.
- [182] D. Tse and P. Vishwanath, “Fundamentals of wireless communication”, *Cambridge University Press*, 2005.
- [183] R. Grobinal and M. Nielson, “Sparse representations in unions of bases”, *IEEE Trans. Info. Theory*, vol. 49, pp. 3320-3325, Dec. 2003.

- [184] D. L. Donoho and X. Huo, "Uncertainty principles and ideal atomic decomposition", *IEEE Trans. Inform. Theory*, vol. 47, pp. 2845-2862, 2001
- [185] M. Elad and A.M. Bruckstein, "A generalized uncertainty principle and sparse representations in pairs of bases", *IEEE Trans. Info. Theory*, vol. 49, pp. 2558-2567, 2002.
- [186] E. J. Candes, T. Tao, "Decoding by linear programming", *IEEE Trans. Inform. Theory*, vol. 51, pp. 4203-4215, Dec. 2005.
- [187] J. A. Tropp, "Just relax: Convex programming methods for identifying sparse signals", *IEEE Trans. Info. Theory*, vol. 51, pp. 1030-1051, Mar. 2006.
- [188] R. Vershynin, "Introduction to the non-asymptotic analysis of random matrices", In *Compressed sensing: theory and applications*, Y. Eldar and G. Kutyniok, editors, Cambridge University Press, Submitted.
- [189] S. Mendelson, A. Pajor and N. Tomczak-Jaegermann, "Reconstruction and subgaussian operators", [arXiv:math/0506239v1 \[math.FA\]](https://arxiv.org/abs/math/0506239v1), 2005.
- [190] D. Pollard, "Empirical Processes: Theory and Applications", *NSF-CBMS Regional Conference Series in Probability and Statistics*, vol. 2, Inst. of Mathematical Statistics and American Statistical Assoc., 1990.
- [191] J. P. Romano, and A. F. Siegel, "Counterexamples in probability and statistics", *Belmont: Wadsworth*, 1986.
- [192] M. E. Davies and R. Gribonval, "Restricted isometry constants where ℓ^p sparse recovery can fail for $0 \ll p \leq 1$ ", *IEEE Trans. Inform. Theory*, vol. 55, pp. 2203-2214, May 2009.
- [193] S. Foucarta and M.-J.Lai, "Sparsest solutions of underdetermined linear systems via ℓ_q -minimization for $0 < q < 1$ ", *Applied and Computational Harmonic Analysis*, vol. 26, pp. 395-407, May 2009.

Vita

Harish Ganapathy obtained his Bachelor of Science and Master of Science degrees in Electrical Engineering from the State University of New York, Buffalo in May 2003 and May 2005 respectively. His industry experience includes internships at Qualcomm Inc. with Qualcomm CDMA Technologies in 2006, at Freescale Semiconductor Inc. with Cellular Products Group in 2007 and again at Qualcomm Inc. with Corporate Research and Development in 2007. His research interests lie (broadly) in optimization as applied to wireless networks, including both physical layer and networking aspects. He is currently pursuing a doctoral degree at the University of Texas, Austin under the supervision of Dr. Constantine Caramanis.

Permanent address: 3301 Speedway, Apt. 209
Austin, Texas 78705

This dissertation was typeset with L^AT_EX[†] by the author.

[†]L^AT_EX is a document preparation system developed by Leslie Lamport as a special version of Donald Knuth's T_EX Program.